pub 4/20/65

OAK RIDGE NATIONAL LABORATORY
operated by
UNION CARBIDE CORPORATION
for the
U.S. ATOMIC ENERGY COMMISSION

ORNL-TM-681

no. 103

A GUIDE TO THE DESIGN OF SHIPPING CASKS FOR THE TRANSPORTATION OF RADIOACTIVE MATERIAL

L. B. Shappert

NOTICE

This document contains information of a preliminary nature and was prepared primarily for internal use at the Oak Ridge National Laboratory. It is subject to revision or correction and therefore does not represent a final report. The information in this document has not been edited or reviewed to provide given public dissemination. Prior approval of the ORNL Patent Branch, Legal and Information Control Department is required.

LEGAL NOTICE

This report was prepared as an account of Government sponsored work. Neither the United States, nor the Commission, nor any person acting on behalf of the Commission:

A. Makes any warranty or representation, expressed or implied, with respect to the accuracy, completeness, or usefulness of the information contained in this report, or that the use of any information, apparatus, method, or process disclosed in this report may not infringe privately owned rights; or

B. Assumes any liabilities with respect to the use of, or for damages resulting from the use of any information, apparatus, method, or process disclosed in this report.

As used in the above, "person acting on behalf of the Commission" includes any employee or contractor of the Commission, or employee of such contractor, to the extent that such employee or contractor of the Commission, or employee of such contractor prepares, disseminates, or provides access to, any information pursuant to his employment or contract with the Commission, or his employment with such contractor.

ORNL-TM-681

Contract No. W-7405-eng-26

CHEMICAL TECHNOLOGY DIVISION

A GUIDE TO THE DESIGN OF SHIPPING CASKS FOR THE TRANSPORTATION OF RADIOACTIVE MATERIAL

L. B. Shappert

APRIL 1965

OAK RIDGE NATIONAL LABORATORY
Oak Ridge, Tennessee
operated by
UNION CARBIDE CORPORATION
for the
U.S. ATOMIC ENERGY COMMISSION

CONTENTS

Page

Abstract 1

1. Introduction 1

2. Evaluation of Criticality and Nuclear Safety 4
   2.1 Problem 4
   2.2 Regulations. 4
   2.3 Methods of Criticality Control 6
   2.4 Selected and Correlated Critical Data 10
   2.5 Methods of Reactivity Analysis 17

3. Heat Transfer 24
   3.1 Problem 24
   3.2 Regulations. 24
   3.3 Heat Removal from Fuel Elements 25
   3.4 Heat Sources 26
   3.5 Heat Removal from a Cask Surface 29
   3.6 Heat Conduction Through a Cask Wall 42
   3.7 Temperatures in Pin Type Fuel Elements 45
   3.8 Lead Bonding 50
   3.9 Fire Protection 54

4. Structural Integrity 66
   4.1 Introduction 66
   4.2 Regulations. 67
   4.3 Unbuffered Cask Testing 68
   4.4 Model Cask Testing 85
   4.5 Buffered Casks 91
   4.6 Energy Absorption Properties of Lead and Steel 100
   4.7 Some Useful Formulas in Cask Design 111
   4.8 Design Considerations. 115
   4.9 Tiedowns 118

CONTENTS (contd)

Page

5. Shielding 125
   5.1 Problem 125
   5.2 Regulation 125
   5.3 Comments on Shielding Design 125
   5.4 Comments on Cask Shielding Material 127

6. Contamination 133
   6.1 Problem 133
   6.2 Regulations 133
   6.3 Fission Product Release from Fuels 134

7. Radiolytic Decomposition and Pressure Buildup in Cask Coolants . . 136

8. Accidents. 138
   8.1 Accident Analyses 138
   8.2 Hazards Analyses of Shipping Casks 140

Acknowledgments 141

Appendix 1. Regulations Applying to the Transport of Radioactive Materials 142

Appendix 2 145

Appendix 3 146

References 147

Distribution 155

A GUIDE TO THE DESIGN OF SHIPPING CASKS FOR THE TRANSPORTATION OF RADIOACTIVE MATERIAL

L. B. Shappert

ABSTRACT

The design of shipping casks for the transportation of radioactive material is governed not only by the physical properties of the source material but also by regulations which place particular limits on internal temperatures, cask structural integrity, surface dose rates, etc. To date, most regulations are still in the formative stage since it is quite difficult to translate desirable performance specifications into cask design specifications; this is particularly true in the area of cask structural integrity.

This guide discusses the proposed regulations along with the latest available data concerning criticality, heat transfer, structural integrity, shielding, and contamination of shipping casks.

1. INTRODUCTION

Since electricity is now being produced in private nuclear reactors and, further, the first private fuel-processing plant has been authorized and will be in operation around 1966, private industry will soon be involved in the shipping of spent fuel from the reactors to the processing plant(s). Prior to the influx of numerous spent fuel shipments, a number of agencies (such as the Atomic Energy Commission, the Interstate Commerce Commission, etc.) have proposed regulations which will, when accepted, govern such shipments in the interest of public safety. The technical sections of the proposed AEC document [Code of Federal

Regulations (CFR) Title 10, Parts 71 and 72] are noted in Table 1.1.*

Table 1.1. Technical Sections

Criticality
Heat Removal
Cask Structural Integrity
Shielding
Cask External Contamination

In order to determine the reasonableness of certain parts in these sections, the U.S. Atomic Energy Commission has supported both experimental and theoretical studies at the Oak Ridge National Laboratory and elsewhere. At ORNL, experimental work has been done on cask structural integrity, cask heat transfer, and fire protection on isotope shipping containers; and theoretical studies have been made on problems of criticality control during spent-fuel shipping.

Du Pont has supported both theoretical and experimental investigations of criticality and structural integrity, in addition to studies on fire protection of large shipping casks. General Electric (Hanford) has built and impact-tested models of buffered isotope shipping casks and, in addition, have made extensive investigations of basic criticality data. The Franklin Institute of Philadelphia has investigated the possibility and reliability of impact-testing exact scale models of casks to determine the effect of impact on the prototype. Other sites, notably Dow Chemical Company (Rocky Flats Plant), Western Electric Company (Sandia Laboratory), and the University of Texas, have programs on impact testing. Underwriters Laboratories have tested shipping casks in a fire. A number of workers

*The AEC regulations covering transportation of irradiated fuel elements discussed in this paper refer to those published in the Federal Register on September 23, 1961, for comment. However, in recent meetings at the AEC Headquarters (November, 1964), revised drafts of CFR Title 10 Parts 71 and 72 were discussed. It is expected that additional revisions will be made as a result of these meetings and another draft will be published in the near future in the Federal Register for comment. A list of most other regulations applicable to the shipment of radioactive material is given in Appendix 1.

have investigated accident probabilities with particular emphasis on truck shipments. The British have spent much time and effort fruitfully in these same areas, with particular emphasis on impact and fire testing.

This report is an attempt to summarize those data which have been developed to date and to present them in a form most useful to those faced with designing and fabricating and/or using casks for irradiated nuclear fuel shipping. In general, data on those parts of the regulations which appear to be most difficult to meet have been stressed; however, an appraisal of all parts of the code has been attempted. Each section contains, first, a short statement of the problems involved in the particular regulation; secondly, a summary of the applicable section of the proposed regulation (CFR Title 10, Parts 71 and 72); and finally, a discussion of design; fabrication and operational methods most likely to result in acceptable cask design.

This paper should be considered a status report since more information is being developed as a result of the numerous testing programs, and many regulations pertaining to radioactive-material shipments have not yet been approved by the appropriate governing bodies.

2. EVALUATION OF CRITICALITY AND NUCLEAR SAFETY

2.1 Problem

When the shipment of fissile material is contemplated, the hazard of accidental criticality while in transit must be carefully studied. If the quantity of ^{235}U to be shipped is less than 350 grams, no criticality hazard exists even if the material is in solution form. The recommended masses for safely handling ^{233}U and ^{239}Pu are 250 g and 220 g, respectively.[1] Larger quantities may be shipped with little criticality hazard if the fissile material (plus any moderator which could become accidentally associated with the material) has the proper form, enrichment, and geometry. The most comprehensive source of critical parameters available may be found in ref. 2.

If the fissile material is in the form of fuel elements, economics normally compel one to consider transport of as many elements per cask as possible. The hazards of such a shipment must be closely examined. Information presented in Sect. 2.3 indicate methods of criticality control which are useful in the shipment of large quantities of fissile material, including the effect that particular variables have on the criticality of a system. With such shipments, the effective multiplication constant for the system in question must be determined either by calculational and/or experimental methods. Nuclear codes, discussed in Sect. 2.5, are available to compute such basic nuclear constants of a particular system. Critical experiments are discussed in Sect. 2.4. Methods of reactivity verification, including the results of two such experiments, are noted in Sect. 2.5.

It may be generally assumed that the criticality hazard of spent-fuel shipments may be successfully controlled with the use of fixed poisons to the extent that heat transfer and not criticality will limit the number of elements to be shipped per cask.

2.2 Regulations

Conditions to be used in the control and evaluation of criticality during the shipment of spent fuel elements, taken from the proposed Code

of Federal Regulations, Title 10, Part 72, are discussed below:

1. The number of fuel elements in a single cask must not exceed 75% of the number required to obtain criticality under conditions specified below, or the effective neutron multiplication constant, k_{eff}, does not exceed 0.9 under the same conditions.
2. For calculational and/or experimental purposes, it must be assumed that water is distributed in and around the cask so as to cause maximum reactivity of the system in question.

   The purpose is to ensure that accidental inleakage, or submergence of the cask in water, would not cause the system to become critical. In addition, if more than trace quantities of beryllium, graphite, or heavy water are expected to be present, further evaluation is required.
3. If reactivity decreases with irradiation, the fuel elements should be considered unirradiated. If reactivity increases with irradiation, then the fuel elements should be considered irradiated to the condition of maximum reactivity.
4. The fuel elements should be considered to be in their most reactive array, unless the proposed spacing will assure less than the maximum reactivity and the fuel elements cannot be rearranged into a more reactive form by, for example, structural damage.
5. Structural materials, including spacers, cask components, and neutron poisons intentionally built into cask components or fuel elements, may be considered if their effectiveness as neutron poisons cannot be reduced by structural damage; by melting of the fuel or neutron poison; or by other mechanisms either under normal conditions of transport or in the event of an accident.
6. Each cask and each shipment, whether including one or more casks, shall be examined for neutron interaction between

casks or other shipments of special nuclear material on the vehicle at the point of origin, trans-shipment, or delivery.

The ability to comply with these standards requires a complete analysis of the cask and fuel combination and an evaluation of k_{eff} under the most adverse conditions. Methods of achieving this analysis and control of criticality are discussed in the following paragraphs.

2.3 Methods of Criticality Control

Two methods of criticality control that are normally considered for spent fuel elements are (fissile) mass restriction and the inclusion of fixed poisons in the shipping cask. The utility of either of these methods in maintaining a subcritical configuration must be considered in the light of the effect of lead, steel, or water reflection and moderation, and the interaction of the cask with other casks containing fissile material. Normally, the most practical of these methods is the inclusion of fixed poisons.

2.3.1 Mass Restriction

When a shipping cask is designed, the configuration and composition of the fuel element usually have been set. The cask cavity is then designed around the shape and size of the element. During the preliminary cask design, a number of different fuel-element loadings normally are considered, and the effect of moderators and reflectors on the loadings is examined. Water is normally assumed to be present except when other moderators, i.e. graphite, are shipped with the fuel.

At some point, as the number of elements in the cavity is increased, criticality might be achieved if the elements were optimally spaced and were water-moderated and reflected. Any number less than this minimum allows excessive leakage of neutrons from the array and criticality cannot be achieved. The proposed regulations noted previously allow 75% of this critical number to be shipped.

Mass restriction can be an important method for criticality control in shipments of research reactor-type fuel whose total decay heat output is not excessive, and whose critical mass constitutes an appreciable

number of elements. For example, a minimum of 15 fresh, 168-gram ^{235}U fuel elements of the MTR type (Materials Testing Reactor) are required to attain criticality under water in the most optimum spacing.[3] Thus, eleven elements could be shipped in one cask with little concern for criticality. The cask should, however, be evaluated for possible interaction with other units of fissionable material.

2.3.2 Fixed Poisons

A neutron poison can be used in a cask to increase the amount of fissile material transported at one time and still keep the effective multiplication constant below 0.9. Poisons that are normally considered are those that have a high macroscopic absorption cross section for thermal neutrons and are relatively inexpensive, such as boron and cadmium. The boron may be fabricated in an aluminum matrix (Boral) or incorporated in stainless steel. Cadmium sheets are normally bonded between aluminum or steel for mechanical support and containment. The arrangement of the poison is quite important and, to be most effective, should be distributed, as much as possible, uniformly throughout the cask.

In special cases, it might be necessary for the poison to be accompanied by a moderator. Moderators that are normally considered are paraffin, water, and concrete.

An example of a cask which requires the use of fixed poisons is an annular solution carrier which has been used to transport uranyl (^{233}U) nitrate (see Fig. 2.1). The annular vessel has a solution thickness of 2 in., a volume of 175 liters, and is covered with a 30-mil-thick cadmium sheet which is "black" to thermal neutrons but "transparent" to fast neutrons. Fast neutrons that diffuse out of the vessel and become moderated in the paraffin or concrete cannot return. The cask was tested prior to shipment with 225 g/liter ^{233}U solution and was found to be quite unreactive.

A second example of a cask which uses a neutron poison to prevent criticality is the BMI-1 shipping cask[4] designed to transport 24 irradiated MTR type fuel elements (Fig. 2.2). The cask, weighing 23,000 lb when fully loaded, contains two identical baskets, one on top the other,

ORNL-LR-DWG 50865AR1

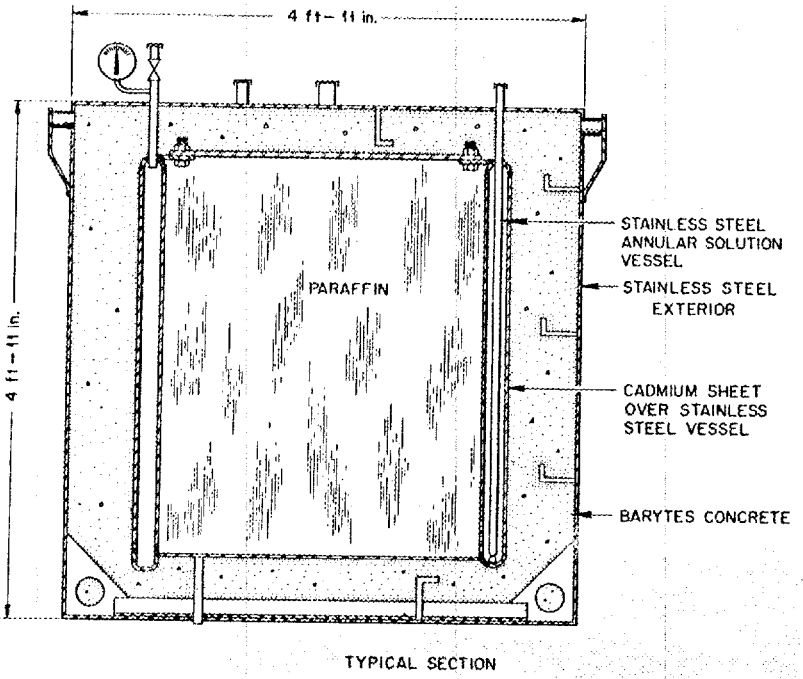

Fig. 2.1. Annular Uranyl Nitrate Solution Carrier.

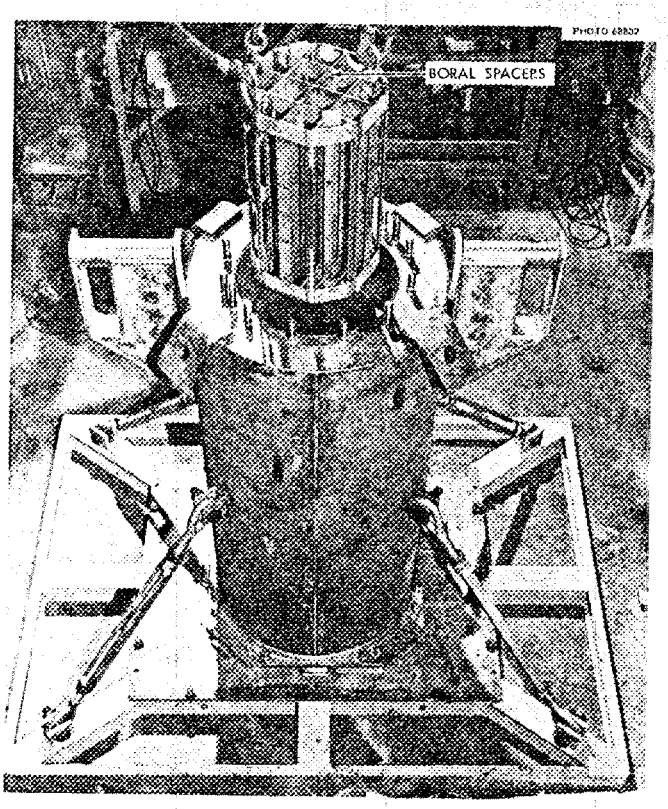

Fig. 2.2. BMI-1 Shipping Cask with One Fuel Basket Removed.

which provide both positioning stability and a neutron poison for the fuel. The central divider plates are constructed of Boral; the outside surfaces are open with the fuel elements constrained by angle irons on the corners to facilitate radiation heat transfer during dry shipment.

Another cask which employs a fixed poison to control criticality was designed by the National Lead Company (Model NL-BF-MTR-775) to be used for transporting MTR-type fuel elements. The geometry of the fuel array is roughly that of a right circular cylinder, 22-1/2 in. in diameter by 27 in. long with five 1/4-in. Boral plates dividing the fuel elements into six compartments, each 3-1/8-in. wide (see Fig. 2.3). The subcriticality of this cask containing both fresh and irradiated fuel has been experimentally checked and is described in Sect. 2.5.2.

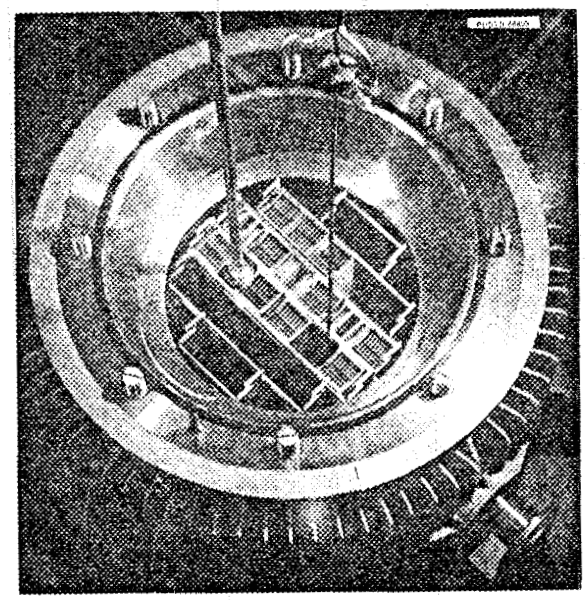

Fig. 2.3. National Lead Company Shipping Cask for Research and Test Reactor Fuels, Partially Loaded with Plate-Type Fuel Elements.

The poison in a cask should be checked periodically to ensure its effectiveness; such an instrument is described by Anthony[5] and consists of a small neutron source and a detector attached to a forked probe. The source is placed on one side of a divider plate, which is underwater, while the detector is on the other side. A meter indicates, in relative units, the number of neutrons striking the detector. The device was tested on a cadmium plate, and voids with a diameter as small as 1-1/4 in.

were easily detected.

Additional data are available in which heterogeneous poisons, such as steel rods, copper, Boral, and boron steel-plate partitions, have been used to poison highly enriched homogeneous systems.[6,7]

2.4 Selected and Correlated Critical Data

Normally, the critical mass of ^{235}U, in mixtures of ^{235}U and ^{238}U, is minimized when it is mixed homogeneously with a moderator.[1] Uranium containing up to approximately 5% of ^{235}U is an exception. The minimum critical mass under these conditions may be obtained by lumping the fuel in rods or slugs and arranging them in a lattice. This is due to the fact that epithermal neutrons are easily trapped in the ^{238}U resonance structure when the fuel and moderator are intimately mixed. When the fuel is lumped, the neutrons have a higher probability of becoming thermalized in the moderator, thus escaping the ^{238}U resonances.

Critical data which have been calculated by Brown for slightly enriched (1.03 to 5.0%) uranium rods moderated in light water are presented below.[8]

Figure 2.4 shows the minimum critical mass produced with the optimum rod spacing and moderation as a function of rod enrichment. (The minimum critical mass was calculated in a spherical geometry and is, therefore, conservative for all other geometries.) Figure 2.5 cross-plots the minimum critical mass as a function of uranium enrichment and is extended above 5% enrichment based on homogeneous systems.[2] Thus, if the mass of uranium to be shipped is less than the minimum critical for the enrichment and conditions noted in Figs. 2.4 or 2.5, the system would be subcritical in light water. It is recommended that if Figs. 2.4 and 2.5 are used to determine the amount of ^{235}U that can be shipped in one container, a safety factor of 45% be applied to the mass as read from the graphs. These curves are valid if the uranium is in the oxide or metal form.

It is often desirable to make shipments which contain masses greater than the minimum critical as noted in Figs. 2.4 and 2.5, such as in the case of reactor fuel elements. If the geometry of the fuel in a shipment is such that excess neutron leakage occurs at the surface of the array

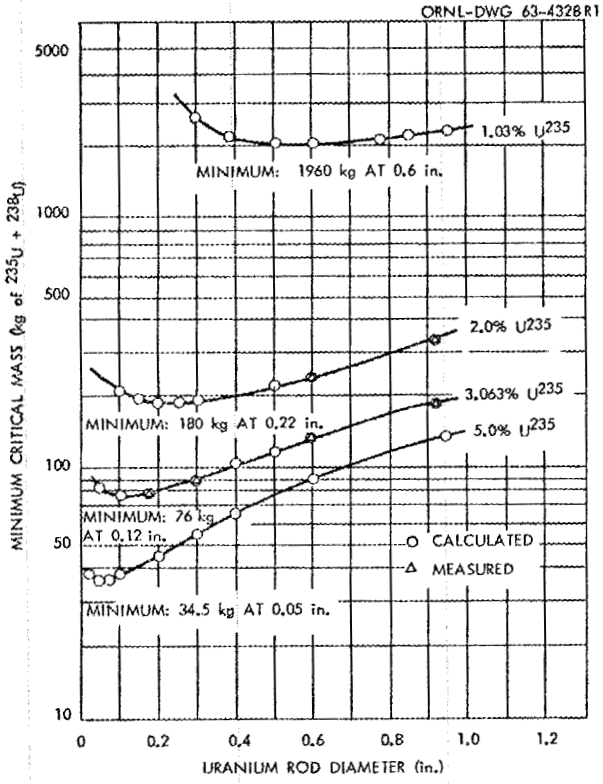

Fig. 2.4. Minimum Critical Mass of Total Uranium as a Function of Uranium Rod Diameter for Uranium Rods in Light Water. (No safety factor included.)

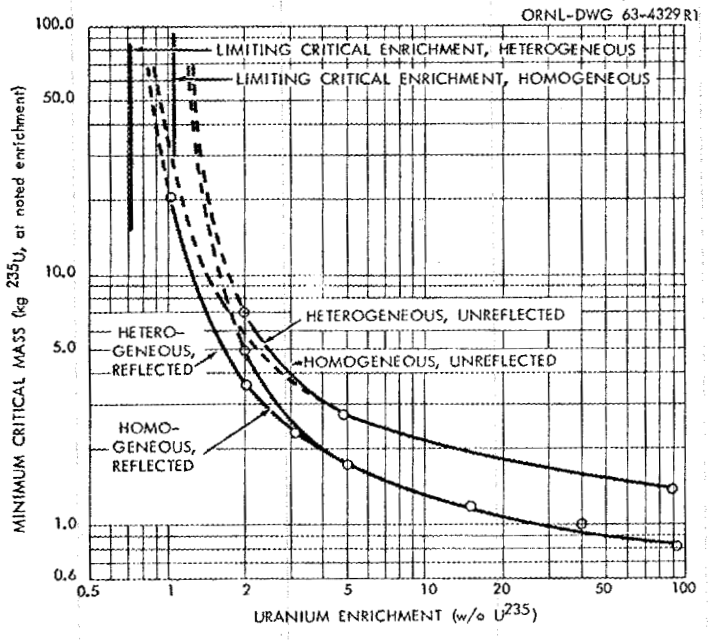

Fig. 2.5. Minimum Critical Mass of ^{235}U for Heterogeneous and Homogeneous Uranium-Water Systems as a Function of ^{235}U Enrichment. (No safety factor included.)

(assuming optimum conditions of light water moderation and reflection), criticality cannot be achieved and the shipment may be safely made without resorting to neutron poisons. This is more likely to be the case when shipping unirradiated fuel, since the individual elements may be separated by larger distances without incurring a weight penalty as would be the case if the elements were shielded.

Two useful parameters in establishing nuclear safety limits for fuel elements in arrays are (a) the minimum critical mass of uranium required in a unit of area to be critical in light water and (b) the minimum critical mass of uranium required per unit of length to be critical in light water. The former parameter is shown in Fig. 2.6 for uranium rods up to 5% enriched, and the latter is shown in Fig. 2.7 for both uranium up to 93% enriched and 93% enriched UO_2 in a mixture of UO_2-ThO_2 in light water. The use of Figs. 2.6 and 2.7 can best be illustrated by an example.

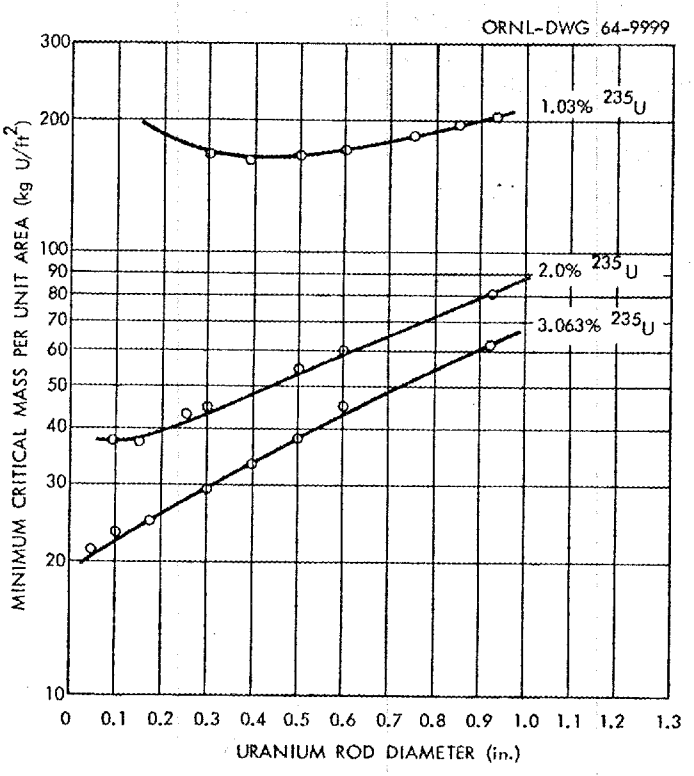

Fig. 2.6. Minimum Critical Mass Per Unit Area as a Function of Uranium Rod Diameter for Uranium Rods in Light Water.

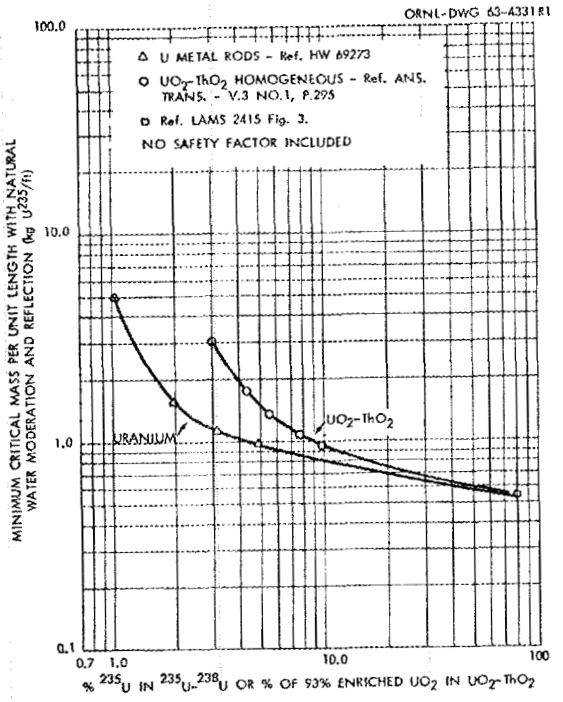

Fig. 2.7. Minimum Critical Mass Per Foot as a Function of ^{235}U Enrichment.

Problem 2.1. Employing both Figs. 2.6 and 2.7, determine the number of unirradiated EGCR fuel elements that may be safely shipped in one vehicle. Some of the fuel element specifications are given in Table 2.1.

Table 2.1. EGCR Fuel Element Specifications

Type	7-pin cluster
Dimensions	3.155-in. diameter by 28.27 in. long
Active length	26.625 in.
Kg uranium per element	8.70 kg
Enrichment	2.46%
Kg ^{235}U/element	0.214 kg
Fuel pellet diameter	0.707 in.

Solution: From Fig. 2.6, the minimum critical mass per unit area for this fuel enrichment and pellet diameter is 55 kg/ft^2; since

$$(55\ kg/ft^2)/(8.70\ kg/element) = 6.34\ elements/ft^2\ ,$$

then an infinite plane array containing 6.34 $elements/ft^2$ would just achieve criticality if flooded and reflected with light water. The regulations permit a shipment of 75% of this critical number; thus it is possible to ship a plane array of EGCR fuel elements containing 4.75 $elements/ft^2$ and remain subcritical under all flooding conditions.

In order to use Fig. 2.7, the kilograms of ^{235}U per foot of active length of fuel element must be known. For the EGCR element, this value is

$$0.214\ kg\ ^{235}U/2.22\ ft\ of\ element = 0.0965\ kg\ ^{235}U/ft\text{-}element\ .$$

For an enrichment of 2.46%, the minimum critical mass of uranium per unit length from Fig. 2.7 is 1.23 kg $^{235}U/ft$. Therefore,

$$(1.23\ kg\ ^{235}U/ft)/(0.0965\ kg\ ^{235}U/ft\text{-}element) = 12.75\ elements\ .$$

Based on this result, a 9-element array (75% of 12.75, rounded off) of unirradiated fuel may be stored or shipped without criticality problems.

It should be pointed out that since this calculation is based on an uranium content per foot of length, the 9-element array may be any length; therefore, as many EGCR elements as necessary may be stacked vertically, so long as the array does not exceed 9 vertical rows of elements.

These calculations are conservative and somewhat restrictive; if it is required only to ship a limited number of elements in one vehicle, the results may be adequate. If, however, a large number of elements must be shipped in one vehicle and the required geometry cannot be guaranteed, then additional criticality calculations must be made. Such calculations are discussed in Sect. 2.5.

2.4.1 Research Type Reactors

Critical experiments have been made utilizing Oak Ridge Research Reactor (ORR) and Bulk Shielding Facility (BSF) fuel elements.[9] These elements are the MTR plate type, clad in aluminum, and normally contain between 140 and 200 grams of 93% enriched uranium per element.

The elements were arranged in approximately square arrays, one element high, and the spacing between the elements was varied. The results are shown in Fig. 2.8 and Table 2.2 in terms of the critical number of fuel elements as a function of the distance between locating bosses. (The locating bosses are mounted on the end boxes of the elements and extend laterally on all four sides.) These distances can be converted to plate-to-plate spacing by adding 0.44 in. to the distances between bosses parallel to the fuel plates and 0.164 in. to the distance between bosses perpendicular to the plates. (See Table 2.2)

The optimum spacing of these elements is about 0.2 in., which corresponds to an H/U atom ratio of 370. This is approximately the same ratio that is associated with the minimum critical mass of other fuel elements of this same general type (e.g. 10 plate elements with 15- or 20-mil aluminum cladding).

The increase in the number of ORR elements required for criticality, as the spacing between elements increases (see Fig. 2.8) indicates that an infinite array of these elements spaced 1-1/2 in. apart probably would be subcritical.

In other experiments utilizing this plate-type fuel element,[9] the effect of placing 20-mil-thick cadmium sheets between rows of closely

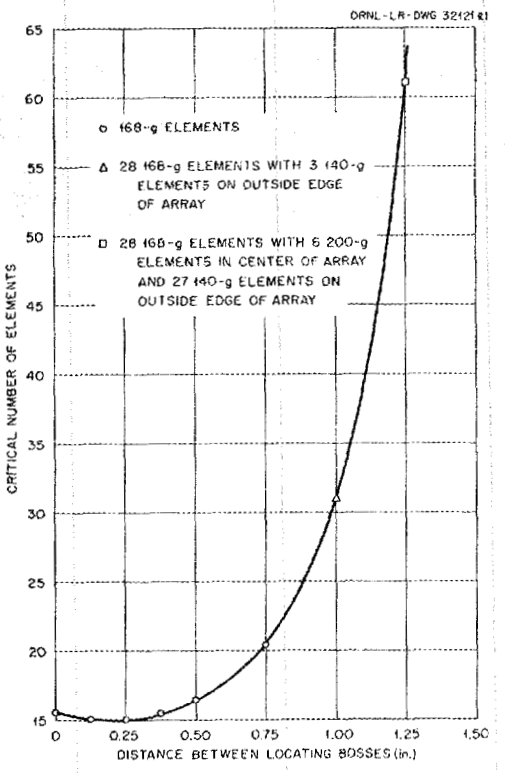

Fig. 2.8. Critical Number of ORR Fuel Elements in Approximately Square Arrays in Water as a Function of the Distance Between Locating Bosses.

Table 2.2. Critical Number of ORR Fuel Elements in Approximately Square Arrays in Water

Distance Between Locating Bosses (in.)			
Bosses Parallel to Fuel Plates	Bosses Perpendicular to Fuel Plates	Approximate Critical Array	Approximate Critical Mass (g of ^{235}U)
0	0	15-1/2 168-g elements	2575
1/8	1/8	15 168-g elements	2510
1/4	1/4	15 168-g elements	2515
3/8	3/8	15-1/2 168-g elements	2575
1/2	1/2	16-1/2 168-g elements	2775
3/4	3/4	20-1/2 168-g elements	3450
1	1	28 168-g elements 3 140-g elements[a]	5200
1-1/4	1-1/4	28 168-g elements 6 200-g elements[b] 27 140-g elements	9575
1/8	3/16	15 168-g elements	2510
0	1/8	15 168-g elements	2510
0	1/4	15 168-g elements	2505
0	3/8	15 168-g elements	2520
0	1/2	15-1/4 168-g elements	2550
1/8	0	15-1/4 168-g elements	2540
1/4	0	15-1/4 168-g elements	2545
0	0	12 168-g elements 4 140-g elements[c]	2575
0	0	13 168-g elements 3 140-g elements[b]	2622
0	0	18-3/4 140-g elements	2615
0	0	13 200-g elements	2620

[a]On outside edge of array.

[b]In center of array.

[c]Dispersed throughout array.

packed elements in water was investigated. The elements were arranged in an 11-by-12 array and had an average loading of 160 g ^{235}U per element. There was no appreciable multiplication of source neutrons noted.

2.5 Methods of Reactivity Analysis

The shipment of fissile material requires an accurate estimation of criticality hazard involved under the most adverse conditions. In the case of the shipment of fuel elements, the conditions that are normally postulated are that fresh fuel (or fuel in its most reactive condition) becomes moderated and reflected with light water distributed in and around the cask. (For a more complete description of required conditions, see Sect. 2.2.)

The most reliable information concerning the criticality hazard of a system containing a specific arrangement of fissile material and moderator can be obtained by performing critical experiments on the fuel in question under the conditions of interest.

A second source of information may be available from critical experiments which have been performed on fuel elements that closely resemble the elements in question. Also for some specific cases, nuclear safety may be based upon published critical data such as that presented in Sect. 2.4.

Multigroup machine calculations often can be used to predict the reactivity of a specific fuel and shipment. If appropriate, critical experiments have not been made, this may be the only method available. Such machine calculations should be used to predict known results of critical experiments using fuel that resembles, as closely as possible, the fuel under consideration, as a check on the calculational method.

The reason this check is so important is that it is sometimes difficult to obtain reliable cross-section data for the core material. If the code with its cross sections can be used to predict known effective multiplication constants in particular experiments, then a higher degree of confidence is achieved in a prediction of other similar fuel arrangements.

There are a number of multigroup reactor codes available which can be used to calculate k_{eff} for the fuel and cask in question. A partial listing is given in Table 2.3.

Table 2.3. Available Codes

Code Name	Type	No. of gps.	No. of Dimensions	Reference
CURE	Diffusion	No restriction	2	KAPL 1724
EQUIPOISE-2	Diffusion	4	2	ORNL-CF-60-11-67
MODRIC	Diffusion	50	1	K-1520
PDQ	Diffusion	few	2	WAPD-TM-179
DSN	Transport	No restriction	1	LAMS-2346
SNG	Transport	No restriction	1	LASL T-1-159
TDC	Transport	No restriction	2	LAMS-2346

Often two of these codes can be combined and utilized more effectively together than by themselves. For example, MODRIC is a one-dimensional 50-group code but has the ability to accept a predetermined axial buckling. If the axial buckling is not included, or if it is not accurately known (as will probably be the case), then the code computes the parameters as if the fuel were infinitely long. This will be conservative, but may be acceptable. If not, MODRIC, a diffusion code, may be used to determine weighted constants (cross sections and diffusion constants) for a few energy groups, which, in turn, can be used in a two-dimension, few-group transport code, such as EQUIPOISE, PDQ, or TDC. An example of this method, which has the advantage of obtaining greater accuracy for shorter computing times and smaller costs, is presented in Sect. 2.5.1.

The availability of nuclear codes is noted in Appendix 2.

2.5.1 Comparison of Calculated and Measured Critical Data for a Simulated N.S. Savannah Core

Critical experiments called "Marty II" and "Marty III" have been performed on 4% enriched UO_2 fuel elements arranged in a core similar to that of the N.S. Savannah.[10] These experiments utilized 16 fuel elements instead of the 32 elements contained in the prototype core and were used to compare the critical water heights of a stainless-steel egg-crate core

(Marty II) to that of an aluminum egg-crate core (Marty III) for a variety of control rod patterns.

The multiplication factors of these systems were measured. An attempt was then made to predict these multiplication factors utilizing machine codes and a four-group analytical model.[11]

A desire to account for the two dimensional aspects of the N.S. Savannah core led to the use of the PDQ code, which is a 2-dimensional diffusion-theory code limited to four or less energy groups. The full-group capabilities of the code were utilized to handle the strong absorption properties of the core I control rods.

Strongly absorbing regions, such as control rods, can be represented in the PDQ code by a current-per-unit-flux-boundary condition at the surface of the absorbing region. To obtain realistic transport-theory values for the control-rod boundary conditions, the one-dimensional SNG transport-theory code was employed.[12] The SNG code also served to obtain reaction rates throughout the strongly absorbing UO_2 fuel region where, again, diffusion theory was not expected to apply. The resulting analytical model was thus a combination of one-dimensional transport-theory and two-dimensional diffusion-theory codes.

The calculated results are compared with experimental results in Fig. 2.9.

ORNL-LR-DWG 52970R3

	MARTY II		MARTY III	
ROD PATTERN	k_d EXP	k_s CALC	k_d EXP	k_s CALC
	1.043 ± 0.001	1.055	1.16 ± 0.02	1.180
	1.024 ± 0.001	1.030	1.13 ± 0.02	1.148
	1.0011 ± 0.0001	1.000	1.09 ± 0.01	1.099
	1.013 ± 0.001	1.021	1.11 ± 0.01	1.126

Fig. 2.9. Comparison of Calculated and Experimental Multiplication Factors in Marty II and Marty III Critical Experiment.

The expression k_d refers to the experimentally measured "dynamic" multiplication factor while k_s refers to the calculated "static" multiplication factor.[13] (The "dynamic" multiplication factor implies that k_{eff} is different than one, i.e., the reactor is on a period, and the delayed neutron groups have a different effective lifetime than when the reactor is "static" or not on a period. Most calculations assume a delayed neutron lifetime equal to that of the static system, and as $|k_{eff}-1|$ becomes larger, this assumption becomes less valid.

A comparison of the experimentally measured and the calculated values of k (see Fig. 2.9) are in close agreement. This method of analysis may be applied to poisoned arrays of this fuel which are to be transported in shipping casks, to estimate how far such an array is from becoming critical under the conditions specified in the regulations.

2.5.2 Neutron Multiplication Measurements

A practical method for determining the reactivity of a particular system is by making multiplication measurements on the system. Such measurements may be made prior to cask design to determine critical parameters that could effect the design or after cask design and fabrication to verify calculations.

Such measurements are made by adding fuel elements to a subcritical array (which includes a neutron source) and monitoring the neutron flux or count rate. The relative multiplication factor, M, may be determined by comparing the count rate with the fuel present to count rate with no fuel (just the neutron source) present.

The inverse of the neutron multiplication factor (1/M) can then be plotted as the ordinate against the number of elements (or the mass of fissionable material), which gives that particular value of M, and the curve may be extrapolated to the point where 1/M is equal to zero ($M \rightarrow \infty$) to determine the number of elements required to make the system critical. If the system is highly poisoned, the extrapolation may indicate an infinite number of elements would not produce criticality. The closer the experimental system gets to criticality, the more accurate the extrapolation will be.

This method is quite useful in indicating the subcriticality of a specific system, but multiplication measurements made under one set of conditions cannot be applied to a second set of conditions; measurements must be repeated.

Such experiments can be carried out both in the shipping cask and in the laboratory. Recently, clean Experimental Gas Cooled Reactor (EGCR) fuel assemblies were tested to determine the maximum reactivity for a particular loading which might be expected during shipment of the elements.[14] A total of 28 fuel assemblies were available for the test. The assemblies, each of which consisted of a cluster of seven stainless-steel tubes containing UO_2 pellets fastened into a graphite sleeve, were placed on a triangular pitch in a stainless-steel tank, and the system was flooded with water (see Fig. 2.10).

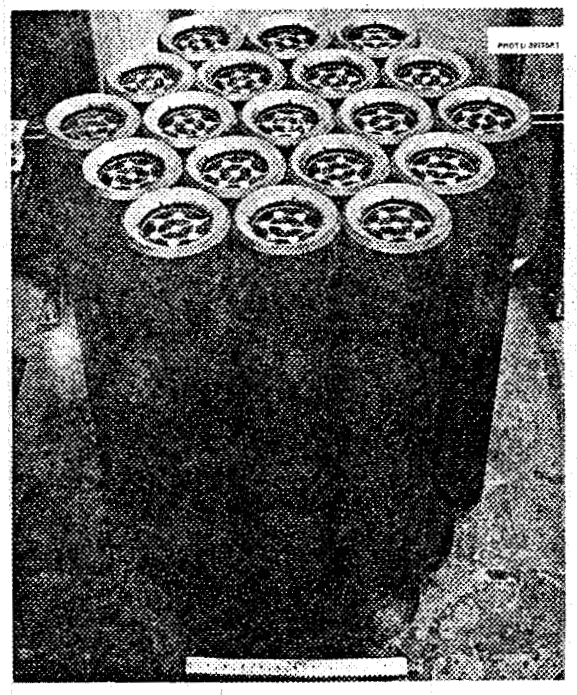

Fig. 2.10. Typical EGCR Fuel Element Arrangement.

Spacing between the assemblies was varied, but the most reactive arrangement was with the graphite sleeves touching each other. The reciprocal neutron multiplication curve is shown in Fig. 2.11. It was concluded that as few as 40 assemblies might be made critical when reflected and moderated by water, but the exact number is uncertain due

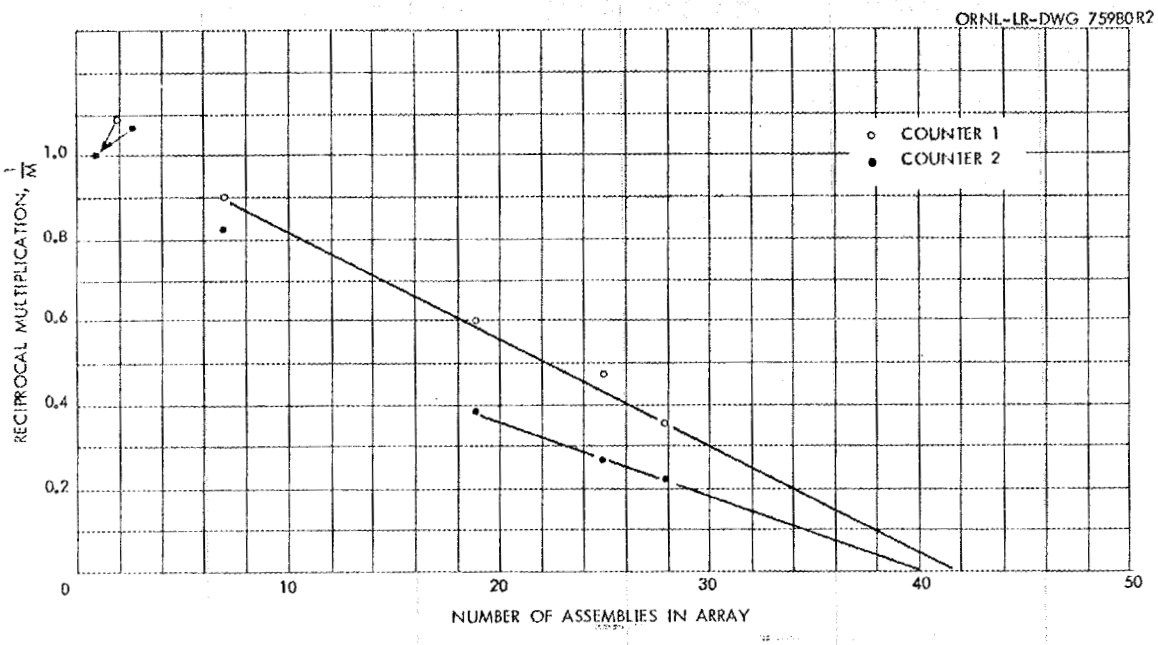

Fig. 2.11. Reciprocal Neutron Multiplication Curve for EGCR Fuel Assemblies in Close-Packed Triangular Lattice, Water-Moderated and Reflected.

to the long extrapolation. In any case, 28 elements under the conditions specified cannot be made critical.

A second example of using multiplication measurements to experimentally investigate the criticality hazard of a shipment of fuel elements was demonstrated when National Lead Company made such measurements as various MTR type fuel elements were loaded into their Model NL-BF-MTR-775 cask.[15] (This cask is described in Sect. 2.3.2.)

The reciprocal multiplication curve (Fig. 2.12), carried to the capacity of the cask (28 elements), indicates shipments of the elements and loadings tested would be safe and that criticality would not be possible with this general fuel-poison geometry.

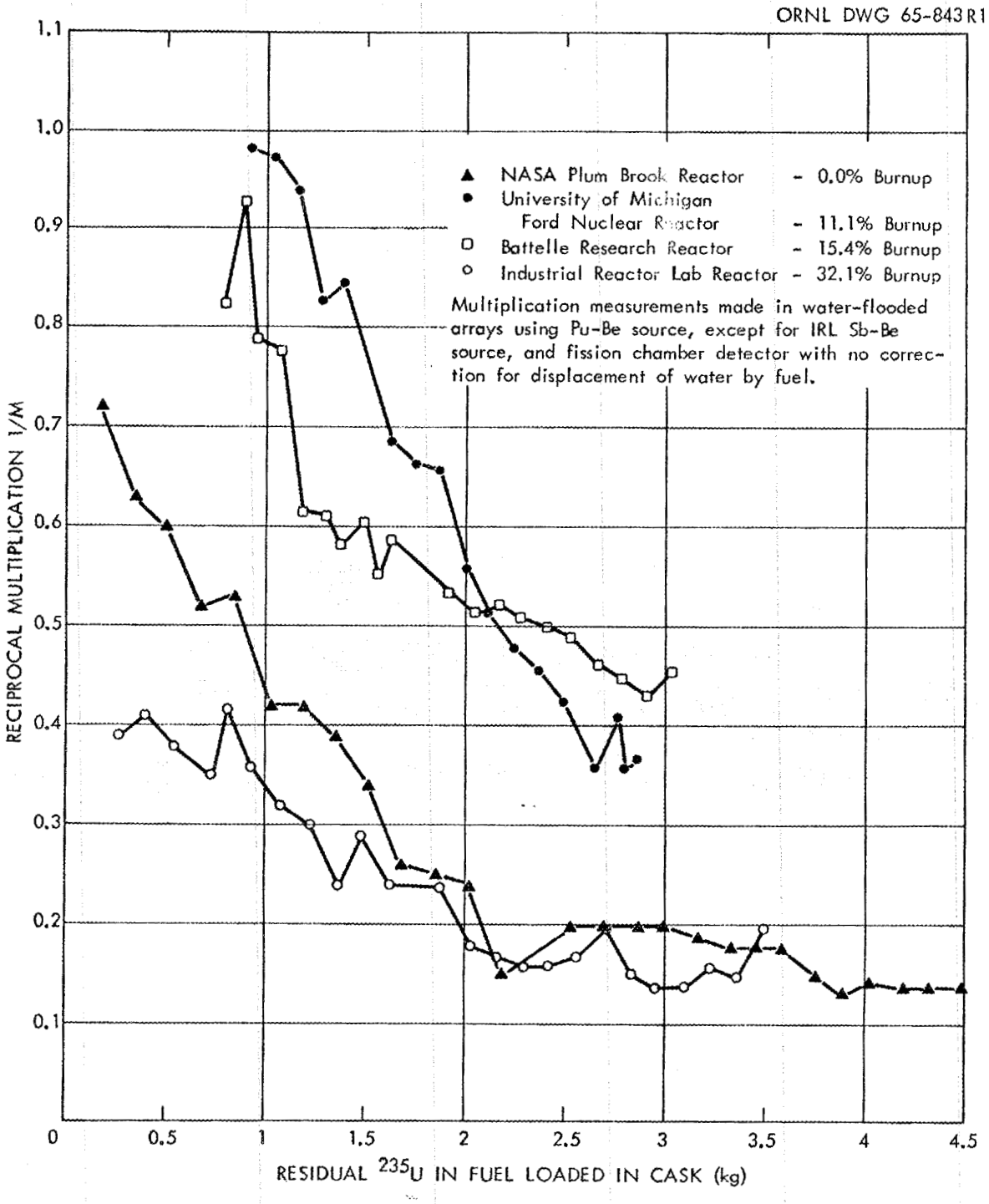

Fig. 2.12. Reciprocal Multiplication Curves for Various MTR-Type Fuel Elements in a Cask.

3. HEAT TRANSFER

3.1 Problem

It is necessary that the temperature throughout a cask that is used to transport irradiated fuel elements be kept within certain predetermined limits during shipment; excessive temperatures in the cavity could cause structural failure of the fuel element cladding. A fuel element is considered failed if fission products can leak into the primary coolant and contaminate the cask interior. (Section 6.2 presents acceptable limits on the contamination of the primary coolant.) Fuel that is expected to release excessive fission products into the cask cavity (which may include unclad fuel) should be canned prior to shipment.

The most probable cause of fuel element failure during shipment is overheating due to inadequate heat removal. High temperature weakens the cladding of the fuel and causes increased internal pressure of gaseous fission products.

The heat load that the cask must dissipate occurs primarily from fission product decay and, to a lesser extent, solar heating. Heat removal from the cask may be by forced or natural circulation of a coolant through or around the cask. If liquid is used as a coolant, then hazards analysis must examine the consequences of a loss of the liquid to determine whether or not the resulting fuel temperatures would be excessive.

3.2 Regulations

The temperature of any easily accessible cask surface should not exceed 180°F. The temperature of the fuel elements and fixed poisons inside the cask should be kept below their failure temperature, even under accident conditions. The proposed maximum temperature limit for the hottest element, under normal conditions, in the cask is (a) 300°F, (b) the fuel operating temperature in the reactor, or (c) 300°F below the failure temperature, whichever is greater. Under accident conditions, the temperature should go no higher than 200°F below the failure temperature. Limit (c) implies an experimental determination while limits (a) and (b) should be known.

Failure temperature is defined as the minimum temperature at which one cask, full of initially sound fuel elements, will, within 48 hours, release to the primary coolant 100 curies of beta-gamma or one curie of alpha radioactivity.

Primary gaseous or liquid coolants, i.e., coolants which are in contact with the fuel, must not be circulated outside of the shielding of the cask. The temperature of any liquid primary coolant must remain 20°F below its boiling point at the anticipated operating pressure of the cask.

The intent of these regulations is to prevent the release of radioactive material, particularly in a mobile form, such as a gas or aerosol. Attention should be paid particularly to the amount of radioactive iodine in the fuel at the time of shipment, since it could constitute a serious biological hazard should it escape.

All temperatures calculated for the contents of the cask should assume an ambient air temperature of 100°F and the maximum solar heat load anticipated during the shipment.

3.3 Heat Removal from Fuel Elements

Heat is normally removed from spent fuel elements by either of two schemes. The first and simplest is to allow air to remain in the cavity, contacting both the elements and the inner cask wall. Heat is transferred from the elements to the wall by natural convection of the air and by radiation. The heat is then conducted through the cask shield and dissipated to the atmosphere by natural convection and radiation. This is generally the least efficient, but safest, method of heat removal since it is unlikely that the air could be accidently replaced by a less effective coolant.

A second scheme that is usually considered is that of filling the cask cavity with water. Heat transfer from the fuel to the cask walls by the water will be almost entirely by convection, and the fuel element temperatures will be lower than if air was used as a coolant. The heat is then conducted through the shielding and dissipated in the same manner as described in the previous paragraph.

A modification of this method is to force-circulate a secondary

coolant, e.g., water, through the cask cavity (which would contact the primary coolant and not the fuel itself) and dissipate the heat from an air-cooled radiator outside of the cask. Much greater amounts of heat may be dissipated in this way, but any mechanical method of heat removal should have a back-up system. If the primary and back-up systems become inoperative, or the liquid coolant completely leaks away (a possible result of a severe accident), the heat must still be removed without allowing the fuel to fail due to excessive temperatures.

3.4 Heat Sources

3.4.1 Fission Products

Two sources of heat which should be considered in determining the maximum temperature of the spent fuel in the cask are the fission products in the fuel and the solar heat absorbed by the cask. The former source normally has the largest effect on the temperature distribution throughout the cask.

The amount of decay heat produced from ^{235}U fuel may be estimated from Fig. 3.1 (ref. 16). The ordinate, P_s/P_o, is the ratio of decay power to operating power. The abscissa is the decay time and the parametric curves, the operating time.

Problem 3.1. Determine the amount of decay heat produced from an element that had operated for 1 year in a reactor at a power level of 1 Mw per element and was removed and cooled 120 days.

Solution:

$$T_o = 365 \text{ days}$$
$$T_s = 120 \text{ days}$$
$$P_o = 1{,}000{,}000 \text{ watts per element}$$

From Fig. 3.1

$$P_s/P_o = 5.4 \times 10^{-4}$$

Hence, for one element

$$P_s = (P_s/P_o)(P_o) = (5.4 \times 10^{-4})(1{,}000{,}000) = 540 \text{ watts}$$

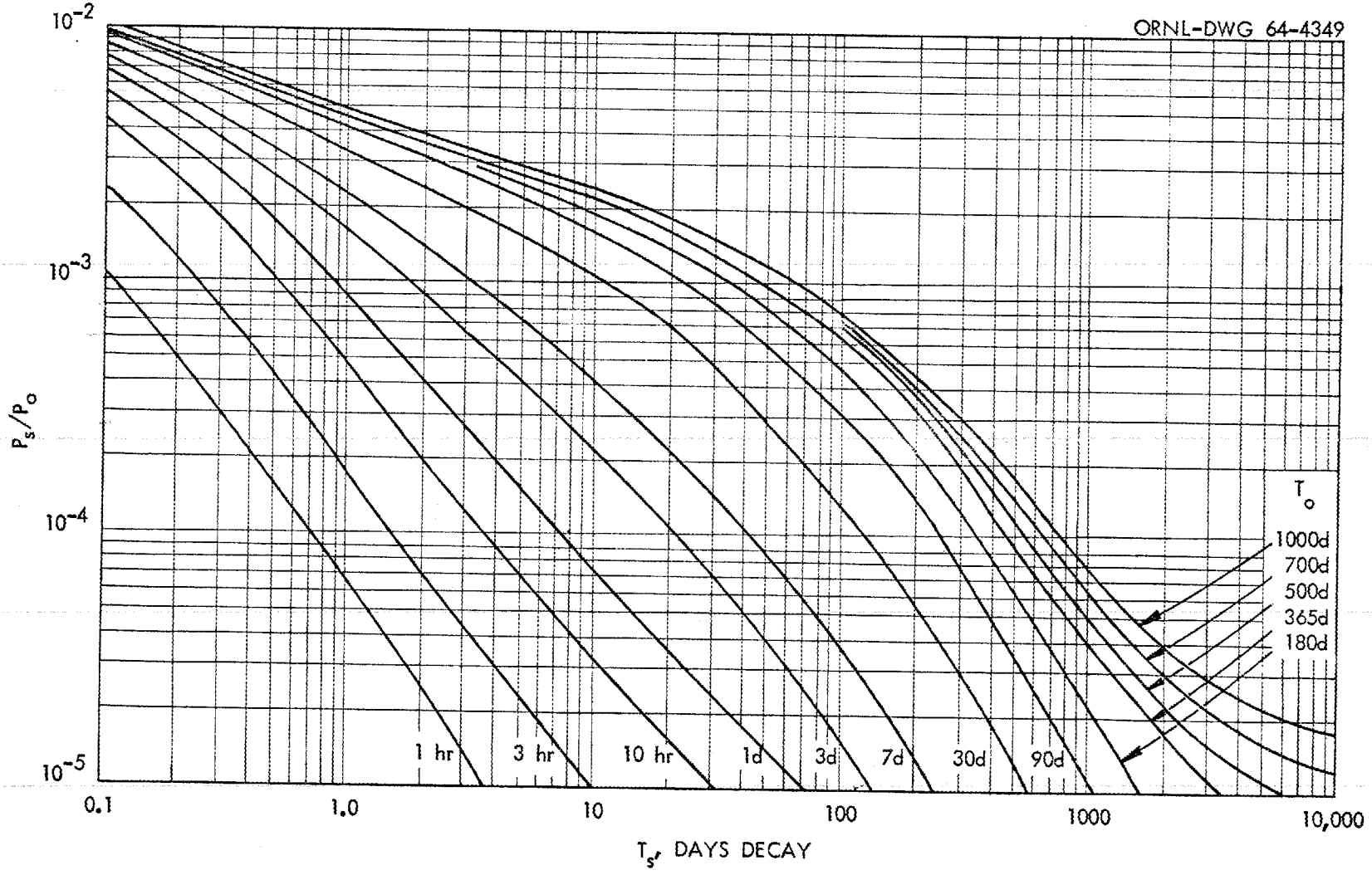

Fig. 3.1. Decay Heat, P_s from ^{235}U Fuel as a Function of Operating Power, P_o, Operating Time, T_o, and Decay Time, T_s.

3.4.2 Solar Radiation

The rate at which the earth intercepts solar energy on a surface normal to the sun's rays at a point above the earth's atmosphere is 442 Btu/hr-ft^2; this value is known as the solar constant.[17] The amount of solar radiation received at a point on the surface of the earth on a clear day when the sun is at the zenith varies with a mean value of 70% generally considered sufficiently accurate for engineering purposes.

Total solar radiation is made up of both direct radiation from the sun and diffuse or scattered solar radiation. On clear days, the fraction of scattered radiation is a function of the sun's position and varies from about 16% of the direct solar radiation, if the sun is directly overhead, to about 130%, if the sun is very low in the sky.[18]

Figure 3.2 indicates that Q_{si} is the total amount of incident solar and diffuse radiation as a function of time of day falling on horizontal and vertical surfaces at a latitude of 42°N at the summer solstice.[19]

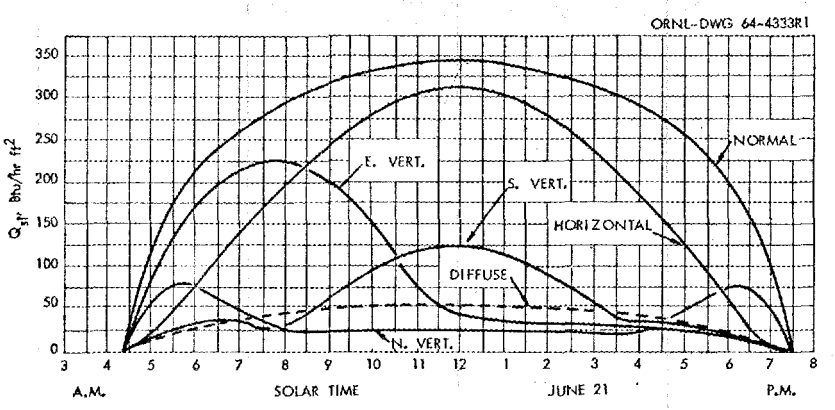

Fig. 3.2. Incident Solar Energy on Clear Days, Latitude 42°N.

The curves marked N. VERT., S. VERT., and E. VERT. indicate the total amount of solar plus scattered radiation received by vertical surfaces facing north, south, and east, respectively. The solar energy received by a vertical west wall may be considered as the reverse of that given for E. VERT. The curves marked horizontal and normal indicate the solar energy received by a horizontal surface and a surface that is always normal to the sun's rays.

All curves include the contribution of diffuse radiation to the total

heat load; the diffuse radiation for a horizontal surface is also separately noted in Fig. 3.2.

To determine the heat load affecting the surface, the incident heating value, Q_{si}, given in Fig. 3.2 must be multiplied by the absorptivity (emissivity), ϵ_{solar}, of that surface. Thus, $Q_{solar} = Q_{si}\epsilon_{solar}$. It is important to remember that the absorptivity (emissivity) on a surface is a function of the wave length of the radiation, and there may be a significant difference between the values obtained from the literature for low-temperature sources (100 to 2500°F) and for the sun. Table 3.1 presents the emissivities of various surfaces as a function of wave length or average temperature.

Note that for most polished metals, the emissivity (absorptivity) of the surface is higher when exposed to solar radiation than if the surface is exposed to lower temperatures or longer wave-length radiation. There are paints that may be applied to such surfaces to reverse the situation. White zinc-oxide paint has a low value of emissivity at solar-wave lengths (0.18), but at 100°F the emissivity is high (0.95). This is the ideal situation in that a surface freshly painted with zinc-oxide paint would absorb little solar radiation, yet would have a high emissivity at lower operating temperatures.

3.5 Heat Removal from a Cask Surface

Heat transfer from the surface of the cask is normally accomplished through the mechanisms of natural convection and radiation. The former mechanism is usually the most significant with the exception that if the cask were in still air, convective transfer could drop to a point where a significant part of the heat would be transferred by radiation. This is considered the worst condition which might be found in normal transport, and calculations of cask equilibrium temperatures should be based on this assumption.

Convective heat-transfer coefficients are low ($\bar{h}_c$ = 1 to 3), even at large temperature differences in still air. In the case of most large heat-transfer surfaces placed in still air, turbulent air flow probably exists if the vertical heat-transfer height is greater than 2 ft. Assuming that turbulent flow does exist, in which case the significant length of the

Table 3.1. Emmissivities of Surfaces at Various Temperatures Including that Associated with Solar Temperatures

Material	Wave Length and Average Temperature				
	9.3 μ 100 F	5.4 μ 500 F	3.6 μ 1000 F	1.8 μ 2500 F	0.6 μ Solar
Metals					
Aluminum					
Polished	0.04	0.05	0.08	0.19	~0.3
Oxidized	0.11	0.12	0.18		
24-ST weathered	0.4	0.32	0.27		
Surface roofing	0.22				
Anodized (at 1000 F)	0.94	0.42	0.60	0.34	
Chromium					
Polished	0.08	0.17	0.26	0.40	0.49
Iron					
Polished	0.06	0.08	0.13	0.25	0.45
Cast, oxidized	0.63	0.66	0.76		
Galvanized, new	0.23	....	....	0.42	0.46
Galvanized, dirty	0.28	....	....	0.90	0.89
Steel plate, rough	0.94	0.97	0.98		
Stainless Steel					
18-8, polished	0.15	0.18	0.22		
18-8, weathered	0.85	0.85	0.85		
Steel tube					
Oxidized	....	0.80			
Tungsten filament	0.03	....	....	~0.18	
Paints					
Aluminized lacquer	0.65	0.65			
Cream paints	0.95	0.88	0.70	0.42	0.35
Lacquer, black	0.96	0.98			
Lampblack paint	0.96	0.97	....	0.97	0.97
Red paint	0.96	....	....	....	0.74
Yellow paint	0.95	....	0.5	....	0.30
Oil paints (all colors)	~0.94	~[illegible].9			
White (ZnO)	0.95	....	0.91	....	0.18

cask (the vertical height) disappears from the formulas for calculating $\bar{h}_c$, the exact cask dimensions are not necessary to calculate the heat transfer coefficient. Under these conditions, McAdams[20] recommends the simplified dimensional equation (for cylinders or plane surfaces in air under turbulent conditions),

$$\bar{h}_c = C_1 \Delta t^{1/3} \tag{1}$$

where C_1 is assigned the value of 0.19 for vertical planes and cylinders, 0.18 for horizontal cylinders, 0.22 for heated plates facing up, and Δt is the temperature difference between the cask surface and ambient air in degrees F.

The amount of heat lost by radiation depends upon the cask geometry, emissivity, the absolute temperature of the cask and of the radiation receiver, and is given by the formula

$$Q/A = \sigma \, \underline{F}_{12} \, (T_1^4 - T_2^4) \tag{2}$$

where Q is in Btu/hr, A in ft^2, $\sigma = 0.173 \times 10^{-8}$ Btu/ft^2-hr-$°R^4$, $\underline{F}_{12}$ is the grey-body shape factor which can be written $F_A F_E$ (the product of the geometric shape factor, F_A, and grey-body factor, F_E), and T_1 and T_2 are the absolute temperatures of the source and enclosing body, respectively.

It is convenient to determine an equivalent radiant heat-transfer coefficient so that a total heat-transfer coefficient may be computed as follows:

$$h_t = \bar{h}_c + \bar{h}_r \quad . \tag{3}$$

If the heat transferred by radiation can be expressed by the equation

$$Q/A = \bar{h}_r \, (T_1 - T_2) \tag{4}$$

then by equating this to Eq. (2) the effective radiant heat-transfer coefficient may be calculated by

$$\bar{h}_r = \sigma \, \underline{F}_{12} \left[\frac{T_1^4 - T_2^4}{T_1 - T_2} \right] \tag{5}$$

Since, according to Sect. 3.2, the cask surroundings are assumed to be 100°F, a plot of $\bar{h}_r$ vs $T_1 - T_2$ is given in Fig. 3.3, where T_2 is assumed to be 560°R (100°F), and $\underline{F}_{12}$ was assumed equal to ϵ_1, the emissivity of the cask surface.

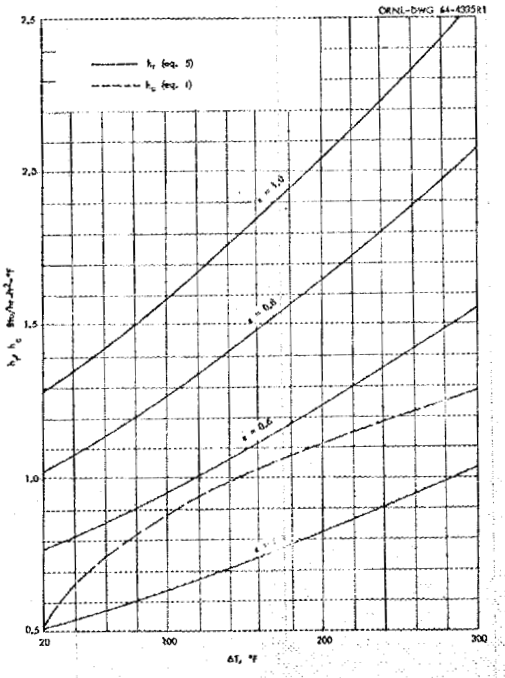

Fig. 3.3. Convective and Radiative Heat Transfer Coefficients as a Function of ΔT.

The cask surface temperature, t_2 (in °F), may be determined from the nomograph shown in Fig. 3.4, which is based on Eqs. (1) and (5). Only the emissivity of the cask surface ϵ and its heat flux Q/A are required to estimate t_2.

The cask temperature is affected by not only the heat flux produced by the radioactive source but also the diurnal solar heat load. The diurnal solar heat load will change the equilibrium temperature of the cask surface and cause it to vary in a cyclic manner throughout the shield. The temperature change on the interior surface of the shield will be damped in magnitude and will lag the temperature change on the cask surface. The situation is complicated by the fact that only part of the cask intercepts the sun's rays, and the heat will be transferred not only radially but also circumferentially to the cooler side.

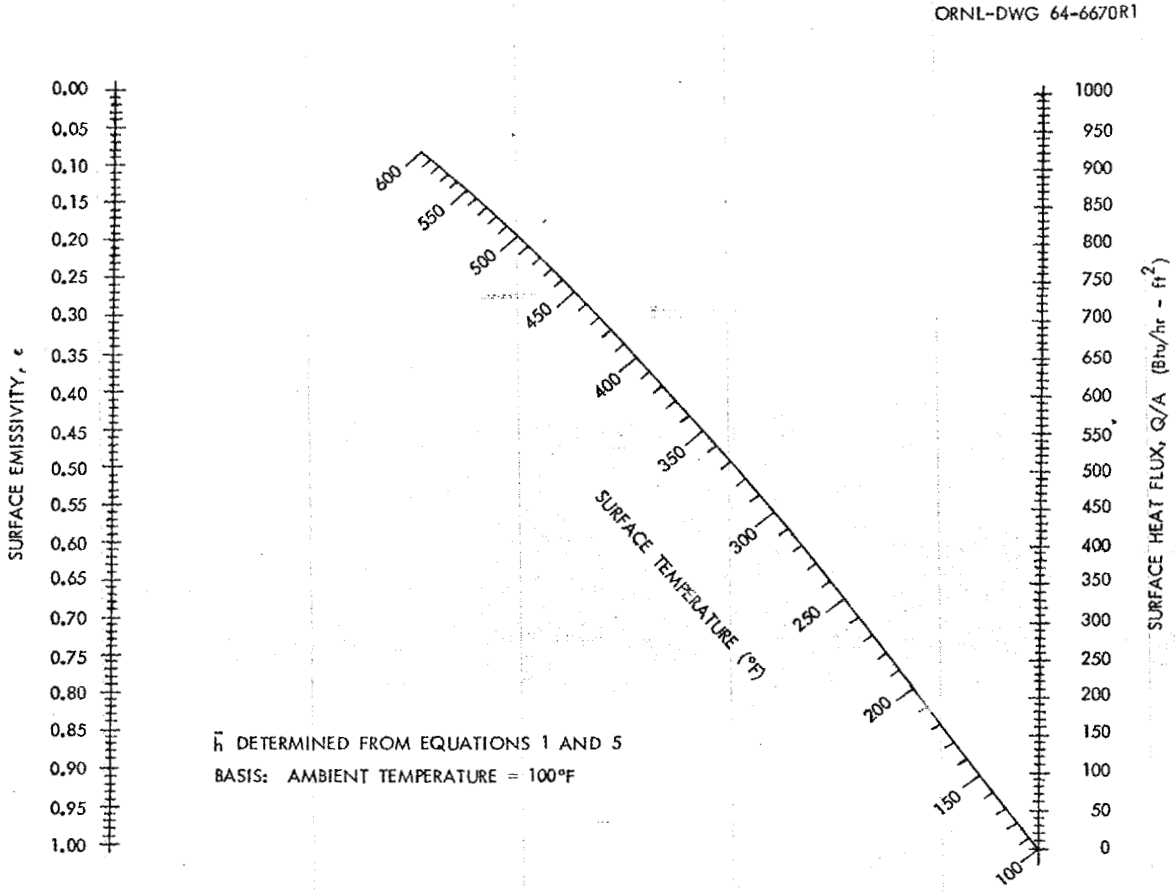

Fig. 3.4. The Cask Surface Temperature in Still Air Based on the Surface Heat Flux and Emissivity.

Figure 3.5, which indicates the increase in temperature of the external cask surface per unit of effective solar heat flux as a function of $\bar{h}$ for several cask sizes, was determined on the supposition that the entire cask surface was exposed to the additional solar heat flux. To calculate the average temperature increase of the cask on this basis would obviously be conservative, although the local temperature increase where the ϕ_{solar} is maximum could approach this value.

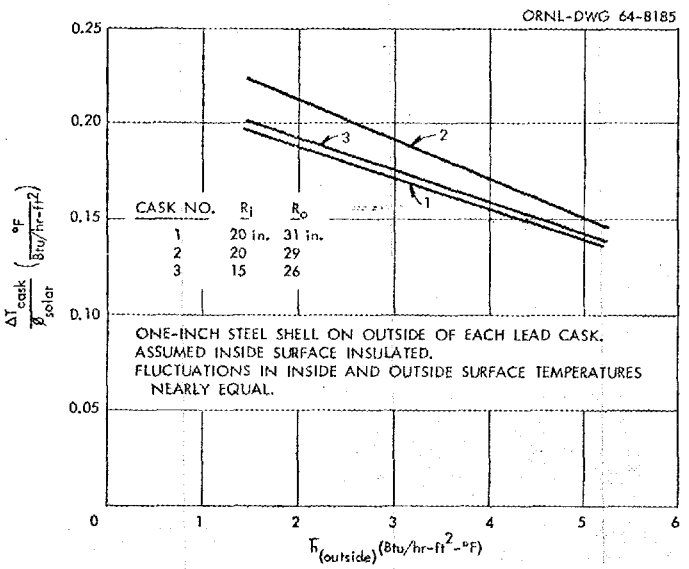

Fig. 3.5. Amplitude Response of Cask Temperatures to Solar Heat Flux of Frequency = 1 Cycle/Day for various Effective Outside Heat Transfer Coefficients.

The mathematical model of the cask, from which Fig. 3.5 was determined,[21] assumed that the temperature gradient at the inside wall was zero. Under these conditions, the temperature rise produced on the inside cask wall was within a few percent of that produced on the outside wall. That is, through 10 in. of lead, little damping occurred. Even though appreciable damping can occur to the temperature fluctuation when the heat is conducted to the cooler side of the cask, it is likely that there is a much smaller circumferential temperature variation around the inside cask wall than the outside. It may, therefore, be reasonable to determine the average inside temperature variation from Fig. 3.5 based on the solar flux averaged over the entire outside surface; the inside temperature fluctuation

determined in this way should give a reasonable approximation to the actual value.

Problem 3.2. A steel-shelled, lead-filled cylindrical cask whose inside and outside radii are 20 in. and 31 in., respectively, has an outside surface heat flux due to its radioactive source of 400 Btu/hr·ft^2. The air temperature is 100°F and the cask is sitting in the summer noonday sun. The emissivity of the cask surface is 0.6. Assuming the maximum solar heat flux is averaged over the entire surface, determine the maximum inside cavity surface temperature increase due to the solar heat load.

Solution. Since $\epsilon = 0.6$ and $Q/A = 400$ Btu/hr·ft^2, then from Fig. 3.4, the surface temperature of the cask from the radioactive source is

$$t_s = 278°F$$

and

$$\bar{h} = \frac{Q/A}{t_s - 100} = \frac{400}{178} = 2.25$$

The maximum effective solar heat flux may be estimated from Fig. 3.2, assuming the cask's longitudinal axis is in an east-west direction. In that case, at noon the sun's rays would be normal to the cask's projected cylindrical surface (i.e., the cask's length times diameter) which is a factor π less than the entire surface area. Since at noon, including diffuse radiation,

$$\phi_{si} = 345 \text{ Btu/hr·ft}^2$$

for a normal surface, then the solar heat flux averaged over the surface is

$$\bar{\phi}_{solar} = \frac{1}{\pi}\phi_{si}\epsilon = \frac{1}{\pi} \times 345 \times 0.6 = 66 \text{ Btu/hr·ft}^2$$

Since

$$\bar{h} = 2.25$$

and from Fig. 3.5

$$\frac{\Delta T}{\phi} = 0.182$$

then

$$\Delta T = (0.182)(66) = 12\,^{\circ}F$$

Approximately this maximum temperature increase would be expected on the inside cavity surface under the conditions specified.

3.5.1 Use of Fins on a Cask

Since the heat load on the cask is normally rejected to the atmosphere from the cask surface, the use of fins on the cask surface will result in lower temperatures throughout the cask. The total surface area of the fins does not, however, dissipate heat with the same efficiency as the cask prime surface. The convective heat transfer coefficient is reduced since the temperature decreases along the fin.

In addition, the effective radiation heat transfer coefficient of the entire cask can also be reduced because one fin may "see" a considerable amount of the adjacent fin which is about the same temperature and the prime surfaces "view" of the surrounding radiation receiver will be partially blocked by fins.

Since the fins generally do not dissipate as much heat per unit area as does the prime surface, it is convenient to determine how efficient the fins are so that a modified total surface area (fins plus the prime surface) may be manipulated as if it were all at the same temperature as the prime surface.

The effective surface area of fins may be determined from the equation

$$A_{eff} = A_{fins}\eta_{eff} \tag{6}$$

The fin efficiency η_{eff} may be evaluated from the equation[22]

$$\eta_{eff} = (\text{Tanh } ML)/ML \tag{7}$$

where

$$M = \sqrt{\frac{2h_t}{kt}} \tag{8}$$

and

$h_t = h_c + h_r'$, the total heat transfer coefficient, Btu/hr-ft^2-°F

$h_r' = (1 - F)\bar{h}_r$, the modified radiation heat transfer coefficient, Btu/hr-ft^2-°F

$\bar{h}_r$ = radiation heat transfer coefficient (Fig. 3.3)

F = view factor for the surface in question

k = the thermal conductivity of the fin material, Btu/hr-ft-°F

t = fin thickness, ft

L = fin width, ft

Since the view factor, F, represents the ineffective area fraction available for radiant heat transfer, $\bar{h}_r$ must be multiplied by (1 - F) to obtain an effective radiation heat transfer coefficient.

The view factor, F, is given for opposed parallel rectangles in Fig. 3.6 and for direct radiation between adjacent rectangles in perpendicular planes in Fig. 3.7 (ref. 23).

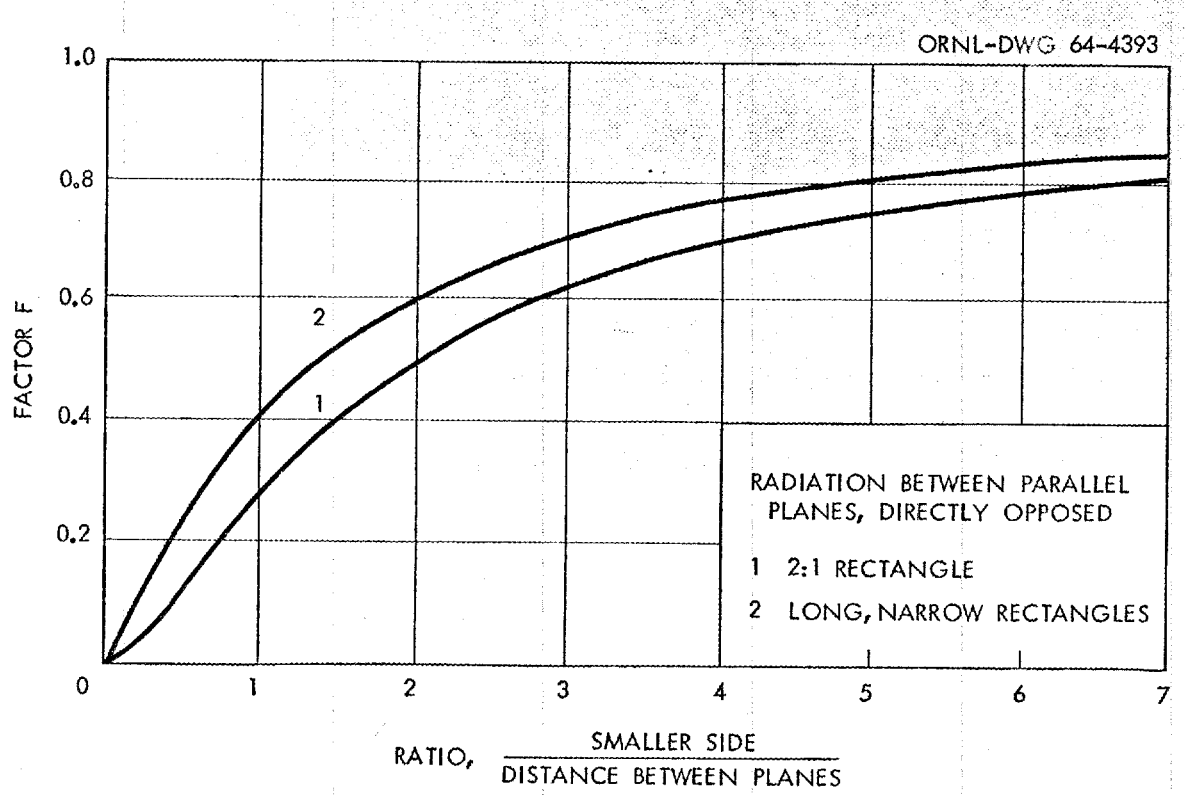

Fig. 3.6. View Factor F for Opposed Rectangles.

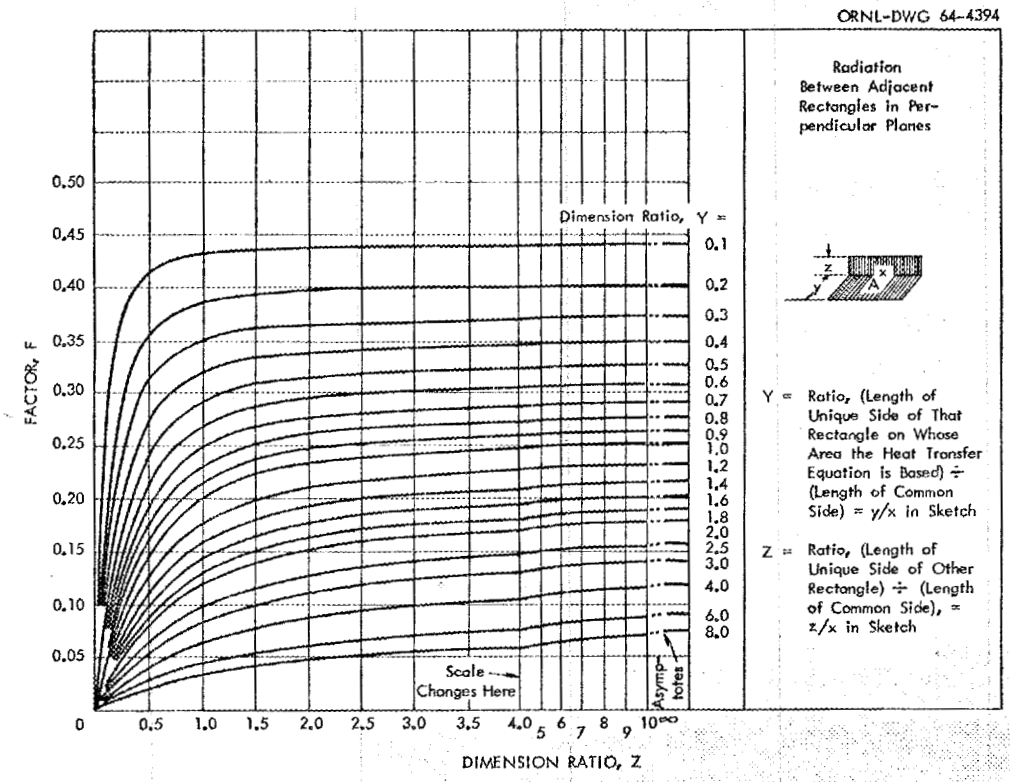

Fig. 3.7. View Factor F for Direct Radiation Between Adjacent Rectangles in Perpendicular Planes.

Problem 3.3. It is necessary to build a steel-shelled, lead-filled shipping cask to transport four spent Yankee Atomic Power Reactor fuel elements which were operated for 417 days and decayed for 100 days. The cylindrical cask, designed to transport the elements vertically, has a 24 in. I.D., a 45 in. O.D., and a height of 150 in. The outer shell is 1-in.-thick stainless steel which has an emmissivity and thermal conductivity of 0.6 and 9 Btu/hr-ft-°F, respectively. Determine the surface temperature of the cask (1) assuming no fins and (2) assuming 1/2-in.-thick fins, 4 in. wide spaced on 3-in. centers, are welded to the surface and run the height of the cask. For simplification, assume that all of the heat is transferred from the cylindrical surface and none from the cask ends.

Specifications of the Yankee fuel are given in Table 3.2.

Table 3.2. Specifications of Yankee Atomic Fuel

Core thermal power	480 mw
Irradiation time (full power days)	417 days
Burnup	8200 Mwd/Mt U
Pins per fuel element	380
Elements per core	76
Length of element	124 inches
Active length	90 inches
Decay time before shipment	100 days

Solution 1. The operating power of an average element may be determined from Table 3.2.

$$P_o = 480 \text{ mw}/75 \text{ elements} = 6.33 \text{ mw/element}$$

Since T_o equals 417 days and T_s equals 100 days, P_s/P_o from Fig. 3.1 is 6.35×10^{-4}. Thus

$$P_s = (P_s/P_o)(P_o) = (6.35 \times 10^{-4})(6.33 \times 10^6 \text{ watts})$$
$$= 4000 \text{ watts} = 13{,}650 \text{ Btu/hr}$$

Neglecting the ends, the cask surface area without fins, A_s, equals:

$$A_s = \pi D_o L = \pi(45)(150) = 21{,}300 \text{ in.}^2 = 148 \text{ ft}^2$$

The decay heat from four average elements, Q, = (4)(13,650) = 54,500 Btu/hr and

$$Q/A_s = 54{,}500/148 = 368 \text{ Btu/hr-ft}^2$$

Since the emissivity $\epsilon = 0.6$, from Fig. 3.4, the surface temperature (assuming an ambient air temperature of 100°F) is

$$170°F + 100°F = 270°F$$

Solution 2. Based on an original square foot of prime surface without fins, the surface area of the fins = (4 fins)(4 + 4 + 0.5)/12 in. = 2.84 ft^2 and the base surface area = 1 ft^2 - (4 fins)(0.5)/12 in. + 0.835 ft^2. Therefore, the total area with fins = 2.84 + 0.835 = 3.675 ft^2/ft^2 of original prime surface.

The efficiency of the fins is given by Eq. (7) and is affected by F, the view factor of the fins and prime surface.

To determine the view factor F, the geometry of the fins must be examined (see Fig. 3.8).

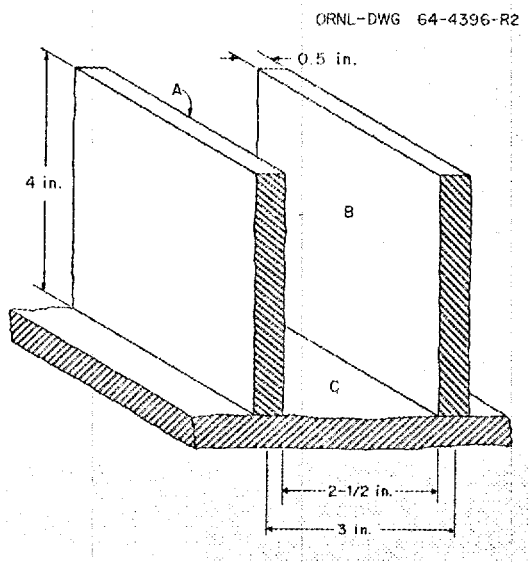

Fig. 3.8. A Schematic Drawing of the Cask Fins.

The view factor F_{ab} for opposed parallel rectangular surfaces A and is given in Fig. 3.6 and depends upon the ratio of fin height to fin spacing; in this case the ratio is

$$4 \text{ in.}/2.5 \text{ in.} = 1.60$$

and

$$F = 0.55 \ .$$

The view factor $F_{ca(cb)}$ for radiation from surface C to surface A (or B) may be determined from Fig. 3.7 and is a function of the ratios of fin height to length (z/x) and fin spacing to length (y/x). In this case, the fins run the length of the cask (150 in.), and the ratios are:

$$z/x = 4/150 = 0.0267$$

$$y/x = 2.5/150 = 0.0167$$

Thus,

$$F_{ca} \text{ (and } F_{cb}) = 0$$

The total view factor is therefore 0.55.

In order to determine $\bar{h}_r$, a trial-and-error approach is necessary. A value of $\bar{h}_r$ is assumed, the cask surface temperature calculated and a re-examination of $\bar{h}_r$ must be made based on the computed Δt; if the error is too great, the process should be repeated.

A reasonable value for $\bar{h}_r$ may be estimated if the assumption is made that the fins are at the same temperature as the prime surface; then Fig. 3.3 and Fig. 3.4 can be used.

The surface area with fins = 3.675 ft^2/original ft^2 of cask surface. The total surface area is, thus, 3.675 x 148 = 544 ft^2. Since Q/A = (54,500 Btu/hr)/545 ft^2 = 100 Btu/hr, the surface temperature t_s determined from Fig. 3.4 (ϵ = 0.6) equals 162°F.

From Fig. 3.3 for a Δt of (162 - 100)°F = 62°F,

$$\bar{h}_r = 0.85$$

$$h_r' = (1 - F)\bar{h}_r = (1 - 0.55)(0.85) = 0.38$$

$$h_c = 0.75$$

and, therefore,

$$h_t = 0.38 + 0.75 = 1.13 \ .$$

Thus, from Eq. (8)

$$M = \sqrt{\frac{2(1.13)}{(9)(0.0417)}} = \sqrt{6.0} = 2.45$$

$$ML = (2.45)(4/12) = 0.82$$

and

$$\eta_{eff} = (\tanh 0.82)/0.82 = 0.675/.82 = 0.82$$

The effective area = (0.82)(2.84) + 0.835 = 2.34 + .835
= 3.14 ft^2/ft^2

of the original cask surface; thus,

the total effective area = (3.14)(148) = 464 ft^2
Q/A = 54,500/464 = 118 Btu/hr-ft^2

From Fig. 3.4, the surface temperature t_s = 170°F

From Fig. 3.3, for a t_s of 170°F (Δt = 70°F),

$$\bar{h}_r = 0.87 \quad \text{(compare with 0.85 assumed)}$$

$$h_c = 0.78 \quad \text{(compare with 0.75 assumed)}$$

The original values of $\bar{h}_r$ and h_c are accurate enough to preclude recalculating t_s.

Thus, the cask surface temperature could be reduced from 270°F to 170°F by the use of fins. Since the fins would lower the surface temperature to below 180°F, it would not be necessary to surround the cask with some protective framework to prevent direct contact by unauthorized persons as required by the regulations noted in Sect. 3.2.

3.6 Heat Conduction Through a Cask Wall

The amount of heat being conducted through the walls of a cylindrical cask is given by

$$Q = \frac{k}{x_2 - x_1} A_{1m} \Delta t \tag{9}$$

where

$$A_{1m} = \frac{A_2 - A_1}{\ln(A_2/A_1)} \tag{10}$$

and A_1 and A_2 refer to the inside and outside surface area, respectively; k, the thermal conductivity of the shield material; x_1 and x_2 the inside and outside radii, respectively; and Δt the temperature difference from the inside to the outside of the shield (Fig. 3.9). The temperature drop across the shield may be estimated from Eq. (9) by assuming no heat is lost through the ends of the cask and by knowing the heat source and the cask dimensions.

It is quite possible that if a cask shield material is lead, an air gap will develop between the lead and the outer steel shell during cask fabrication (see Sect. 3.8). Such a gap will cause a temperature drop across the air film which will, in turn, increase the cavity temperature. If the gap is small, heat transfer will be mainly by conduction, and the temperature drop across it may be computed by the usual method, shown by Eq. (11).

ORNL-DWG 63-4337R1

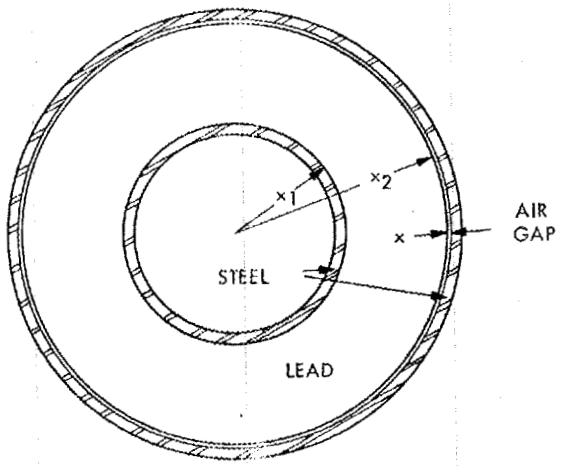

Fig. 3.9. Schematic of Cylindrical Cask.

$$\Delta t = \frac{Qx}{kA_2} \tag{11}$$

where

Q = heat transferred across the film, Btu/hr

x = the thickness of the air film, ft

k = the thermal conductivity of the air at the average temperature, Btu/hr-ft-°F

Problem 3.4. Calculate the inside wall temperature of the finned cask described in problem 3.3. Assume a 1/32-in. air gap between the outer steel shell and the lead. The inner and outer steel shell thicknesses are 1/2 in. and 1 in., respectively, and the cask has 9 in. of lead shielding.

Solution. From problem 3.3,

$$A_1 = \pi D_i L = \pi(25)(150) = 11{,}800 \text{ in.}^2 = 82 \text{ ft}^2$$

$$A_2 = \pi D_o L = \pi(43)(150) = 20{,}300 \text{ in.}^2 = 141 \text{ ft}^2$$

The temperature drop across the outer shell may be calculated as if the shell were a flat plate. In this case, Eq. (11) is applicable and

$$\Delta t = \frac{Qx}{A_2 k}$$

where

$Q = 54{,}500$ Btu/hr

x = the shell thickness, 1/12 ft

$k = 9$ Btu/hr-ft-°F

$$\Delta t = \frac{(54{,}500)(1/12)}{(141)(9)} = 3.6°F$$

The temperature across the air film is calculated in a similar way. The surface area inside of the outer shell, at the air film, is 138 ft^2. The outside surface temperature was computed to be about 170°F (problem 3.3) and k_{air} may be evaluated at somewhat above that temperature, say 200°F.

$$k_{air} = 0.0174 \text{ Btu/hr-ft-°F}$$

and

$$\Delta t = \frac{Qx}{Ak} = \frac{(54{,}500(1/32)}{(138)(0.0174)(12)} = 59°F$$

The temperature drop through the lead shield may be determined from Eq. (9).

$$A_{lm} = \frac{A_2 - A_1}{\ln(A_2/A_1)} = \frac{141 - 82}{\ln(141/82)} = \frac{59}{\ln(1.72)} = 109 \text{ ft}^2$$

Rearranging Eq. (9)

$$\Delta t = \frac{Q(x_2 - x_1)}{k\,A_{lm}}$$

where

$$x_2 - x_1 = 9/12 = 0.75 \text{ ft}$$

$$k = 19 \text{ Btu/hr-ft-°F}$$

$$\Delta t = \frac{(54{,}500)(0.75)}{(19)(109)} = 19.7°F$$

The temperature drop through the inner shell may be calculated from Eq. (11).

$$\Delta t = \frac{(54{,}500)(1/24)}{(82)(9)} = 3.1°F$$

The temperature at the inner cask wall is, therefore:

$$\begin{array}{r} 170 \\ 59 \\ 3.6 \\ 19.7 \\ 3.1 \\ \hline 255\,^{\circ}\mathrm{F} \end{array}$$

Almost 70% of the temperature drop through the shield occurs across the air gap. This emphasizes the importance of a good bond between the lead and outer steel shell in order to keep temperatures in the cavity as low as possible.

3.7 Temperatures in Pin Type Fuel Elements[24]

Most power reactor fuel elements are made up of fuel pins that form a square array. If water is not used as a coolant in the shipment of such elements, the pins would have to lose heat by natural convection to the air circulating in the cask and by radiation of heat from one pin to another. The determination of the maximum pin-cladding temperatures of a large array of pins under such conditions is quite complicated. Therefore, experiments were conducted in order to investigate the more important factors affecting the transfer of heat and to determine if an effective and reasonably accurate method can be found for calculating the maximum temperature in a pin-type fuel element under a given set of conditions.

Stainless-steel tubes with a measured emissivity of 0.55 were electrically heated to simulate the pins of a spent fuel element. These pins, 2 ft long and 0.312 in. in diameter, were nested into 2-by-2-square array modules by use of transite end plates and spaced on 0.68-in. centers (Fig. 3.10). Larger arrays were built up from the modules to a maximum of 64 pins. The four pins of each module were wired in series and heated electrically at various heat inputs in order to cover a wide range of heat fluxes.

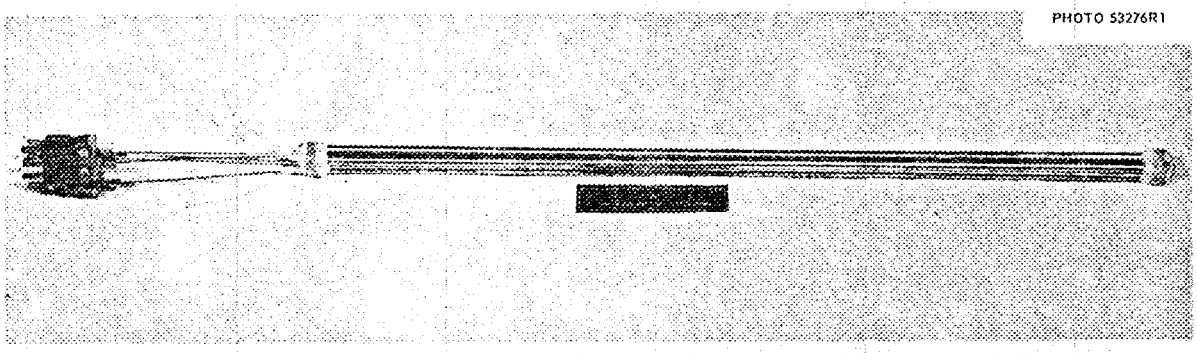

Fig. 3.10. Sub-Bundle of a Mock Reactor Fuel Element.

A model of a fuel bundle, after being assembled from the modules, was then placed into a section of stainless-steel pipe, which simulated the inside shell of a cask (see Fig. 3.11). The resistance of lead shielding to heat flow was simulated by wrapping various thicknesses of of asbestos cloth around the outside of the steel pipe.

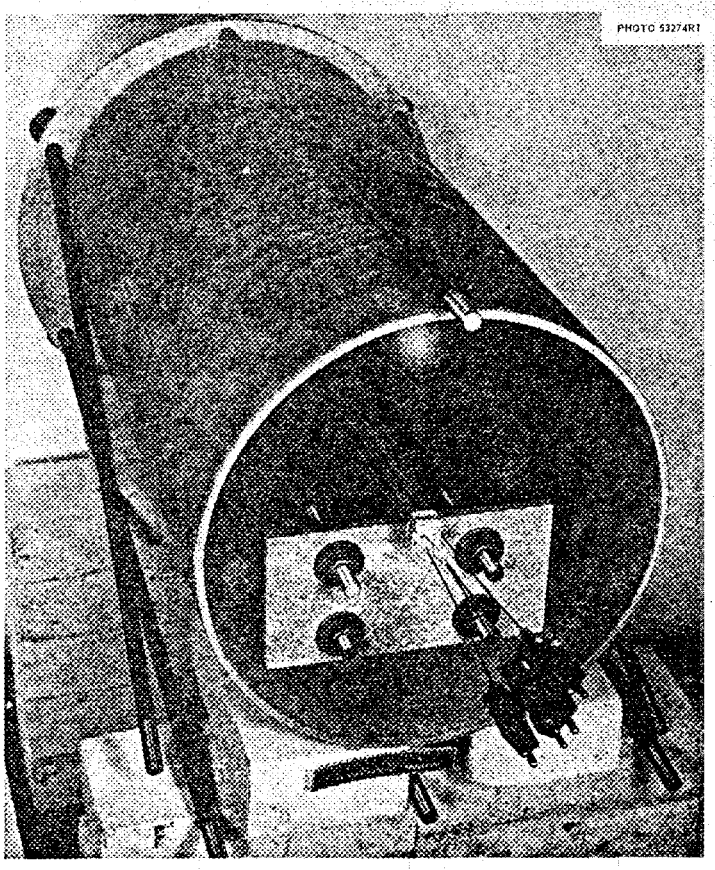

Fig. 3.11. Fuel Sub-Bundle and Container.

The mathematical model used to predict the pin temperatures assumed only radiant heat transfer from pin to pin. This was done because radiation is the controlling mode of heat transfer in a dry, air-filled cask cavity, if the fuel pin temperatures are high, and the mathematics of the model was simplified. Since no attempt was made to account for convection, the results based on radiant heat transfer should be conservative in the sense that the predicted temperature in the center of the bundle would be higher than the measured temperature.

The basic equation that describes the radiant heat flux from surface 1 to surface 2 is of the form

$$\frac{Q}{A_1} = A_2 \underline{F}_{12}\, \sigma(T_1^4 - T_2^4) \tag{12}$$

where

σ = Stefan-Boltzmann constant

T_1, T_2 = absolute temperatures of tubes 1 and 2

Q = net radiation from 1 and 2

A_1, A_2 = areas of 1 and 2

$\underline{F}_{12}$ = radiation factor between 1 and 2

The radiation factor $\underline{F}_{12}$ is a complicated function of the areas, emissivities, and view factors not only for radiation between fuel pins 1 and 2 but between all surfaces of the system. For reasonably high emissivities (0.5 or greater), the factor can be approximated by

$$\underline{F}_{12} = \frac{1}{\frac{1}{F_{12}} + 2\left(\frac{1}{\epsilon} - 1\right)} \tag{13}$$

where

F_{12} = view factor

and

ϵ = the emissivity of all surfaces (assumed to be identical).

This is exact only when 1 and 2 are the only radiating or receiving surfaces.[25] For very low emissivities, the factor can better be estimated by a more complicated procedure.[26]

Since power reactor fuel pins are normally closely spaced, it was assumed that a centrally located fuel pin in a square array would radiate only to four adjacent tubes, four diagonal tubes, and eight other tubes located adjacent to the diagonal tubes. The total heat, Q_i, radiated by a central pin must be totally intercepted by these sixteen tubes (under these assumptions) and may be summed up as follows:

$$Q_i = \sigma A \sum_{j=1}^{16} \frac{T_i^4 - T_j^4}{\frac{1}{F_{ij}} + 2(\frac{1}{\epsilon} - 1)} \tag{14}$$

This equation was written for each tube in a bundle and solved simultaneously in a code for each T_i^4 by a trial-and-error procedure on an IBM-7090 computer. The code is presented in reference 24.

Experiments to verify the calculated temperatures were run with the mocked-up fuel element and cask in a horizontal and vertical position. Heat outputs ranged from 0.002285 to 0.0986 watts per centimeter of tube length. (This compares to the heat output of a Yankee fuel element, described in problem 3.3, of 0.046 watts per centimeter.) Thermocouples inserted into some of the tubes were used to measure tube temperatures. It was assumed that the temperature did not vary around the perimeter of the fuel pin.

Although there were obvious signs of convective heat transfer (the temperatures in the horizontal bundles were not symmetrical about a horizontal plane through the center of the bundle), the predicted temperatures were reasonably close to those measured (see Figs. 3.12, 3.13, and 3.14). Good agreement was obtained in all cases where the temperatures were high (> 200°C) and where the cask fit reasonably tightly around the fuel bundle. In this case, radiation was controlling and convection was reduced to a minimum. These are the conditions under which heat transfer is likely to be a problem in fuel shipping and, therefore, are of most interest.

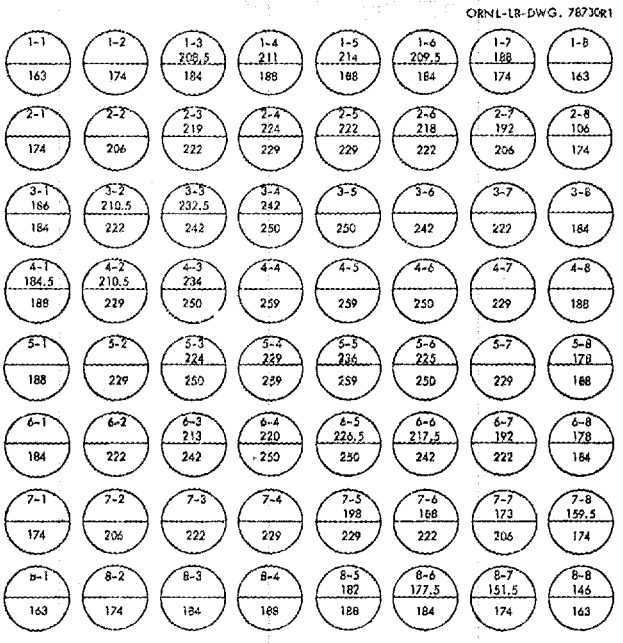

Fig. 3.12. Predicted and Experimental Temperature Distribution in a 64-Tube Bundle, Square Array, Horizontal Position. Predicted temperatures (°C) are shown in the lower half of the circles. Q = 0.0514 w/cm of tube; average cask wall temperature = 79.0°C.

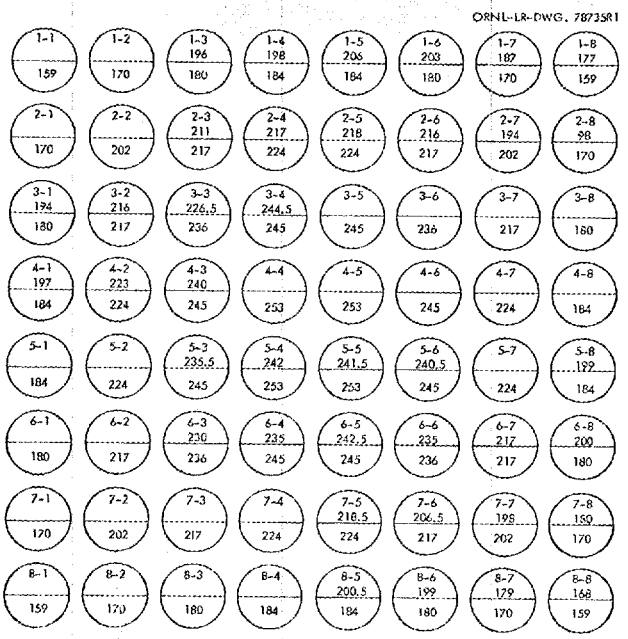

Fig. 3.13. Predicted and Experimental Temperature Distribution in a 64-tube Vertical Bundle at the Midpoint. Predicted temperatures (°C) are shown in the lower half of the circles. Q = 0.04852 w/cm of tube; average cask wall temperature = 79.4°C.

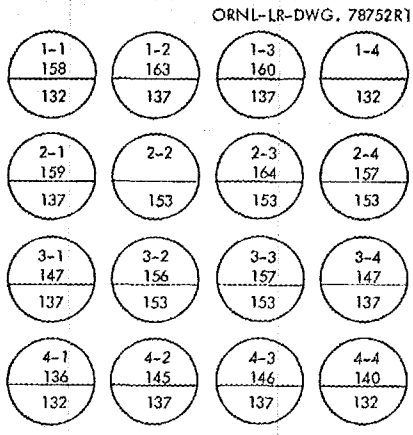

Fig. 3.14. Predicted and Experimental Temperature Distribution in a 16-Tube Bundle, Square Array, Horizontal Position in a 6-in. Cask. Predicted temperatures (°C) are shown in the lower half of the circles. Q = 0.043 w/cm of tube; average cask wall temperature = 70.0°C.

3.8 Lead Bonding

When lead-filled casks are to be used for transporting highly burned short-cooled fuel with large heat generation, it is quite important to obtain as complete a bond between the lead and the steel shells as possible. Without adequate bonding, air gaps between the lead and the outer shell of the cask can develop, which could cause excessive temperatures in the cask cavity (see problem 3.3).

Air gaps are seldom a problem between the inner shell and the lead. A very tight mechanical bond develops there as the lead is cooled during the fabrication process. Such a bond would likely occur even if the inner shell were not tinned prior to lead pouring.

Lead can be bonded more easily to carbon steel than to stainless steel; however, the latter is often more desirable due to its resistance to many decontaminating agents. Therefore, some casks have been designed with a stainless-steel-clad carbon-steel shell to take advantage of both desirable properties.

A number of methods have been used successfully to obtain a good lead-to-steel bond, and most cask fabricators have their own methods. One procedure is to tin the steel surfaces and maintain at least 1/4 in. of liquid flux over the molten lead as it is poured. During the pouring, the cask is kept hot with torches around the level of the lead, and the bottom

portion of the cask is allowed to cool. As the lead in the bottom solidifies and contracts, molten lead from above fills the voids.

Another method, which was successfully used in building the 70-ton casks for Du Pont, entails tinning the steel prior to pouring the lead, pouring the lead, keeping it molten until the cask is completely poured, and then spraying all surfaces of the cask with water.[27] The cooling is rapid and proceeds from the surfaces inward to a point about halfway between the inner and outer steel walls. During the solidification of the lead, liquid lead from above runs into the voids in the center created by the contracting lead.

A third method which has been suggested for producing a good mechanical bond is to use an alloy of lead and bismuth.[28] If enough bismuth is added, the mixture will actually expand, rather than contract, on solidification. However, the melting point of the Pb-Bi alloy is appreciably lower than that of pure lead, and bismuth costs about $2.25 a pound in ton lots as opposed to lead at about 12 cents a pound.

Figure 3.15 shows a section of a small annular container in which a mixture of 55% bismuth and 45% lead was poured around a core of lead to obtain a high-quality mechanical bond between the alloy and steel. Figure 3.16 shows the results of a simple lead pouring in which the walls were tinned and which resulted in an inadequate bond at the outer steel shell.

It is possible to design the cask in such a way that a good bond between the lead and the outer shell is not required for efficient heat removal. Figure 3.17 shows a sectioned cask in which iron fins can be welded to the inside of the outer shell.[29] These fins are made in such a way that they bend and give as the lead expands and contracts under varying heat loads while still maintaining mechanical contact with the lead. This provides a good path for heat to be conducted from the lead to the outer steel shell under all heat loads.

A cask of this design has been built and tested for its heat removal ability.[30] The cask, designed to transport 19 WTR-type fuel elements (Westinghouse Test Reactor), weighs 30,000 lb and will dissipate 7 kw of heat at ambient temperatures of 100°F with the cavity temperature no more than 277°F.

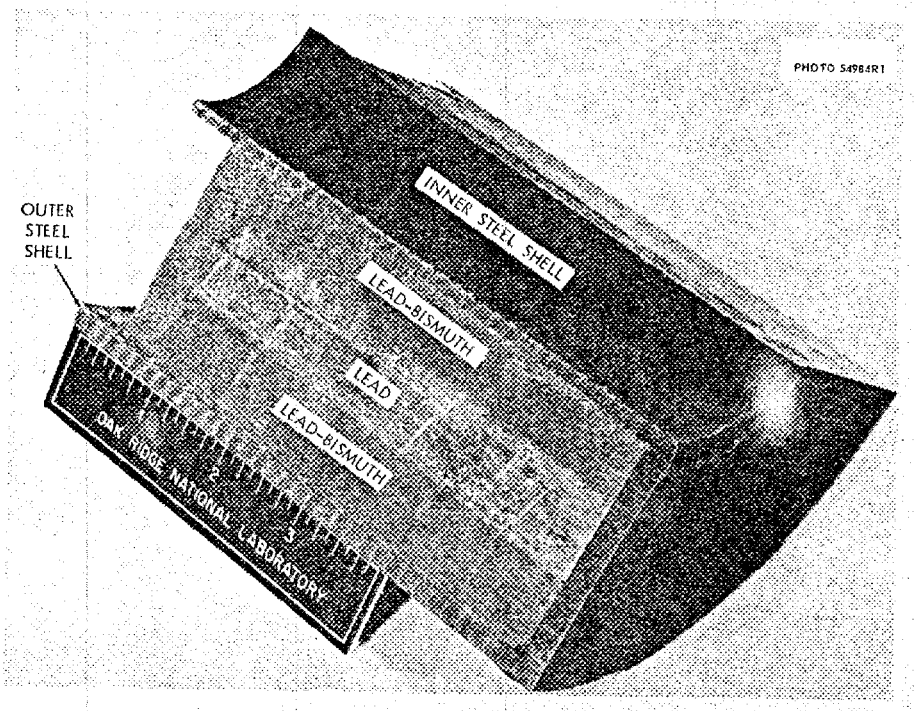

Fig. 3.15. A Sectioned Annular Container with a Good Bond Between the Shielding and Shells.

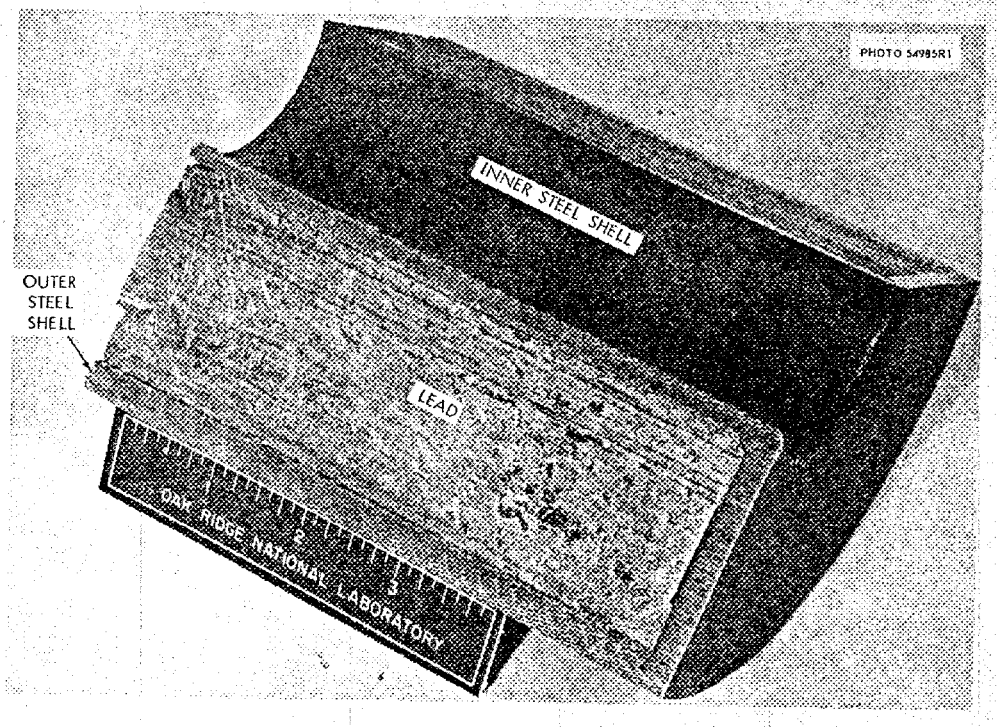

Fig. 3.16. A Sectioned Annular Container with a Poor Bond Between the Shielding and Outer Shell.

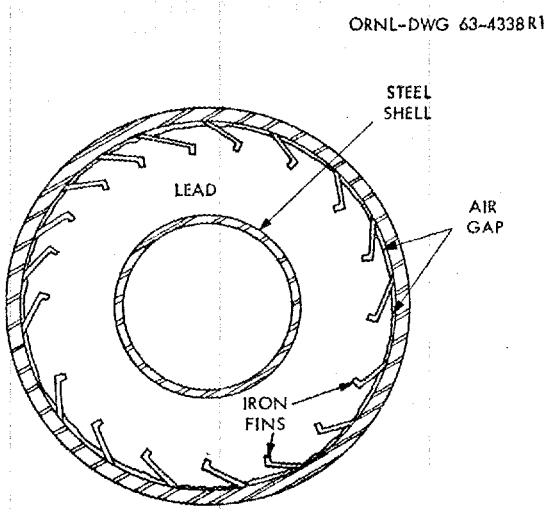

Fig. 3.17. Schematic of a Sectioned Cask Containing Internal Heat Transfer Fins.

Heat transfer tests to verify this design characteristic were performed with an electrical heat source of 5.5 kw in the cask cavity. Thermocouples were used to determine the temperature profile through the cask wall (see Fig. 3.18). Note that the temperature drop between the outer lead surface and the surface of the outer shell was only about 15°F, indicating that the fins satisfactorily performed their function.

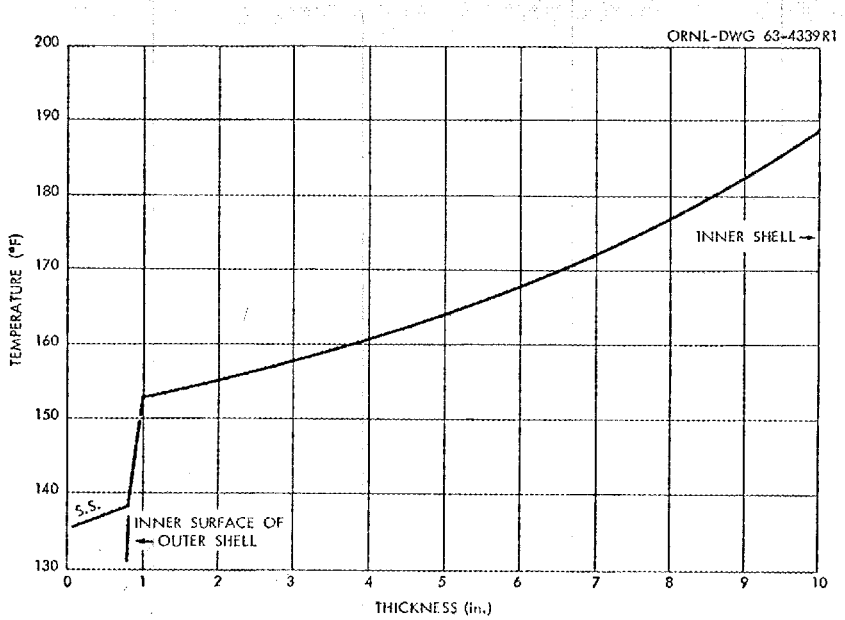

Fig. 3.18. Temperature Profile Through Lead Shield in WTR Cask with a Power Input of 5.5 kw.

3.9 Fire Protection

The involvement of a cask in a fire is one of the worst type of accidents that could occur during shipment. Lead expands as its temperature increases at a faster rate than steels that normally contain it (see Sect. 5.4). Consequently, in a fire pressure of molten lead could rupture the steel shell and leak away. Cavity pressure would increase, particularly if a liquid coolant were present, which could cause the containment to be violated. Fission products would be dispersed from the cask. Even though the probability of involving a cask in a fire may be low, an examination of the consequences is far from academic since the potential monetary loss is so great.

The proposed regulations (CFR Title 10, Part 72) state that the cask should be able to withstand a standard 1-hour fire (the time-temperature curve is given in appendix 3) without creating excessive hazards; i.e., the surface dose rate could increase to 1 r/hr, but fission products should not be lost from the cask.

If the types of fires in which heavy casks may become involved are examined, then the British recommendation that a half-hour fire test is sufficient, has merit.

Containers which weigh over several tons are not likely to be placed in a building during transit. These casks would, most probably, be involved in a petroleum fire caused by an accident involving, say, a railroad car containing such fuel. The burning rate of a pool of hydrocarbon fuel varies from about 10 to 15 in./hr of pool depth. In order to postulate a 1-hr fire which completely envelopes the cask and produces the maximum heat flux over the entire cask, the fuel would most likely have to be trapped in some natural depression (possibly a ditch with no run-off) and the cask suspended about 30 in. above the pool. In order to burn for 1 hr, the pool depth would have to be possibly 15 in. deep.

Such a situation is difficult (although not impossible) to imagine, and even though a half-hour open-air fire, under optimum burning conditions, seems to be a conservative enough basis to design on, continued shipping experience and accident analysis will be necessary to resolve the question. Until that time, it is recommended that large casks be examined assuming a

1-hr fire.

The situation is generally different in the case of small shipping containers. Such containers may very well be stored in a warehouse in the course of shipment from one point to another and, in this situation, may be subject to a building fire.

It is easy to imagine such a fire lasting at least an hour; under such conditions, the time-temperature curve presented in appendix 3 should be used in assessing the potential hazards under fire conditions.

3.9.1 Characteristics of Open-Air Fire

A limited number of open-air fire tests using JP-4 jet fuel have been performed to date by Armour Research Institute and Sandia Corporation.[31] More tests are being planned. Preliminary results indicate that the fire temperature of large pools is about 1900 ±150°F and the heat flux averages around 47,000 Btu/hr-ft^2.

The heat flux apparently increases with the size of the fire up to about 400 ft^2 of surface area.[32] Between 400 to 2200 ft^2, the heat flux does not appreciably change, but over 2200 ft^2 the flux decreases due to reduced oxygen supply. As noted previously, the burning rate for pools of hydrocarbon fuels appear to vary between 10 and 15 inches of pool depth per hour.

3.9.2 Container Designs which Offer Protection from Fire

Normally, the cask is designed to provide a path for heat to flow from the source to the cask surface. With this design, however, a path for heat input from the cask surface to the cavity is also provided. Since in a fire much of the inergy is transferred by radiation, it would be desirable to build a cask that would reject heat by convection and not accept energy by thermal radiation.

The HAPO buffered cask is designed in this manner (see Fig. 4.15). Hanford's buffered cask provides a thermal barrier in the form of several layers of stagnant air within the buffers' annuli. This helps to insulate the cask from external fires. Under normal conditions, air cools the cask by flowing around several barriers to the innermost annulus, which

forms a chimney around the cask, and then past the cask and out the top of the buffer. In a fire, the hot gases will probably not pass the few entrance barriers, but impinge only on the outer shell;and, certainly, the radiant energy of the flame will be mainly intercepted by the outer surface of the buffer. A simplified fire shield is shown schematically in Fig. 3.19.

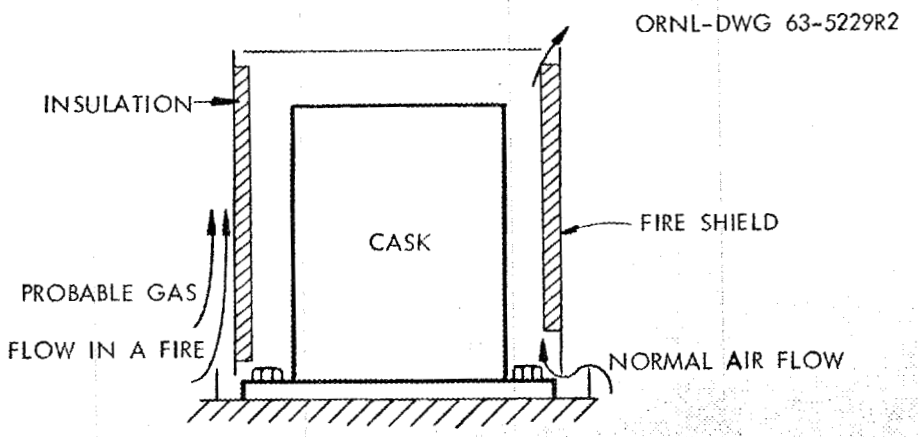

Fig. 3.19. Schematic of Fire Shield.

A type of cask that has met with little approval in the United States, but which the British feel solves most of the problems that are attendant with lead shielded casks in a fire, is the all-steel (or iron) cask. Such casks have the disadvantage of weighing more than a comparable lead shielded cask with the equivalent cavity size and shielding, and would, therefore, cost more to transport across country. But the advantages are, that the shield will not melt at normal fire temperatures; and even though thermal stresses will be present in the steel cask in a fire, the problem of differential thermal expansion between the shield and shell does not occur. If future experience indicates that fire protection is needed on all casks and fire shields fail to provide this protection, then all steel casks may solve the problem.

Relatively small casks, which normally have small internal heat sources, have been enclosed in wooden shields and tested to determine their ability to withstand fire.[33,34,35] The results indicate that about a 3-1/2 to 4 in. thickness of wood offers good thermal protection to the cask for up to an

hour. The hardwoods are somewhat more fire resistant than softwoods, but fire tests performed on pine shields have provided reasonable protection to the enclosed container.

Fire tests have been performed by the Underwriters Laboratories on small shipping casks with no fire protecting shields.[36] In one test, the cask blew up. It was later surmised that several hundred cubic centimeters of water had become trapped inside the steel shell during many years of use. Other casks were dried prior to testing and no further explosions occurred, although loss of lead shielding was common.

Underwriters Laboratories have also tested a wooden fire shield in a fire.[37] They found that in a furnace which followed the time-temperature curve (appendix 3), 3-5/8 in. of maple withstood a 1-hr fire without burning through the wood, and temperatures inside the shield did not exceed 210°F.

3.9.3 Cask Temperatures in a Fire

Methods are available which will permit an estimation of the temperature throughout a cask as a function of time after having been immersed in a fire by making certain assumptions. Such unsteady state heat transfer calculations may be made by hand using a graphical and/or a tabular method employing a finite difference technique. The graphical method, known as the Schmidt plot, is relatively simple even when the boundary conditions become complicated, but is limited to temperatures below the melting point of the cask materials. For a complete description of the theory behind the method, the reader is referred to reference 38.

The unsteady state equation, which applies to heat conduction in a thick-walled cylinder, is

$$\frac{\partial T}{\partial \theta} = a \left(\frac{\partial^2 T}{\partial r^2} + \frac{1}{r} \frac{\partial T}{\partial r} \right) \tag{15}$$

where T is temperature, θ is time, a is the thermal diffusivity, and r is the radius. This equation may be transformed into the finite difference equation (16). To use Eq. (16), the walls of the cylinder must be divided into annular sections of constant Δr, and it is the temperature at the planes between these intervals that is determined as a function of time.

$$T_n^{t+1} - T_n^{t} = \frac{2a\Delta\theta}{(r\Delta\eta)^2}\left[\frac{T_{n+1}^{t} + T_{n-1}^{t}}{2} - T_n^{t}\right] \tag{16}$$

The nomenclature is the same as noted for Eq. (15), but in addition the superscripts indicate the number of time increments ($\Delta\theta$'s) that have elapsed, the subscripts to the position through the cylinder wall, and $\Delta\eta = \frac{\Delta r}{r}$.

The thermal diffusivity, a, of the system is assumed constant; and if $\Delta\theta$ or $r\Delta\eta$ is chosen such that

$$\frac{2a\Delta\theta}{(r\Delta\eta)^2} = 1 \tag{17}$$

then Eq. (16) would become

$$T_n^{t+1} = \frac{T_{n+1}^{t} + T_{n-1}^{t}}{2} \tag{18}$$

which says that the temperature at position n at time increment t + 1 is equal to the arithmetic mean of the temperature at position n + 1 and n - 1 measured at time increment t, and the temperature at any point changes at alternate time intervals. This, therefore, permits a stepwise calculation of temperature as a function of time and temperature history.

For thick-walled cylinders, the wall offers a finite resistance to the heat flow toward the interior of the cylinder. This resistance may be accounted for in construction of the Schmidt plot by extending the cylinder wall a certain distance. This distance is equivalent to $k/\bar{h}r_o$ which is the reciprocal Biot modulus. This reciprocal modulus indicates the ratio of the temperature drop across the solid shield (proportional to k/r_o) to that across the fluid (proportional to $\bar{h}$).

Problem 3.5. A cylindrical steel-shelled, lead-filled cask has an inner radius of 9-1/2 in. and an outer radius of 21 in. The shells are made of mild steel, the inner one being 1/2-in. thick and the outer one 7/8-in. thick. The temperature in the wall is essentially constant at 300°F due to the radioactive material it carried.

Assuming all the heat is transferred by radiation and there are no end effects, determine the time required for the outer surface of the lead shield to reach the melting point when immersed in a fire whose flame temperature is 1900°F and emissivity is 0.85 (1) without a fire shield and (2) with a fire shield similar to that shown schematically in Fig. 3.19. The fire shield is made up of 2 inches of insulating material bonded to a 1/4-in. steel shell surrounding the cask.

For the insulation, assume k = 0.051 Btu/hr-ft-°F, a = 0.01 ft^2/hr and its surface emissivity is the same as the flame, 0.85.

Solution 1. In this analysis the thermal resistance of the outer shell is neglected. The lead shield, shown schematically in Fig. 3.20 is divided into three annular segments, each with a Δr of 3.375 in.

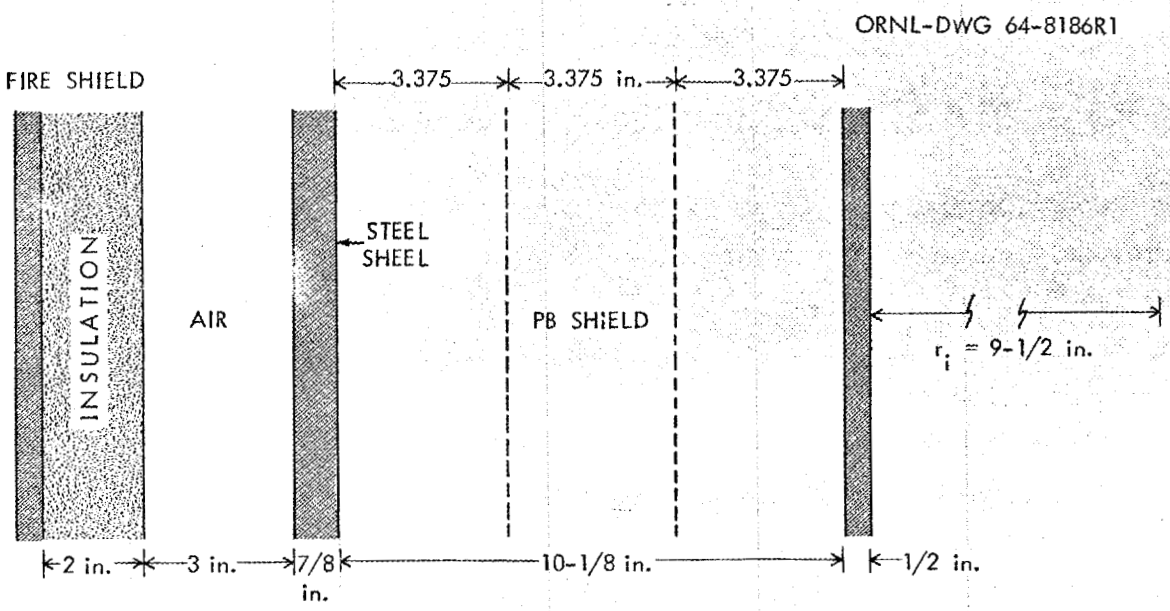

Fig. 3.20. Schematic of a Lead-Shielded Cask Protected by an Optional Fire Shield.

For the lead shield

r_i = 10 in.
r_o = 20-1/8 in.
k = 19 Btu/hr-ft-°F
a = 0.95 ft^2/hr

The values of $\Delta\eta$ corresponding to the annular segments noted in Fig. 3.20 are given in Table 3.3.

Table 3.3. Determination of $\Delta\eta$ for the Lead-Shielded Cask

Sec. No.	Inner Radius in.	Outer Radius in.	Mean Radius in.	$\Delta\eta = \frac{\Delta r}{r}$
1	10.0	13.375	11.688	0.288
2	13.375	16.750	15.063	0.224
3	16.750	20.125	18.438	0.183

Since from Eq. (17)

$$\frac{2a\Delta\theta}{(\Delta r)^2} = 1$$

$$\Delta\theta = \frac{(\Delta r)^2}{2a} = \frac{(3.375/12)^2}{(2)(0.95)} = 0.0415 \text{ hr} \cong 2.5 \text{ min.}$$

Construction of a graph is started by drawing a vertical line at a zero position on a temperature-position plot to represent the surface of the lead shield (see Fig. 3.21). The segment interfaces are then drawn to the right of, and parallel to, the original line at the proper $\Delta\eta$ distances noted in Table 3.3.

Since the cask surface temperature and $\bar{h}$ vary with time, a step-by-step determination of $\bar{h}$ with time must be made to determine the position of the "fictitious cask surface" which is placed to the left of the zero position at a distance equivalent to $k/\bar{h}r_o$.

Equation (5) may be used to compute $\bar{h}$ by assuming that all the heat is transferred by radiation and that $\underline{F}_{12} = F_c F_a$. In this case, since the cask is closely surrounded by the flame and/or the fire shield, the shape factor $F_e = 1$ and F_a, the grey body factor equals

$$F_a = \frac{1}{1/\epsilon_1 + 1/\epsilon_2 - 1}$$

where ϵ_1 refers to the heat source (either the flame or insulation surface) and ϵ_2, the cask surface.

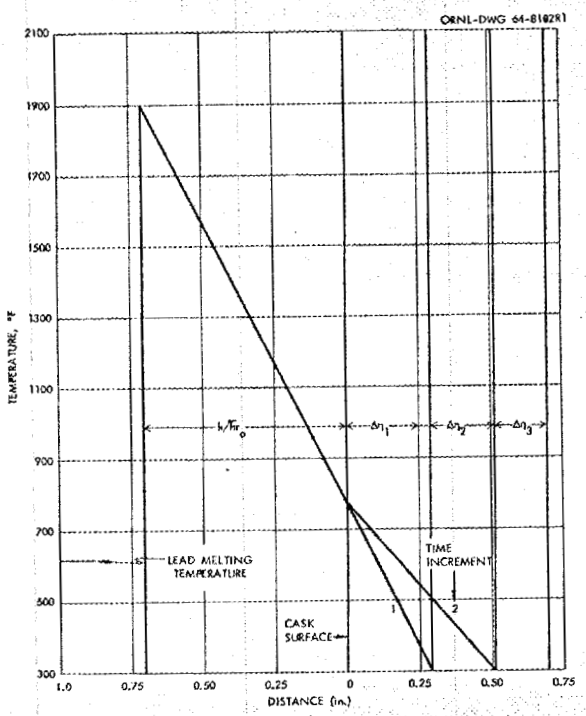

Fig. 3.21. A Determination of the Cask Surface Temperatures as a Function of Time Using the Schmidt Graphical Method.

Thus,

$$F_a = \frac{1}{1/.85 + 1/.55 - 1} = 0.50$$

From Eq. (5)

$$\bar{h} = F_e F_a \sigma \left[T_1^4 - T_2^4\right] \Big/ T_1 - T_2$$

$$= (0.50)(0.173)\left[\left(\frac{T_1}{100}\right)^4 - \left(\frac{T_2}{100}\right)^4\right] \Big/ T_1 - T_2$$

At time zero, the temperature of the flame is 1900°F and the surface temperature of the cask is 300°F. The value of $\bar{h}$ is determined as noted above and is listed below in Table 3.4 along with the corresponding value for $k/\bar{h}r_o$, which is, in this case, 0.720. Note that the temperatures t_1 and t_2 are in degrees Fahrenheit and T_1 and T_2 are degrees Rankine.

Table 3.4. Determination of $k/\bar{h}r_o$ as a Function of Time and Temperature

Increment	Time (min)	t_1 (°F)	t_2 (°F)	$\left(\frac{T_1}{100}\right)^4$ (°R)^4	$\left(\frac{T_2}{100}\right)^4$ (°R)^4	Δt (°F)	$\bar{h}$ (Btu/hr -ft^2-°F)	$\frac{k}{\bar{h}r_o}$
0	0	1900	300	304,000	3,300	1600	16.25	0.720
1	2.5	1900	735					

A "fictitious cask surface" is drawn a distance of 0.720 in. to the left of the zero line and from the intersection of this line with the fire temperature of 1900°F, a straight line is drawn to the first interface in the shield whose temperature is still 300°F. This line intersects the lead surface at 735°F which is just above the lead melting temperature.

These results indicate that if this cask is enveloped by flame whose temperature is 1900°F, that melting of the lead at the cask surface will begin in less than 2.5 minutes after being surrounded by the flames.

Solution 2. When the cask fire shield intercepts the heat from the fire, it will quickly raise the steel plate supporting the insulation to about the fire temperature and the heat will slowly be conducted through the insulation. A time-temperature analysis of the insulated shield may be also handled using a Schmidt plot.

The insulation is thin enough relative to its radius that it may be treated as a slab. The insulation is arbitrarily divided into four 1/2-in. increments and, by replacing $r\Delta\eta$ by Δx in Eq. (17),

$$\Delta\theta = \frac{\Delta x^2}{2a} = \frac{(1/24)^2}{(2)(.01)} = 0.087 \text{ hr} = 5.2 \text{ min}$$

Construction of the graph is similar to that described previously, except the shield surface is assumed to be a constant 1900°F and thus all lines radiate from the intersection of the vertical line representing the cask surface (at point 0) and the horizontal 1900°F line (see Fig. 3.22). The conservative assumption is made that the inner surface of the

fire shield is insulated and no heat escapes. This allows one to draw horizontal temperature lines in the last zone of insulation.

It should be remembered that the temperature in any plane varies only in alternate time increments. Note that the temperature on the inside wall of the insulation does not start to rise until after three time periods have elapsed or 3 x 5.2 = 15.6 min. The time - temperature curve for the inside face of the insulation is replotted in Fig. 3.23.

The cask surface is effected by the temperature on the inside surface of the insulation. Again, assuming the heat is transferred by radiation between these two surfaces, the temperature increase throughout the lead shield may be computed by the use of a Schmidt plot.

The construction is identical to that described in solution 1 of this problem, except that the temperature to which the cask surface is exposed is not 1900°F but the temperature given in Fig. 3.23 as a function of time.

Since the cask is divided into the same annular segments as described in solution 1, the time increment of 2.5 minutes applies as does Eq. (19) for the determination of $\overline{h}$.

To aid in the construction of the Schmidt plot of the cask shield, Table 3.5 was constructed. The results are plotted in Fig. 3.24.

It is seen from Fig. 3.24 that the surface temperature of the cask in 18 time increments (18 x 2.5 + 15.6 min insulation time lag = 60.6 min) has reached only 510°F, which is about 100°F below the lead melting temperature, while the inside wall temperature has increased from 300 to 380°F during the 1-hr fire.

These results indicate the usefulness of a fire shield if a cask is to be protected from a 1-hr fire.

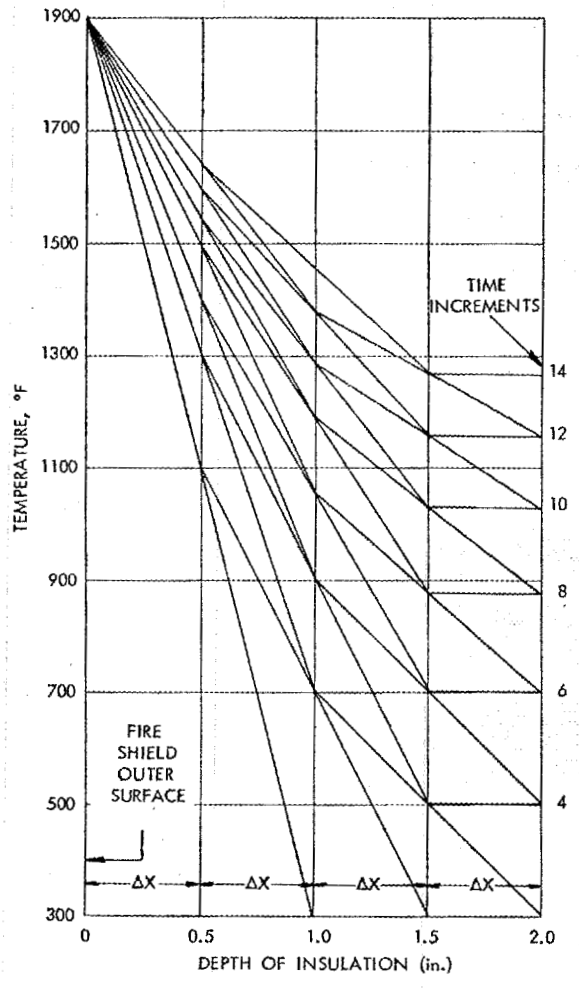

Fig. 3.22. A Plot of the Temperature Distribution through a Fire Shield Using the Schmidt Graphical Method.

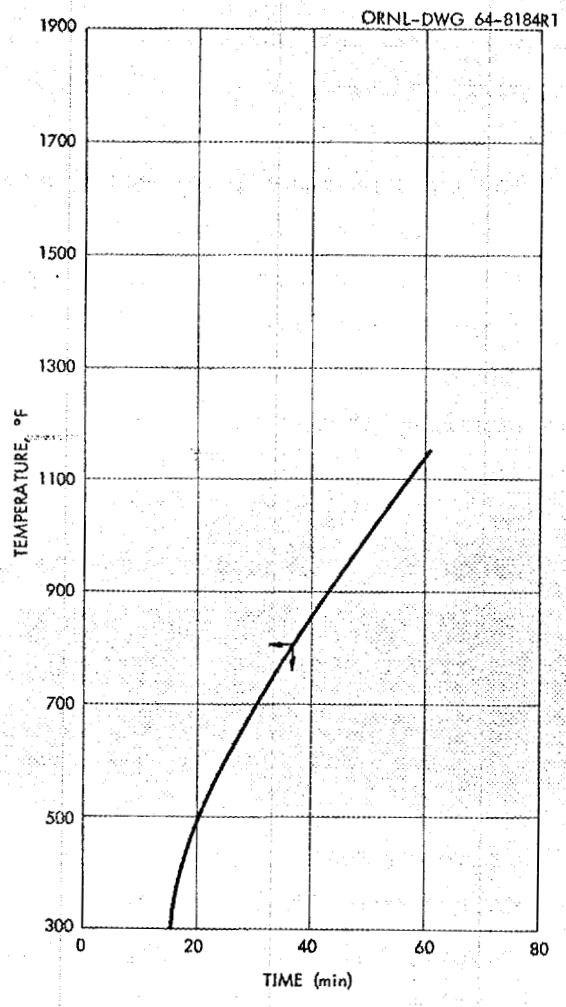

Fig. 3.23. The Time-Temperature Curve for the Inside Surface of the Fire Shield Determined from Fig. 3.22.

Table 3.5. The Determination of $k/\bar{h}r_o$ as a Function of Time and Temperature

Increment	Time (min)	t_1 (°F)	t_2 (°F)	$\left(\frac{T_1}{100}\right)^4$ (°R)^4	$\left(\frac{T_2}{100}\right)^4$ (°R)^4	Δt (°F)	$\bar{h}$ (Btu/hr -ft^2-°F)	$\frac{k}{\bar{h}r_o}$
1	17.5	400	300	5,500	3,350	100	1.86	6.32
3	22.5	535	305	9,400	3,400	230	2.25	5.23
5	27.5	635	315	14,200	3,600	320	2.86	4.11
7	32.5	725	330	19,700	3,900	395	3.46	3.40
9	37.5	815	350	26,400	4,300	465	4.12	2.85
11	42.5	895	375	33,200	4,800	520	4.72	2.50
13	47.5	970	100	41,600	5,500	570	5.50	2.14
15	52.5	1035	435	49,500	6,500	600	6.20	1.90
17	57.5	1100	420	58,700	7,500	630	7.05	1.67
19	62.5	1155	510	67,200	9,000	645	7.80	1.51

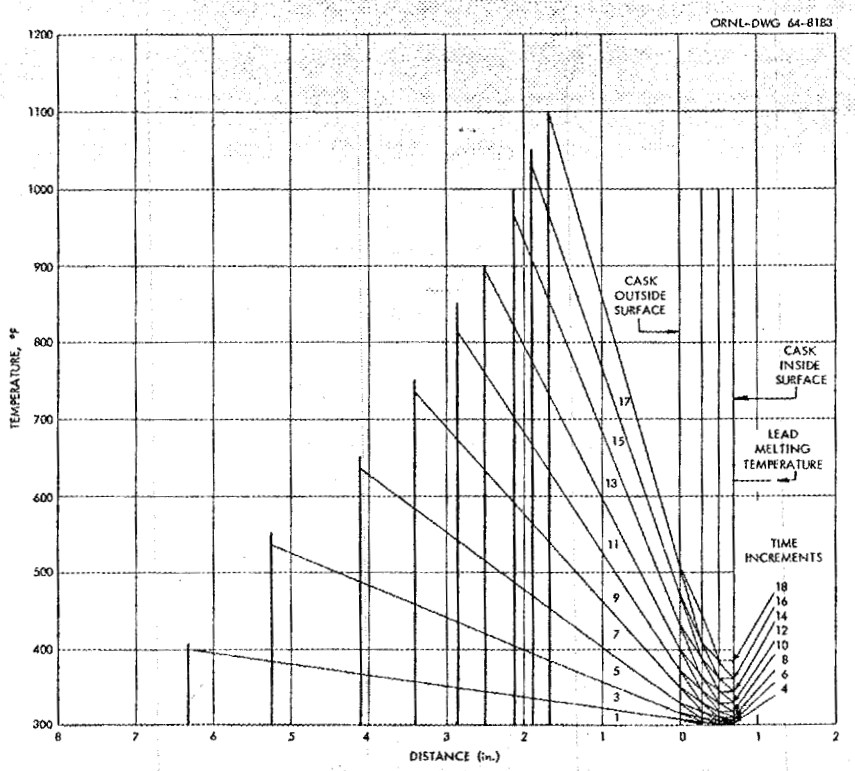

Fig. 3.24. A Plot of the Temperature Distribution as a Function of Time Through a Cask Surrounded by a Fire Shield.

4. STRUCTURAL INTEGRITY

4.1 Introduction

A primary goal of a well designed cask is to protect the public from the release of harmful amounts of radiation during the transportation of the radioactive material. Such releases could occur from a loss of shielding or leakage of the contents from the cask caused by the involvement of a cask in an accident; e.g., impact or fire.

Since the exact nature of such accidents is almost impossible to predict, some arbitrary performance specifications of shipping containers have been set forth by the AEC in the CFR Title 10 Parts 71 and 72.

These performance specifications require, for example, that the cask should be able to withstand a free fall onto an unyielding surface from a specified drop height, the penetrating effect of a piston, and a fire without failure. Because of the almost impossible task of translating such requirements into design specifications, an extensive testing program has developed with the object of determining the effect of various accidents on casks and determining improved methods of cask design from a structural point of view. The available results of the various testing programs, many of which are still in progress, are given in this section.

Two basic policies concerning impact protection may be followed on each new shipping cask design. The first is to build the cask strong enough by itself to withstand credible accidents, and the second is to build a shield or buffer around the cask to absorb most of the impact energy in an accident and, thereby, reduce the amount of stress that the cask itself is subject to. Casks of both types have been built and tested.

Oak Ridge National Laboratory, Du Pont, and The Franklin Institute have performed drops on various-sized unbuffered casks, some of which were scale models of others. Model buffered casks have been tested by the University of Texas. The casks tested to date (all of the steel-shelled, lead-filled type) have shown a remarkable ability to withstand high drops onto a solid surface without cracking the steel shells, although the same casks are relatively vunerable to the punching action of a piston.

The tests also indicated that semi-quantitative results of the deformation of a prototype cask may be obtained by dynamically testing a

scale model of the prototype. Every detail of the prototype does not have to be modeled, but only those features likely to affect the results.

Very small models, less than 1/10 scale, normally are not desirable; welding on such a model is extremely difficult and the weld areas are quite important, since it is in these areas that failure of the shell generally occurs.

The second method of cask protection employs a buffer which encloses the cask. There are several concepts of cask buffers. Hanford has proposed concentric steel shells, held in place by rubber or aluminum honeycomb spacers. Others have proposed simple I-beam cages. Even in the case where no separate buffer is designed, tiedowns will transmit cask shock forces to the transporting vehicle which will then act as a shock absorber to some degree.

Buffered casks have the advantages that the buffer will protect the cask against most impacts, will often provide a thermal barrier in case the cask is involved in a fire, and the force that the cask surface receives in a specified impact can be calculated with a reasonable degree of accuracy.

The disadvantages are that the buffer adds bulk, weight, and complexity which can increase both capital and operating costs.

4.2 Regulations

The more important performance specifications noted in CFR Title 10, Part 72, to which spent-fuel shipping cask should conform from a structural point of view are given below.

1. The cask, when regarded as a simple beam and supported at its ends along the major axis, should be able to withstand a static, uniform load of 10 times the weight of the loaded cask without exceeding the ultimate strength of any part of the cask.
2. The cask, plus any shock-absorbing structure securely fastened to it, should be able to withstand an impact normal to any surface caused by a free fall of 15 ft onto a horizontal, unyielding surface without exceeding the ultimate strength

of any part of the cask or deforming the cask to the extent that fission products are released. (This specification may be raised to 30 ft.)

3. The lid and lid-closing mechanism should be capable of withstanding a force in any direction of at least 60 times the weight of the lid plus contents of the cask without exceeding the ultimate strength of any part of the cask. If the lid projects above the body of the cask, it should withstand 15 times the cask weight without failing.
4. The exterior surface of the cask should be able to withstand a force of 30 times the loaded cask weight applied normal to that surface over a circular area six inches in diameter, without exceeding the ultimate strength of the material of which the exterior surface is constructed. The duration of the force shall be assumed to be not less than 0.016 sec.
5. The cask should be able to withstand a standard one-hour fire test (defined in the American Society for Testing Materials, Design E 119-50) without rupturing the shells and without impairing the shielding ability of the cask.
6. The cask should be able to withstand an internal gauge pressure of not less than 20 psi or twice the operating pressure.

Additional specifications in the area of structural integrity are given in the proposed code, but mainly concern external attachments.

4.3 Unbuffered Cask Testing

Cask impact testing has become an integral part of the overall safety program concerned with shipping of radioactive materials. At present, there is no method of theoretically analyzing the dynamic effect of impact on a cask to determine how safe it is. However, calculations can be made to show that a cask will meet certain criteria based upon static loadings; if the safety factors are high enough for those static loads, the cask can presumably withstand some impact loadings.

The designer has several methods available to determine impact resistance. He may design and build a prototype cask and dynamically test

it (a very expensive method), he may build a scale model of the prototype and test it, or he may examine results of impact tests already performed on a cask similar to his (if such data is available) and infer from the results how his cask will behave under similar test conditions.

None of these methods are foolproof. Full-scale testing is expensive and only a limited number of controlled tests could be made. Model testing is much more reasonable from a cost point of view, but building the model to scale (including welds) is no easy task and the results must be scaled up to the prototype (this does appear feasible - see Sect. 4.4).

Examination of available impact data is certainly the least accurate method, but it is also the least expensive. There is much data which has already been produced and additional testing is being carried out at many different research establishments.

In spite of its obvious limitations, extensive examination of available impact data will provide a good designer with a "feel" of how a particular cask design will behave under specific impact conditions. For this reason, the following sections discuss the results of testing various shipping casks.

4.3.1 Results of Testing of 1.3- and 6-ton Steel-shelled, Lead-filled Casks at ORNL

The impact program at ORNL was implemented with seven cylindrical, steel-shelled, lead-filled casks. Five casks had an 18-in. outer diameter, ~10-in. inner diameter, a 36-in. length, and an outer shell thickness of 0.312 in. Each weighed about 1.3 tons (2,600 lb). The remaining two had a 30-in. outer diameter, an 18-in. inner diameter, a 60-in. length, and weighed about 6 tons (11,350 lb). One of these latter two casks had an outer shell thickness of 0.375 in.; and the other an outer shell thickness of 0.500 in. A schematic drawing of the 1.3-ton cask is shown in Fig. 4.1. The intent of the design was to provide a cask which, in a general sense, could be described as typical so that the results of dynamic loadings on the cask could be studied.

ORNL DWG. 63-3592

CARRIER NO.	SCHED. NO.	DIMENSION A	DIMENSION B
1	80	9.564 in.	9-7/16 in.
2 & 3	20	10.250 in.	10-1/8 in.

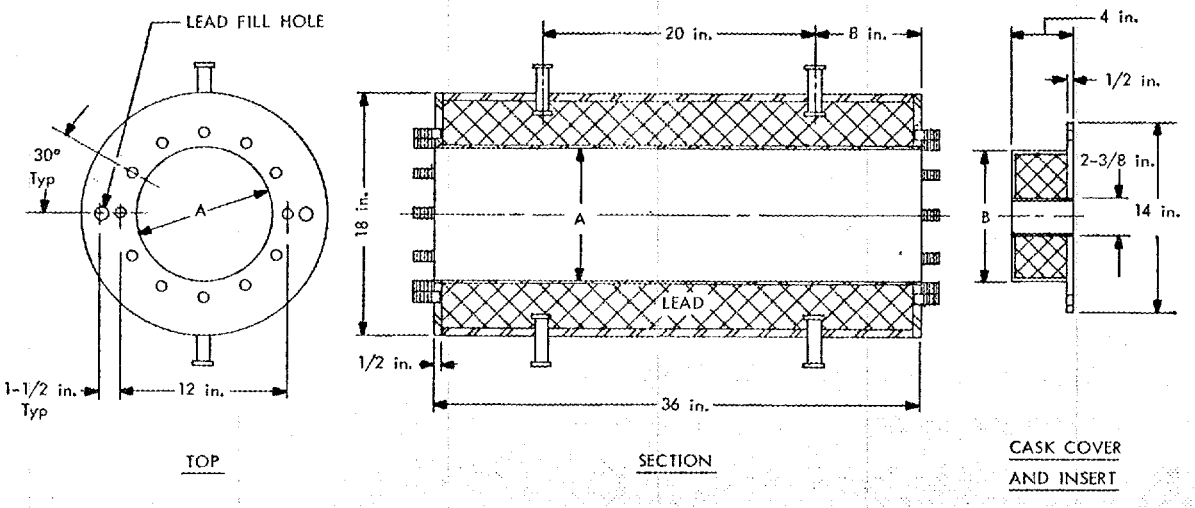

Fig. 4.1. Schematic of 1.3-ton Cask.

These casks were dropped more than 50 times from various heights in horizontal and vertical attitudes, at a 45° angle to impact on edge, onto their lifting trunnions, and onto pistons. A cask was considered to have failed the impact test if a crack or hole was produced in the cask shell, such that lead could leak out if molten.

Instrumentation. - Strain gages, accelerometers, and compressometers comprised the bulk of the instruments on the casks. A schematic picture of the instrumentation is shown in Fig. 4.2.

The compressometers were inserted into the cask cavity to measure the maximum deflection of the vertical internal diameter of the cask cavity at the time of impact.

Permanent Drop Pad. - A permanent drop pad was constructed at ORNL and is shown in Fig. 4.3. It consisted of an 8-ft square of 4-1/2-in.-thick armor plate backed up by a 12-ft square of reinforced concrete 5 ft thick. The concrete square rested on a 3-ft-diam reinforced concrete colume which extended down an additional 7 ft to bedrock.

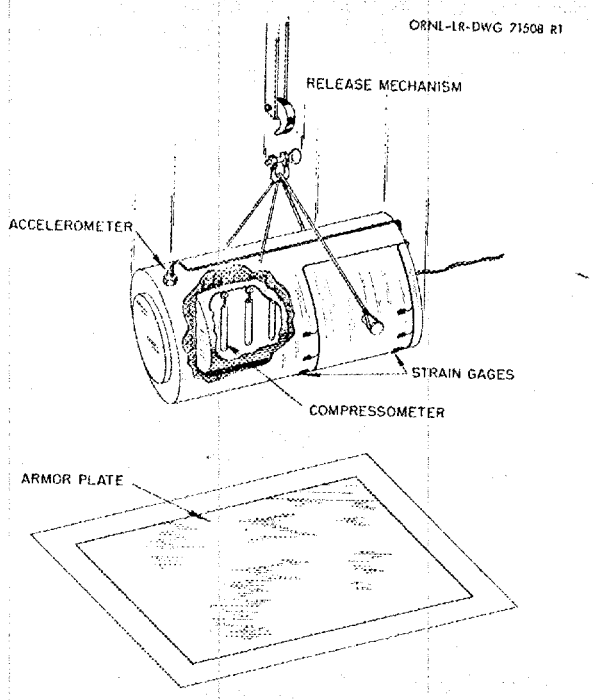

Fig. 4.2. A Schematic of Cask Instrumentation.

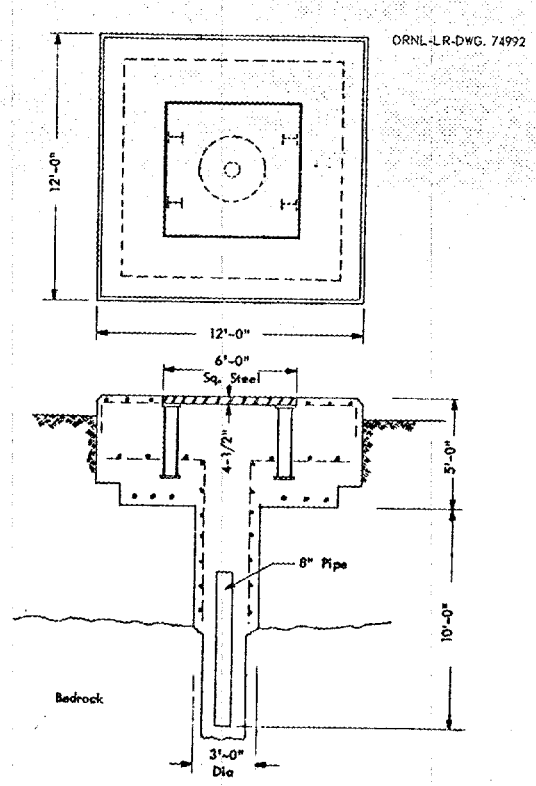

Fig. 4.3. ORNL Cask Drop Pad.

Brittle Lacquer as a Visual Strain Indicator. - One of the most useful tools used in the program was the brittle lacquer which was painted onto the surface of some of the casks prior to impact testing. The lacquer cracked when the strain in the steel shell reached a threshold value (approximately 0.012 in./in.), indicating both the direction and (qualitatively) the magnitude of the strain on the cask surface.

This technique was used to provide an overall picture of strains in the cask shells and to indicate the position and direction of maximum strain so that strain gages could be applied and accurate strain readings recorded. Figure 4.4 shows a crack pattern produced by dropping a 1.3-ton cask horizontally from a height of four feet onto an impacting surface. These patterns were also used in computing the energy absorbed in the steel shells under impact conditions.[39]

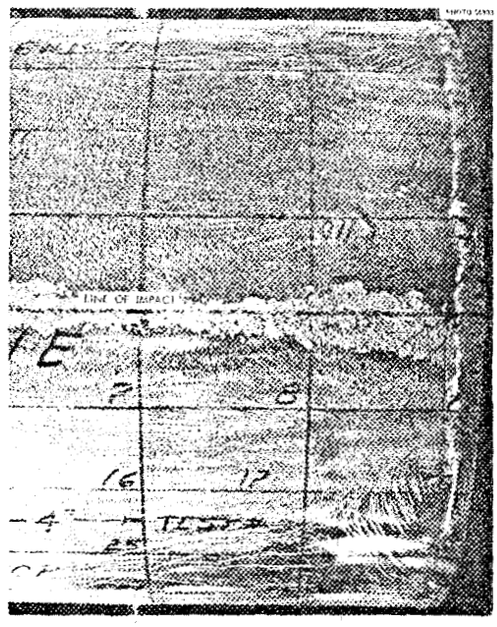

Fig. 4.4. Stresscoat Cracks Resulting from a 4-ft Drop of a 1.3-ton Cask.

Results of Horizontal Drops. - Casks dropped in a horizontal attitude showed a particular tendency to produce a high concentration of stresses in the weld area around the end plates. An example of this may be noted in Fig. 4.5 where the brittle lacquer flaked off as a result of a 2-ft drop of a 6-ton cask. This points up the fact that particular attention must be given to producing quality welds during fabrication of a cask.

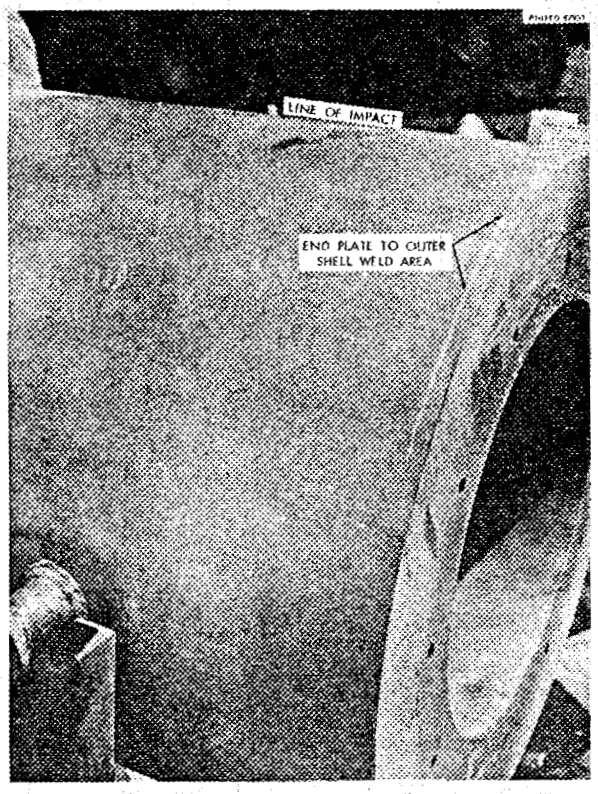

Fig. 4.5. Horizontal Drop of a 6-ton Cask Indicating a High Stress in the Weld Area.

The only failure observed in a horizontal drop was in the end-weld area of a 1.3-ton cask dropped almost 29 ft. The cask had been dropped previously from a height of 15 ft on the same side and 23 ft on the opposite side. The failure may be noted in Fig. 4.6 in the weld area at the point of impact.

The rigidity of the casks dropped in the horizontal attitude is increased by the end plates and closures on the cask. Even so, the casks tended to become oval under impact forces, and many bolts that held the end cover plates in place were sheared off (Fig. 4.6). A measure of the "out of round" produced in the cask interior at the time of impact has been determined from compressometer measurements which are noted in Table 4.1 for the 1.3-ton casks. The maximum deformation refers to the change in cavity diameter at the instant of impact; the permanent deformation was measured after impact and reflects some recovery of the cavity diameter. All drops did not hit perfectly flat which accounts for the larger change in vertical diameter in one end of drop no. 6.

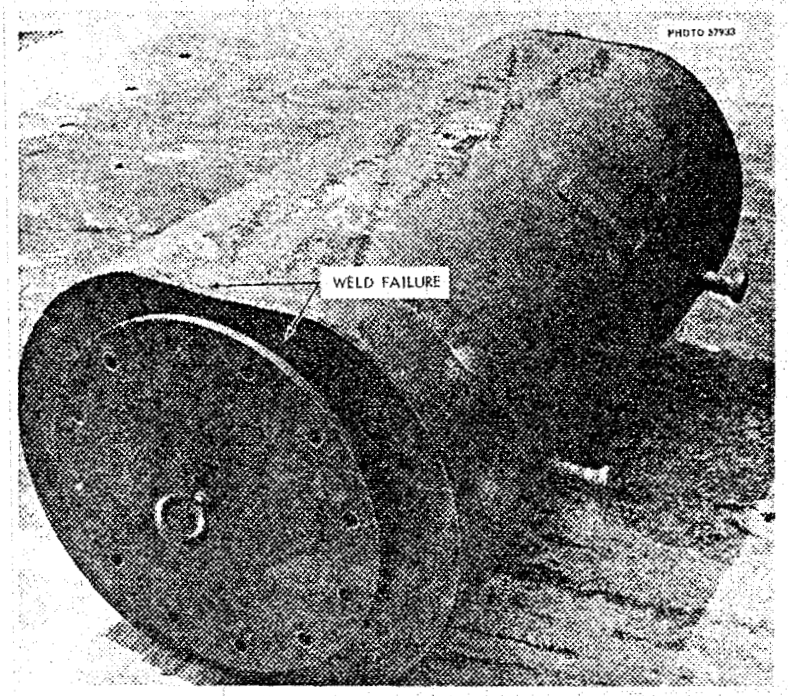

Fig. 4.6. Results of a 1.3-ton Cask Dropped 15 and 29 ft.

Table 4.1. Cavity Deformation in Horizontal Drops, 1.3-Ton Cask.

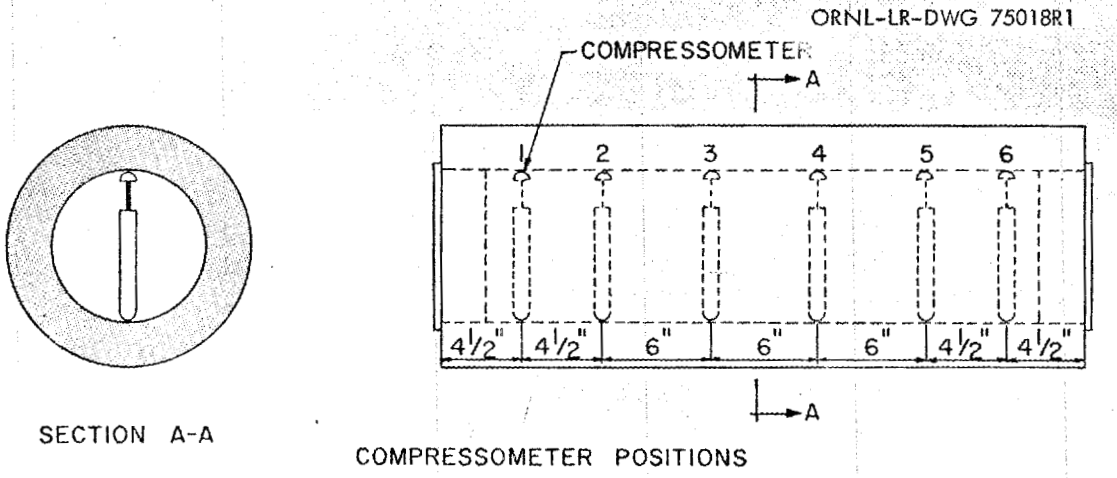

Drop		Maximum Deformation (in.)						Permanent Deformation (in.)					
No.	Height (ft)	1	2	3	4	5	6	1	2	3	4	5	6
6	6	0.161	0.126	0.132	0.118	0.105	0.047	0.050	0.061	0.099	0.073	0.062	0.011
7	8	0.130	0.158	0.173	0.160	0.123	0.104	0.053	0.058	0.059	0.059	0.047	0.090
8	12	0.109	0.096	0.131	0.168	0.185	0.164	0.045	0.046	0.057	0.075	0.094	0.090
9	16	0.128	0.187	0.233		0.244	0.188	0.082	0.108	0.136	0.139	0.146	0.121

It is evident from Fig. 4.6 that the outer steel shell of a cask will flatten along the line of impact as a result of a horizontal drop. The width of the flat varies along the length of the cask, being wide at the ends and narrower in the middle. Measurements of the flat produced as a result of dropping a 1.3-ton cask in a horizontal attitude from a height of 15 ft are noted in Sect. 4.4.1.

Results of Corner Drops. - All corner drops were made with the cask at about a 45° angle to the impact surface. Due to rigging problems, the center of gravity was not directly over the point of impact.

Figure 4.7 shows a sequenced photograph of a cask dropped on its edge from a height of 15 ft. The results of this drop may be seen in Figs. 4.8 and 4.9.

The cask had been coated with a brittle lacquer. Radial strain lines (cracks) in the lacquer at the periphery of the cask were produced on end 1 where the first impact occurred and may be clearly seen in Fig. 4.8 (stress lines occur in a perpendicular direction to the visible strain cracks). This contrasts with the circumferential strain lines produced on end 2 of the cask as a result of the initial impact shown in Fig. 4.9, which were probably caused by the inertia of the lead and inner shell at the time of impact. The second impact, which occurred at end 2, produced radial strains which were superimposed on the original circumferential strains.

Note in Fig. 4.8 the two unstressed "disks" in the cover plate (on opposite sides of the center hole) defined by a high concentration of stress cracks around them. In Fig. 4.9, two similar unstressed disks may be noted outside the cover plate, in the end plate, at a 45° angle from the vertical. These strain cracks define holes through which the lead was poured into the cover plate and into the annular space of the shield and which were subsequently closed by steel disks seal welded in place.

That these cracks in the brittle lacquer indicate weak points in the cask is evident by referring again to Fig. 4.6 where it can be seen that a crack was indeed produced around the lead-fill hole in the end plate. This weakness was noted in many drops.

PHOTOS 58099 THRU 58106R1

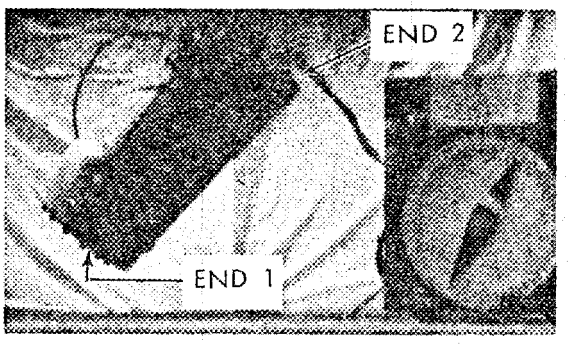

Prior to impact

Second impact - time: 0.102 sec

Initial impact - time: 0.000 sec

Second bounce - time: 0.196 sec

Peak deceleration - time: 0.0083 sec

Third impact - time: 0.391 sec

First bounce - time: 0.071 sec

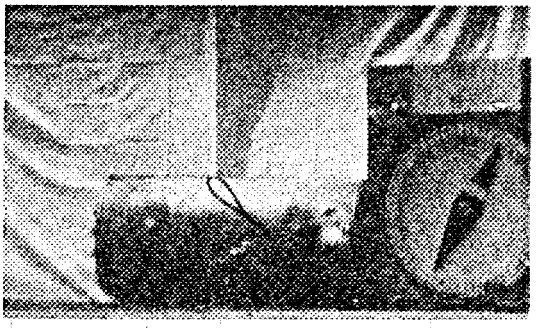

Final position - time: 0.515 sec

Fig. 4.7. Corner Drop of a 1.3-ton Model Shipping Cask; Drop Height 15 ft.

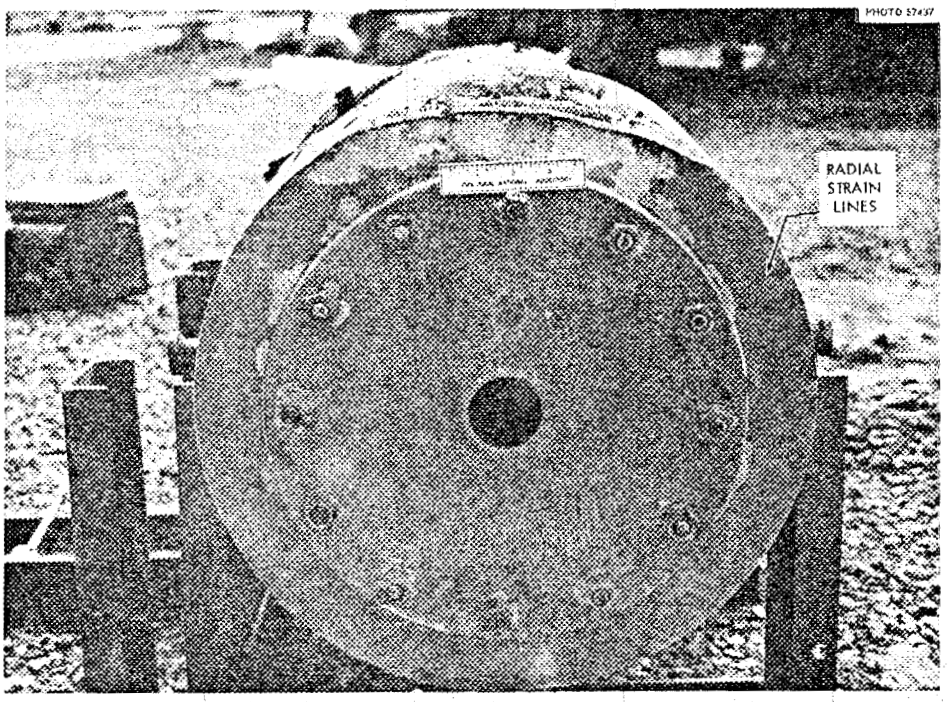

Fig. 4.8. Cracking Pattern in the Brittle Lacquer Caused by a 15-ft-Corner Drop - Initial Impact End.

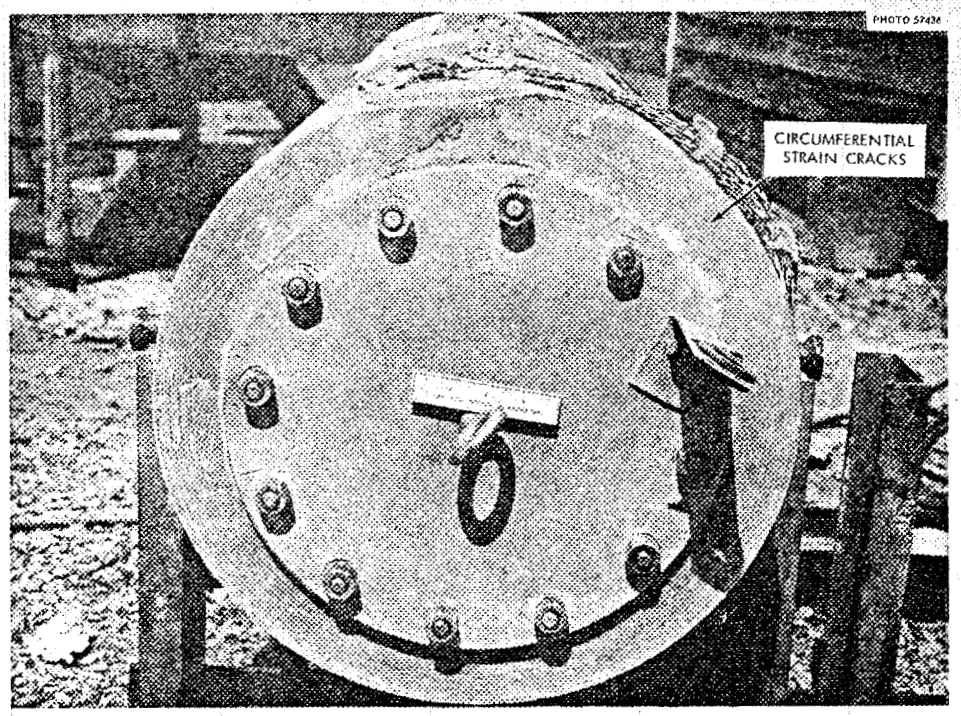

Fig. 4.9. Cracking Pattern in the Brittle Lacquer Caused by a 15-ft-Corner Drop - Second Impact End.

As a result of the 15-ft corner drop, a hairline crack (not visible in Fig. 4.8) in the weld area at the point of initial impact was noted. However, a 23-ft corner drop produced a crack 4 in. long and 1/4 in. wide in the weld area where the end plate joins the outer shell, easily visible in Fig. 4.10.

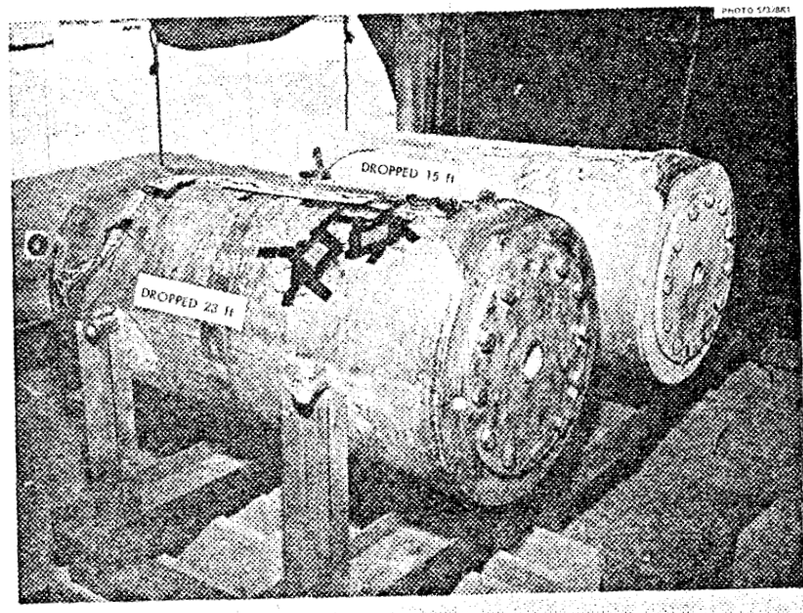

Fig. 4.10. Deformation Produced in 23 and 15-ft-Corner Drops of the 1.3-ton Casks.

Corner drops of the 6-ton casks, in general, gave similar results to those found by dropping the 1.3-ton casks, except that somewhat bigger weld cracks were produced from identical drop heights.

The corner cask drops onto welded zones appear to produce the most damaging impact results on a cask next to the piston drops discussed in the following section. This is due to the fact that the effects are localized and occur at points (corners and welds) that may be weaker than the surrounding metal plate.

The weld failure in corner drops can probably be overcome with design changes in the cask structure. Suggested changes are presented in Sect. 4.8.

Piston Drops. - The proposed code states that a cask should be able to withstand 30 times the weight of the cask applied by a 6-in.-diam

piston for not less than 16 milliseconds. Since this specification has been interpreted by most people to mean a dynamic test, many such tests have been carried out by dropping casks onto a rigidly held penetrator or piston.

The dynamic, or impact test, that is assumed to be equivalent to the specification is a 3-1/2-ft free fall of the cask onto a 6-in.-diam piston without puncture of the shell. This dynamic test was determined in the following way; assuming uniform deceleration of the cask during impact,

$$S = 1/2\ at^2 \tag{20}$$

and

$$V_{max} = at \tag{21}$$

where

s = distance, ft,

a = acceleration, ft/sec^2,

t = time, sec,

V_{max} = maximum velocity, ft/sec .

Substituting Eq. (21) into Eq. (20) and rearranging

$$V_{max}^{\ 2} = 2as \tag{22}$$

Under free fall conditions where s equals H, the drop height, and a $\cong$ 32 ft/sec^2,

$$V_{max}^{\ 2} = (2)(32)(H)$$

or

$$V_{max} = 8\sqrt{H} \quad . \tag{23}$$

Since

$$s = V_{ave}t$$

and assuming that

$$V_{ave} = \frac{V_{max}}{2}$$

then

$$s = \frac{V_{max}}{2}\ t \tag{24}$$

Substituting Eq. (24) into Eq. (20) and noting that a may be replaced by g, where g is any acceleration,

$$1/2\ gt^2 = \frac{V_{max}}{2}\ t$$

or

$$gt = V_{max} \tag{25}$$

Substituting Eq. (23) into Eq. (25),

$$gt = 8\sqrt{H}$$

and

$$H = \left(\frac{gt}{8}\right)^2 \tag{26}$$

The specified deceleration in the regulations was 30 g's, or (30)(32 ft/sec^2) = 960 ft/sec^2 and t = 0.016 sec; substituting into Eq. (26)

$$H = \left(\frac{(960)(.016)}{8}\right)^2 = 3.68 \text{ ft}$$

This drop height was rounded down to 3.5 ft (or approximately 1 meter) and has been unofficially suggested as a standard penetration impact test for shipping containers. The difficulty with this analysis is that the average number of g's that a cask receives from such an impact and the time over which the impact occurs are not independent variables; they are a function of the mechanical aspects (and therefore responses) of the system and a 3.5-ft free fall onto a 6-in. piston generally does not produce the conditions specified above. For example, it was found in dropping the 1.3-ton cask onto a 6-in. piston from a height of 3.5 ft that a decleration shock of about 1500 g's was experienced on the inside shell, close to the point of impact, which lasted for something less than 0.001 sec. Penetration of the outer steel shell did not occur in this particular test.

The number of g's that the cask is subject to varies from point to point on the cask, since it is not a rigid structure and different points decelerate at different rates. In addition, as the piston size decreases for a given cask, the shock becomes less on impact and the deformation or penetration increases. When a 1.3-ton cask was dropped on a 2-in. piston

from 3.5 ft, the piston penetrated about 1-3/8 in. into the lead (as measured from the original cask surface) and the maximum g loading recorded on the inside shell, close to the point of impact was about 700 g's (see Fig. 4.11); the shock impulse lasted approximately 0.001 sec.

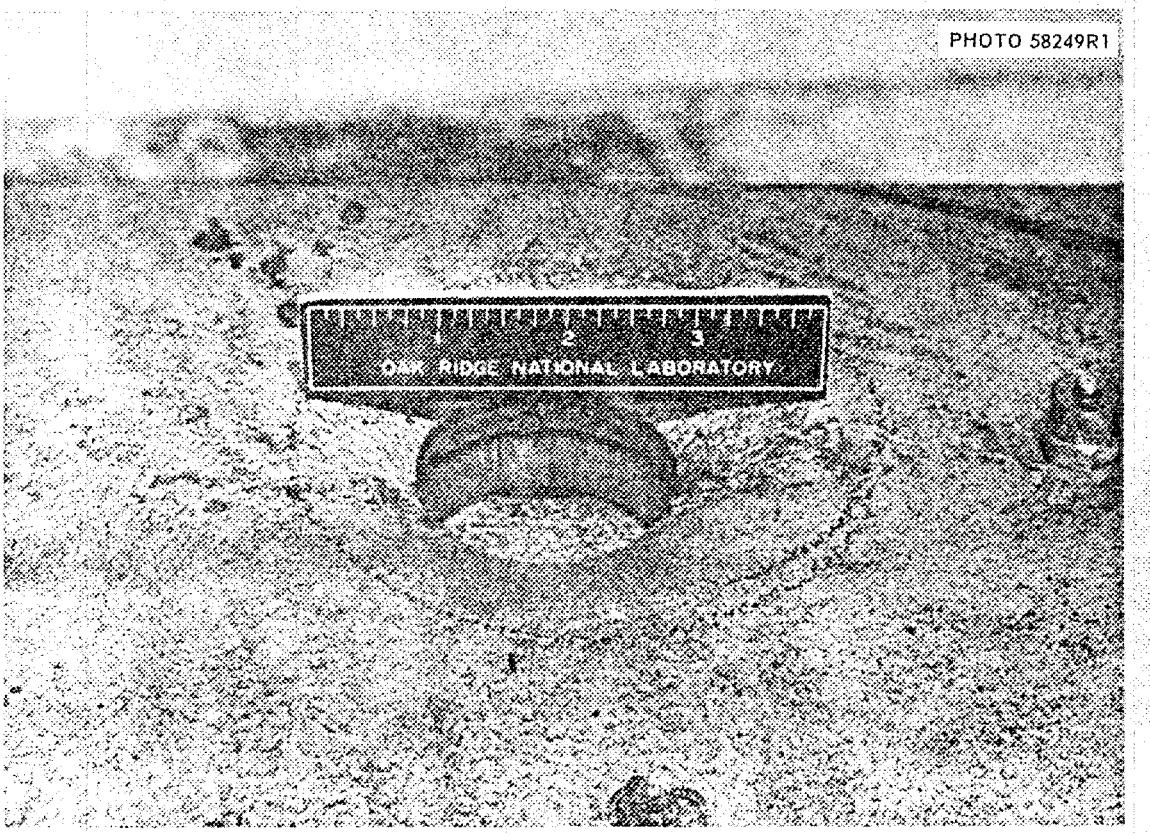

Fig. 4.11. Results of a 1.3-ton Cask Impacting on a 2-in.-diam Steel Piston - Drop Height 3.5 ft.

In other piston experiments, it became evident that the penetration results were affected by the surface condition of the piston. A slightly rounded head does not shear through the outer shell as easily as a flat, sharp-edged piston. All reported results are from drops onto sharp-edged, flat-headed pistons.

The 6-ton casks were dropped onto 4- and 6-in.-diam pistons from various heights and the results are noted in Table 4.2.

The penetration data has been analyzed in detail in Sect. 4.6.

Table 4.2. Results of Piston Tests

Cask Weight (tons)	Approximate Lead Thickness (in.)	Piston Diameter (in.)	Drop Height (ft)	Penetration Measured From Final Cask[a] Surface (in.)	Penetration Measured From Original Cask Surface[a] (in.)
1.3	4	2	2.0	3/16	5/8
(2600 lb)	4	2	3.5	7/8	1-3/8
	4	2	5.0	1-1/2	2-1/8
	4	2	6.5	2-1/4	2-3/4
6.0	6	2	0.5	3/8	7/8
(11,350 lb)	6	2	1.0	1-5/8	2-1/8
	6	4	3.5	1-3/4	2-5/8
	6	4	5.0	3-1/4	4-1/4
	6	4	1.5	3/16	7/8
	6	4	4.0	2-1/16	2-7/8
	6	6	6.0	1/8	1-1/2
	6	6	8.0	3/4	2-3/8

[a]There was a surface indentation in the steel shell as indicated by the difference of the last two columns. It amounted to roughly 1/2 in. for the 2-in. piston, 1 in. for the 4-in. piston, and 1-1/2 in. for the 6-in. piston.

Conclusions. - As a result of the drop tests described in this section, the following generalizations are made:

1. Casks of similar design to those tested will not fail when dropped 15 ft in an attitude normal to any surface of the cask onto a solid surface. It is expected that if the welds are adequate, such casks could survive 30-ft drops under the same conditions. Based on model-testing work discussed in the following sections, this conclusion is expected to apply to casks which weigh 25 tons or greater, although full-scale tests on such casks have not been made.
2. Edge drops from a height of 15 ft or greater produced cracks in the weld area at the point of impact. With proper design, the resistance of a cask edge to impact could undoubtedly be improved (see Sect. 4.8).
3. There is little doubt that the steel shell of a lead-shielded cask is most vulnerable to a penetration type of impact; however,

in none of the tests was the inner shell of the cask ever penetrated by a piston. The maximum drop height was 8 ft, in which a 6-ton cask was dropped onto a 6-in.-diam piston.

4. Important amounts of energy can be absorbed in lead and steel. An analysis of the energy absorption properties of these materials is given in Sect. 4.6. With this information, an estimate of the results of a piston impact of specified proportions can be calculated.

4.3.2 Results of Du Pont's Impact Tests of a 15-ton Shipping Cask[39]

The heaviest shipping cask that has been tested to date, both statically and dynamically, is the Du Pont 15-ton cask (measured weight 28,240 lb) shown schematically in Fig. 4.12.

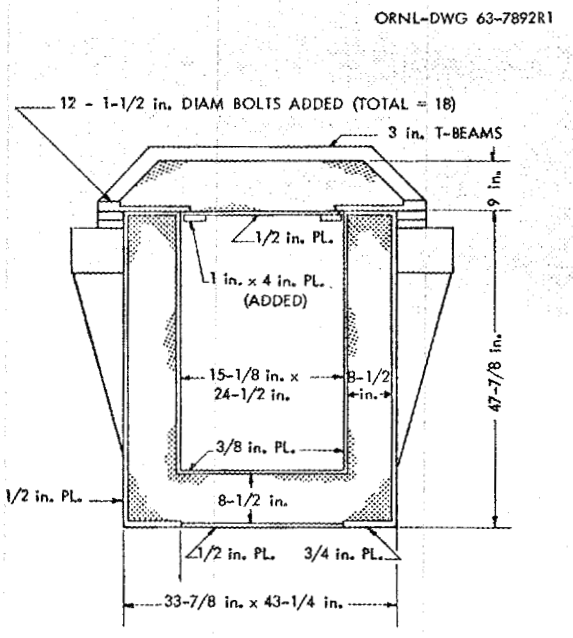

Fig. 4.12. DuPont 15-ton Cask.

The cask was put through a series of eight different static compression tests at Lehigh University, Bethlehem, Pennsylvania. The force was applied by a 5-million-pound capacity Baldwin universal testing machine. Strains at different points on the cask were measured by electric strain gages, and both internal and external deformations were measured. The

results indicated the cask would be most vulnerable to a punching load on the bottom of the cask; although after the impact tests, there appeared to be no correlation between the static and dynamic tests in regard to strain and deflection at a specific location.

The five tests noted in Table 4.3 were conducted with the cask impacting onto a 9-in.-thick piece of armor plate anchored in concrete.

Table 4.3. Drop Tests of a 15-ton Cask

Test	Drop Height, ft	Description of Impact
1	7.5	Flat on bottom
2	15	Flat on bottom
3	30	Flat on bottom
4	3.5	6-in.-diam piston on bottom
5	30	On short bottom edge

As a result of drops 1 to 3, the vertical height of the cask shortened an average of about 1 inch, and both the inside and outside shell bulged outward slightly. No metal fracture was apparent, and the shielding thickness did not appreciably change.

The drop from 3.5 ft onto a 6-in.-diam steel piston sheared through the 1/2-in.-thick steel plate, which covered the lead-fill hole, and penetrated 1-5/8 in. into the lead (a 2-5/8-in. depth from the original surface). This penetration drop is compared with the ORNL penetration drop in Sect. 4.6.3.

The edge drop from a height of 30 ft, created a crack about 10 in. long in a weld area around the lead-fill hole. Previous drops likely contributed to the formation of this crack.

One major consequence of these tests is the indication that large heavy casks with thick lead shields are able to withstand severe impacts, without causing damage to the cask to the extent that the shielding or cask structure itself would be made inadequate as a result.

4.4 Model Cask Testing

Since calculational methods are not available to analytically determine the effect of impact on a cask, other methods have been investigated. One of the most promising methods is that of testing reduced scale models of a prototype shipping container. Franklin Institute in Philadelphia, Pennsylvania, has worked extensively in this area and has constructed and tested models of prototype casks. Results, some of which are described in this section, indicate that there are striking similarities in the damage done to the prototype and its model under identical impact situations.

4.4.1 Results of Testing a Quarter-scale Model of a 1.3-ton ORNL Cask

Several 1/4-scale models (exact scale is 0.274) of the 1.3-ton ORNL cask (which was described in Sect. 4.3.1) have been built by Franklin Institute.[40] These reduced-scale models were tested under identical drop conditions to the prototype casks. The dimensions of the model are given in Table 4.4 along with comparable dimensions of the 1.3-ton ORNL prototype cask.

Table 4.4. Cask Dimensions

	ORNL	Franklin Institute
Length, in.	36	9.864
Inside diameter, in.	10.25	2.809
Outside diameter, in.	18	4.932
Weight, lb	2600	55.0
Scale factor	1	0.274

The scale model cask was first tested by dropping it in a horizontal attitude from a height of 15 ft onto a rigid impacting surface. When the ORNL prototype cask was dropped from this height, one end was observed to impact first; i.e., the longitudinal axis of the cask was approximately 2° from the horizontal. This slight angle was duplicated by Franklin Institute in their tests.

The horizontal drop produced a flattened area in the steel outer shell of the cask and is shown schematically in Fig. 4.13. The width of the flattened portion of the model was accurately measured at 19 different points along the length of the cask. These results were divided by the scale factor to predict results expected of a full-size cask. These predicted results are noted in Table 4.5 and are compared to the ORNL results obtained from testing the full-size cask. The agreement is quite good.

ORNL-DWG 63-5212R1

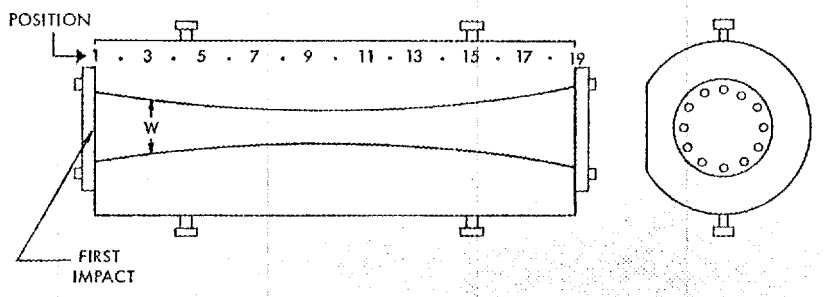

Fig. 4.13. Schematic of the Bottom View of a 1.3-ton Cask After Impact.

Table 4.5. Measured Widths, W, of the Flattened Portion of a 1.3-ton Cask Resulting from a 15-ft Horizontal Drop

Position from Impact End	(.274 Scale) Model Results (in.)	Predicted Full Size (in.)	ORNL Full Size Results (in.)
1	1.454	5.31	5.25
2	1.100	4.02	4.62
3	1.040	3.80	3.75
4	1.000	3.65	3.37
5	0.910	3.82	3.25
6	0.840	3.07	3.12
7	0.840	3.07	3.00
8	0.840	3.07	2.87
9	0.770	2.81	2.75
10	0.770	2.81	2.62
11	0.860	3.14	2.75
12	0.870	3.18	3.00
13	0.880	3.21	3.00
14	0.870	3.18	3.25
15	0.930	3.39	3.50
16	0.990	3.61	3.50
17	1.090	3.98	4.00
18	1.090	3.98	4.75
19	1.234	4.50	4.75

Several model casks were dropped on a rigid piston whose size corresponded with the 2-in.-diam piston upon which the prototype 1.3-ton casks were dropped. The depth of penetration in the model and the predicted full-size penetration are given along with the prototype results in Table 4.6. The predicted results are appreciably lower than the actual full-size results; although as the drop height was increased, agreement became better.

Table 4.6. Results of Drop on Piston

Drop Height (ft)	Model Penetration, Test Results (in.)	Predicted Full Size Penetration (in.)	Full Size Penetration Test Results[1] (in.)
2	0.013	0.047	0.1875
3-1/2	0.151	0.551	0.875
5	0.268	0.978	1.50
6-1/2	0.534	1.95	2.25

[1]Measured from the final cask surface

Additional penetration tests have indicated at least two important factors affect these results. First, the radius of the edge and hardness of the piston have a measurable affect. As the edge becomes sharper and the hardness increases, the piston will penetrate deeper into the lead shielding. Secondly, the amount of energy absorbed per unit volume of lead does not appear to be constant. The reason for this is presently not understood, but the problem is further discussed in Sect. 4.6.

Another quarter-scale model cask was dropped at a 45° angle onto its edge from a height of 15 ft. Particular dimensions of the resulting deformations are noted in Table 4.7. The test results were again scaled up by the scaling factor to predict what would be expected of a full-size cask dropped under these conditions. The table also presents the actual results obtained from dropping the prototype cask. The agreement is remarkably good.

Table 4.7. Results of 45° Corner Drop

ORNL-DWG 63-5213R2

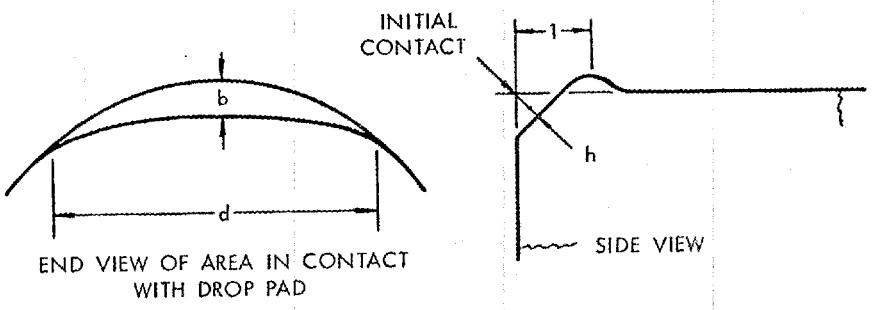

SCHEMATIC OF A CASK AFTER A CORNER DROP

DIMENSION	(0.274 SCALE MODEL) TEST RESULTS	PREDICTED FULL SIZE	ORNL FULL SIZE TEST RESULTS
d	2.44 in.	8.9 in.	9.5
l	0.69 in.	2.5 in.	2.5
b	0.44 in.	1.6 in.	---
h	0.295 in.	1.1 in.	~1.2
AREA	0.68 in.^{2}	9 in.^{2}	---

4.4.2 Results of Testing Models of a 40-ton Cask

Two scale models of a hypothetical 40-ton cask were built by the Franklin Institute to further investigate the scaling factors in impact testing. The first was an exact 1/10-scale model, and the second a nominal 1/4-scale model shown in Fig. 4.14 (actual scale size 0.224). The hypothetical prototype is similar to the Du Pont Chalk River cask which weighs approximately 45 tons. The pertinent dimensions of the two models and the hypothetical prototype are noted in Table 4.8.

Each of the two models was put through an identical series of five drops which is listed in Table 4.9.

Important dimensional measurements of each model were made before and after each drop. The calculated dimensional changes were divided by the appropriate scale factor to obtain a prediction of the deformation of the hypothetical prototype cask. The predicted deformation resulting from the 1/4- and 1/10-scale models, noted in Table 4.10, was then compared and a percent difference of the two predictions, based on the results of the 1/4-scale model, was noted in the third column of Table 4.10.[41]

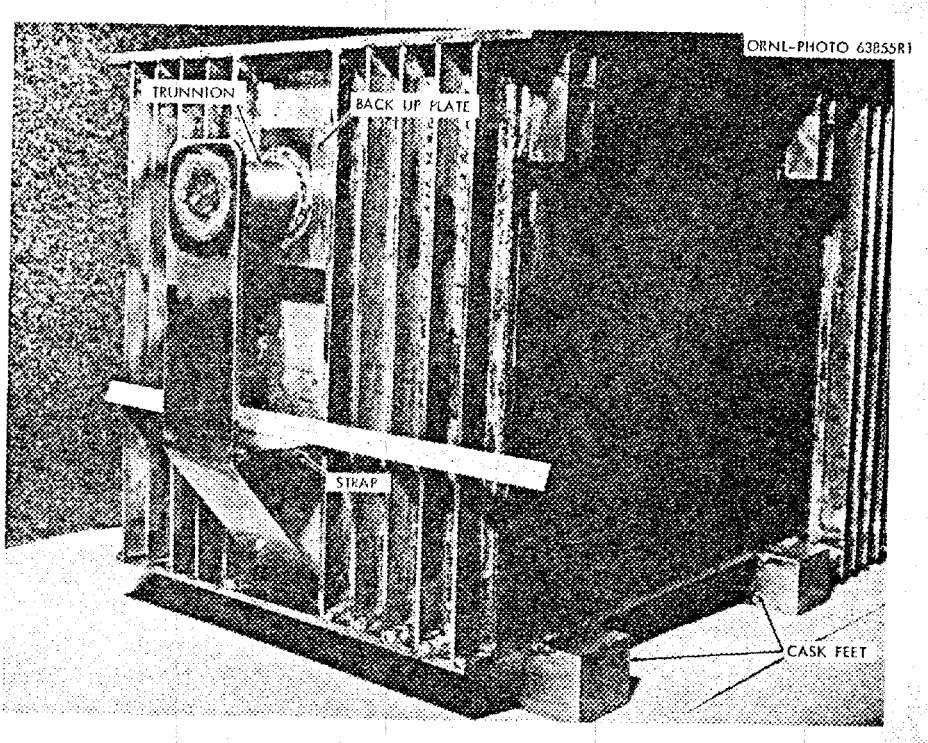

Fig. 4.14. The 1/4-Scale Model of a 40-ton Cask.

Table 4.8. Cask Dimensions

ORNL-DWG 64-9133R1

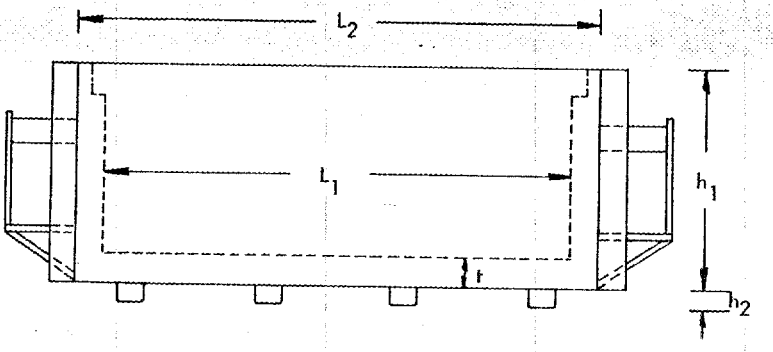

SCALE FACTOR	0.100	0.224	1.00 (PROTOTYPE)
h_1 (in.)	5.05	11.31	50.5
h_2 (in.)	0.60	1.34	6.0
t (in.)	0.76	1.70	7.6
L_1 (in.)	13.20	29.58	132.0
L_2 (in.)	14.82	33.20	148.3
Weight (lbs)	84	905	80,000

Table 4.9. Drop Tests Performed on the Scale Model Casks

Test No.	Test and Position	Drop Height (ft)
1	Flat drop on the bottom	10
2	End drop on a trunnion	15
3	Bottom drop onto a beam	10
4	Side drop on a piston	2
5	Side drop on a piston	4

Table 4.10. Predicted Dimensional Changes in a Prototype Cask Based on Impact Results of a 1/4- and 1/10-Scale Model

Dimensional Change	Predicted Change in Prototype Based on 1/4-Scale Model (in.)	Predicted Change in Prototype Based on 1/10-Scale Model (in.)	Difference Based on 1/4-Scale Model (%)
Average cask width change after drop 1	+1.33	+1.12	-16
Average height change after drop 1	-0.53	-0.42	-20
Trunnion to trunnion length change after drop 2	-7.95	-8.13	+2
Average compression in center of cask bottom after drop 3	-1.95	-1.61	-17
Piston penetration measured from top of fins after drop 4	-5.80	-6.57	+12
Piston penetration through steel shell after drop 4	0	0	0
Piston penetration measured from top of fins after drop 5	-8.90	-8.25	-2
Piston penetration through steel shell after drop 5	-1.96	-2.00	+2

As was done with the heavier 1.3-ton cask and its model discussed in Sect. 4.4.1, the tests on the heavier (1/4-scale model) cask were performed at the Oak Ridge National Laboratory, while the tests on the lighter(1/10-scale model) cask were performed at the Franklin Institute. It should, therefore, be noted that some small, unavoidable differences in the testing procedures occurred between the two sites, but this is not enough to alter the general conclusions, which are:

1. Impact testing of scale models of a prototype cask is a practical method of determining, with reasonable accuracy, expected gross deformations in the prototype cask under specific conditions.
2. Such model tests may be employed to predict methods of obtaining stronger and safer casks.
3. Such tests can be carried out at reasonable costs.

4.5 Buffered Casks

The buffer concept, as designed by Hanford to protect both the HAPO I and II casks (Fig. 4.15), is made of concentric steel shells surrounding the lead-shielded cask and held in place by rubber shock absorbers. The top and bottom of the buffer is reinforced by strong I-beam spiders and plates. The buffer was designed to reduce the impact force on the surface of the cask to 50 g's when the cask and buffer were dropped in any orientation on a solid surface from a height of 30 ft. This design criterion is indicative of the ability of the buffer to control the distance through which the cask decelerates. Since most of the systems' kinetic energy is dissipated by the shock-absorbing devices, the uniform surface loading on the cask may be specified and controlled. Pertinent information on the HAPO I and II casks is given in Table 4.11.

In order to test the adequacy of the design and to make a complete analysis of the buffering system, an impact testing program of model buffered casks was undertaken at the University of Texas.[42]

One-quarter scale models of the HAPO cask and buffers were built. Two types of material were used in the buffer to absorb the impact energy: rubber, which is the same as on the full-scale buffers, and a specially-designed aluminum honeycomb material. The aluminum honeycomb may be used

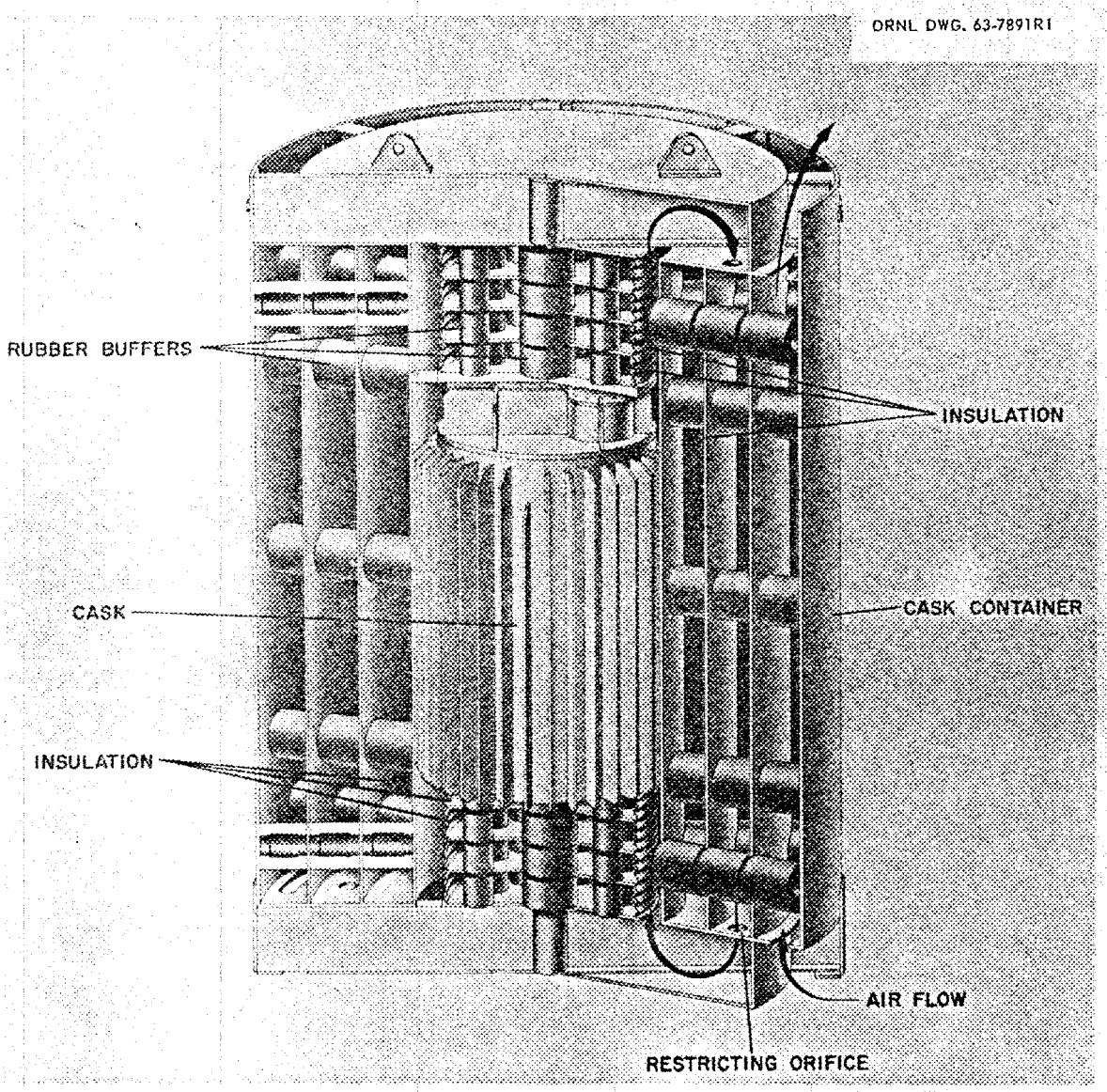

Fig. 4.15. Hanford's 1A Cask and Buffer Shield.

Table 4.11. Statistics of the HAPO Buffered Casks

Cask	HAPO I	HAPO II
Type insert	Slurry filter	Slurry filter
Weight: cask	40,000 lb	18,000 lb
buffer	35,000 lb	23,000 lb
Size: cask	52" diam x 71" high	40" diam x 56" high
buffer	10' diam x 14' high	8' diam x 12' high
Number available	1	2
Heat transfer medium	Woods-metal (MP= 160°F)	Woods-metal (MP=160°F)
Lead thickness, in.	8.75	6.5
Emergency design	Impact at 44 ft/sec	Impact at 44 ft/sec
Conditions	Total insulation for 48 hr. Flame impingement for 2 hr.	Total insulation for 48 hr. Flame impingement for 2 hr.
Design pressure	20 psig	200 psig
Design temperature	1000°F	1000°F
Maximum allowable shipping pressure	10 psig	100 psig
Rated maximum heat Gen. Btu/hr	23,500	11,600
Proposed shipment		
Desired isotope	cerium-144	strontium-90
Curies	500,000	up to 170,000
Normal decay heat Generation, Btu/hr	17,000	8,600
Chemical composition	$CeSO_4$-XNa_2-SO_4	$SrCO_3$
Physical state	Stable, dried salt	Stable, dried salt

for future buffers since its properties are less susceptible to temperature changes and can be used to design smaller buffers with the same energy absorbing capabilities as the large buffers that use the rubber shock absorbers.

4.5.1 Energy Absorbers[43]

The first buffer designs specified hard rubber as a shock-absorbing medium. This rubber had previously been tested and had known desirable properties; that is, it had a high "specific energy" (up to 2000 in.-lb of energy per cubic inch of material) at fast rates of compression under impact. Under these conditions, the rubber becomes primarily an energy absorber with little rebound. The stress-strain curve for rubber is shown in Fig. 4.16. Since the deflection is proportional to the applied force, a considerable thickness of rubber is necessary to absorb the total kinetic energy of the cask. A second drawback of rubber is that it stiffens under winter temperatures which, in turn, reduces its energy-absorption capabilities.

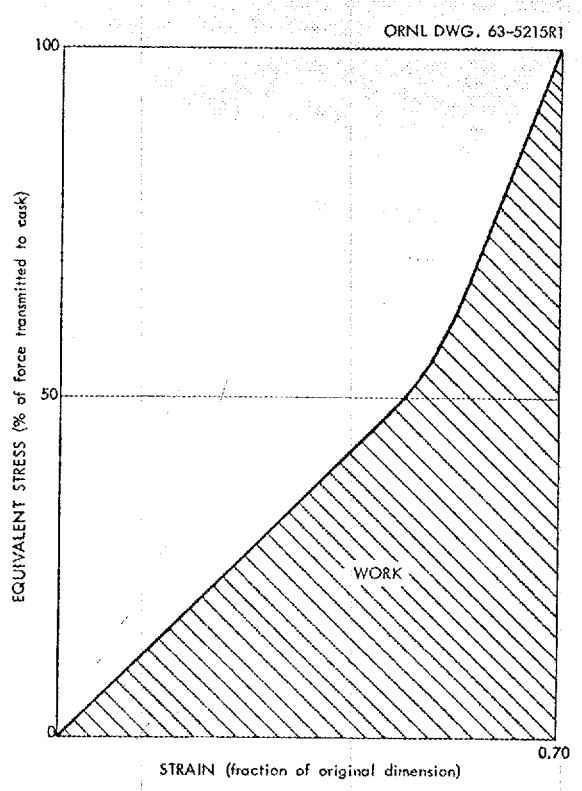

Fig. 4.16. Stress - Strain Relationship of Rubber Compounds

Other materials that might possibly effect a size and weight reduction at a reasonable cost have been examined to determine whether their energy absorption properties are adequate. Corrugated paper honeycomb and foamed plastics, although inexpensive, do not appear suited to resist the concentrated loads imposed by heavy casks. Metal honeycombs were then examined and, even though it is recognized that such material could be used only once per accident, appeared satisfactory. Since stainless steel is expensive, emphasis in the testing program was placed on aluminum honeycombs. They are available with crushing strengths of 300 to 1200 psi or higher. The crushing strengths, relatively independent of crushing velocities, may be designed for a specific application.[42,44]

Energy absorption characteristics of aluminum honeycomb were studied at the University of Texas.[45,46] This material has cross-laminated corrugations and is made in various foil thicknesses, corrugation heights, and lamination patterns. Stress-strain curves for a typical honeycomb under static loading and impact velocities of 50 to 100 ft/sec are shown in Figs. 4.17, 4.18, and 4.19. As indicated in Fig. 4.17, there is a point, after the material is compressed to 20 to 30% of the initial thickness, at which the honeycomb becomes almost solid and further compression is attainable only at high loadings. The energy absorption capability of such a system is completely irreversible.

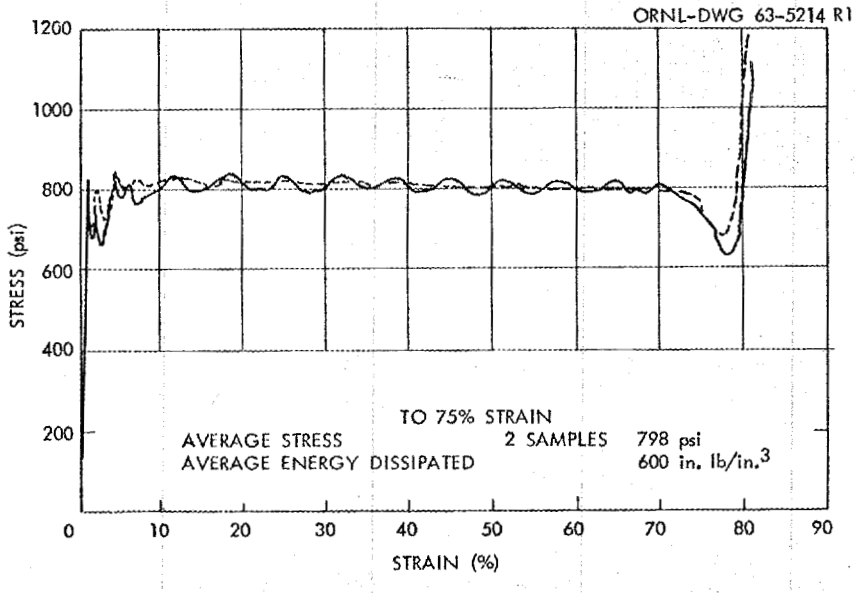

Fig. 4.17. Static Stress-Strain Curves for PR-A-O Type Aluminum Honeycomb.

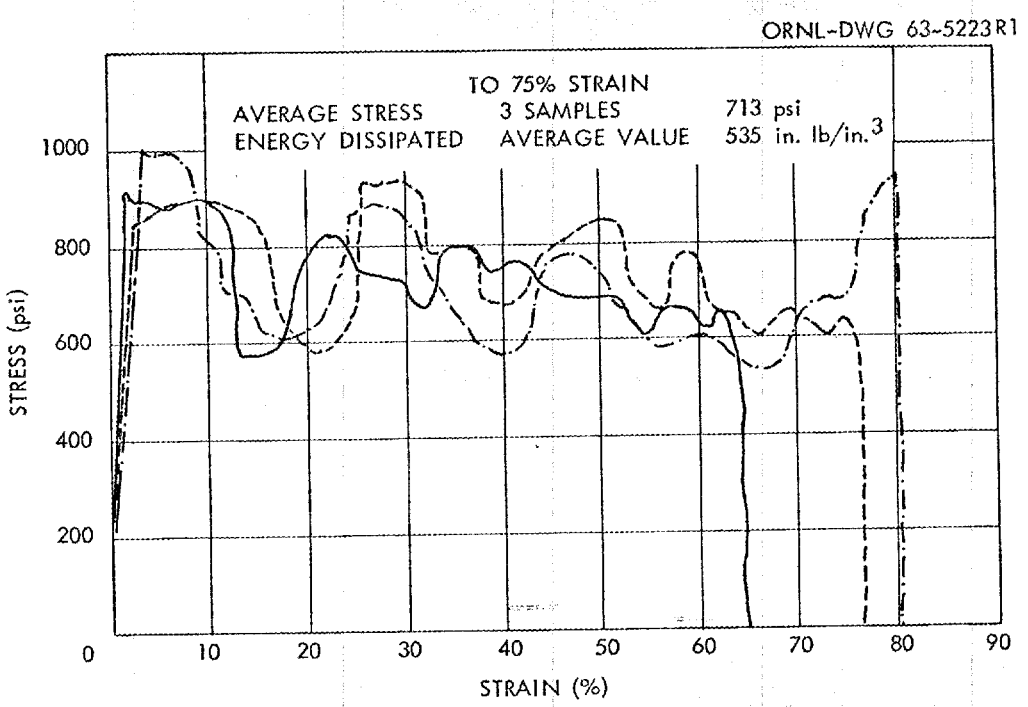

Fig. 4.18. Dynamic Stress-Strain Curves for PR-A-O Type Aluminum Honeycomb Impacted at 50 fps.

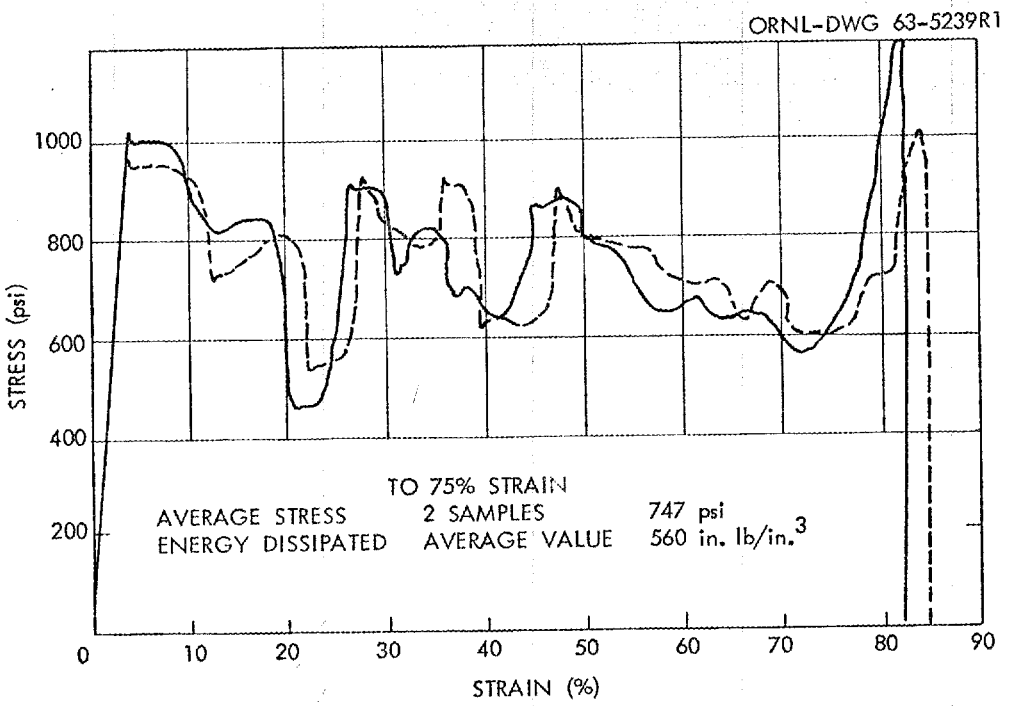

Fig. 4.19. Dynamic Stress-Strain Curves for PR-A-O Type Aluminum Honeycomb Impacted at 100 fps.

The material's characteristics are listed in Table 4.12. Note that the honeycomb is slightly stronger under static loading than impact loading. The amount of energy that this particular material can absorb under an impact load is around 550 in.-lb/in.^{3}.

Table 4.12. Energy Dissipation and Average Stress

Material	Impact Velocity (fps)	Average Stress (psi)	Energy Dissipated (in.-lb/in.^{3})	Strain (%)
PR-A-0	0 (Static)	798	600	75
PR-A-0	50	713	535	75
PR-A-0	100	747	560	75

Recently another method of absorbing large amounts of energy has been investigated which employs as its working element a frangible metal tube.[47] The tube is pressed over a die which is shaped so that the tube will expand, split and fragment when a force is applied to one end of the tube (see Fig. 4.20). This process is capable of absorbing large amounts of energy per unit weight of tubing.

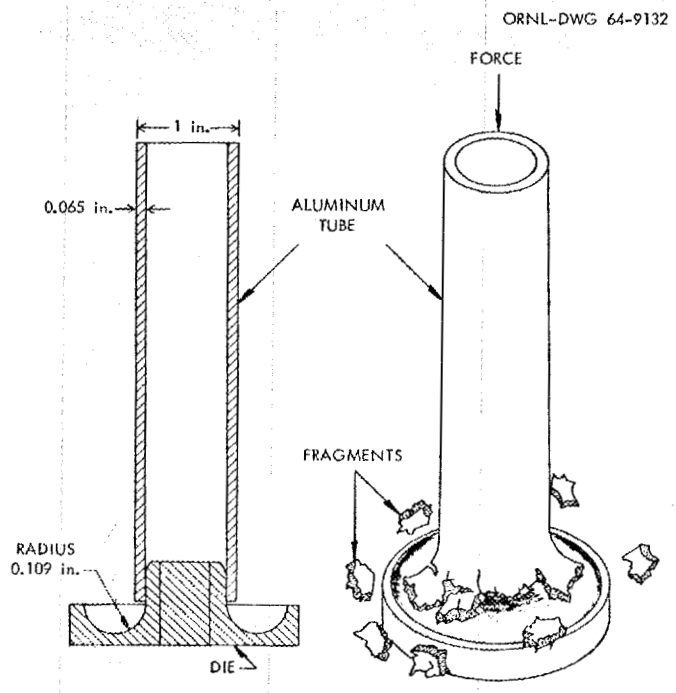

Fig. 4.20. Sketch Illustrating Fragmenting Process.

Under the conditions investigated, a 1-in. outside diameter aluminum tube with a wall thickness of 0.065 in., when forced over a die whose radius, r, was 0.109 in., absorbed over 7000 ft-lb of energy per foot of tubing. The load, in this case, was applied at a rate of 1 in. per minute. This is equivalent to an energy absorption capability of over 30,000 ft-lb of energy per pound of aluminum. Indications are that, under an impact load, this tube and die combination could absorb as much as 50% more energy in the fragmenting process.

Such a process might easily be adapted to provide impact protection for large, heavy casks during transportation.

4.5.2 Results of Testing and Quarter-scale Model of the Buffered Cask

Both the rubber and aluminum buffered model casks were tested under impact conditions. Aluminum honeycomb was placed between the concentric shells of the buffer in different patterns, as shown in Figs. 4.21 and 4.22. The casks and buffers were then dropped from 30 ft in various orientations onto a drop pad that approximated a solid, unyielding surface.

ORNL DWG. 63-82R1

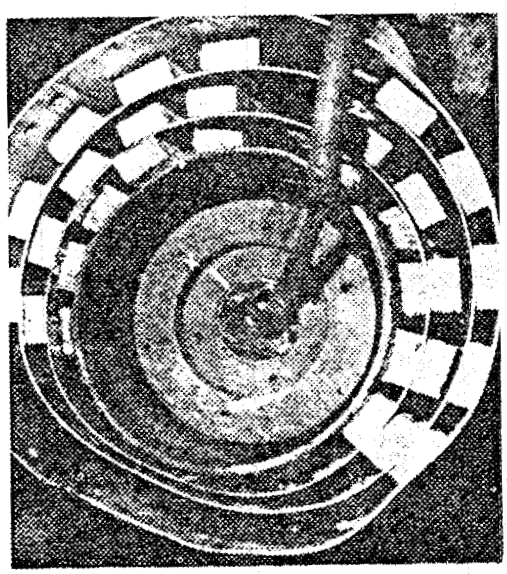

Fig. 4.21. An Aluminum Honeycomb Buffer After Impact - Top View.

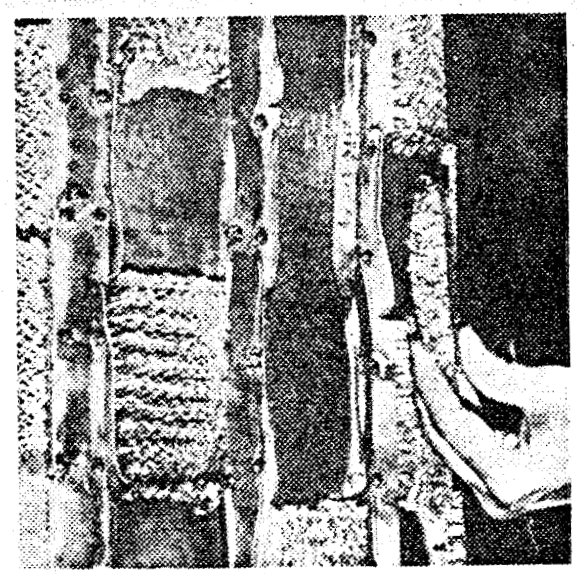

Fig. 4.22. A Buffer Showing the Crushed Aluminum Honeycomb After Impact.

An analysis of the scaling laws indicated that the deceleration received by the cask inside the buffer should be inversely proportional to the scale factor. Since the HAPO system was designed to reduce the deceleration of the cask to 50 g's when impacting from a 30-ft fall, a deceleration of 200 g's was expected on the 1/4-scale models when dropped from the same height.

An acceleration, velocity, and displacement record of the rubber buffer model is shown in Fig. 4.23. The maximum deceleration of the cask received in this drop from 30 ft was 224 g's, but the "smooth peak" value was about 200 g's which is in excellent agreement with the predicted value.

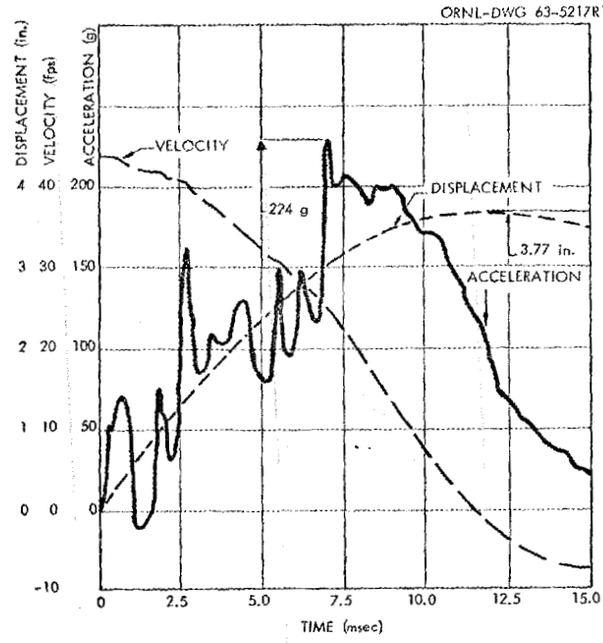

Fig. 4.23. Acceleration, Velocity and Displacement Record for a 30-ft End Drop of a Rubber Buffer Model.

A similar record for an aluminum honeycomb buffer model is shown in Fig. 4.24. The cask received a peak deceleration of 300 g's with a "smooth peak" value of considerably under 200 g's. This is certainly within acceptable limits and, if required, the honeycomb may be redesigned such that the "averaged" impact results will agree more closely to the specifications.

The use of a buffering system holds promise, particularly for shipments in which the cask is of a moderate size and in which the radioactive material could be particularly hazardous if the cask inner cavity was

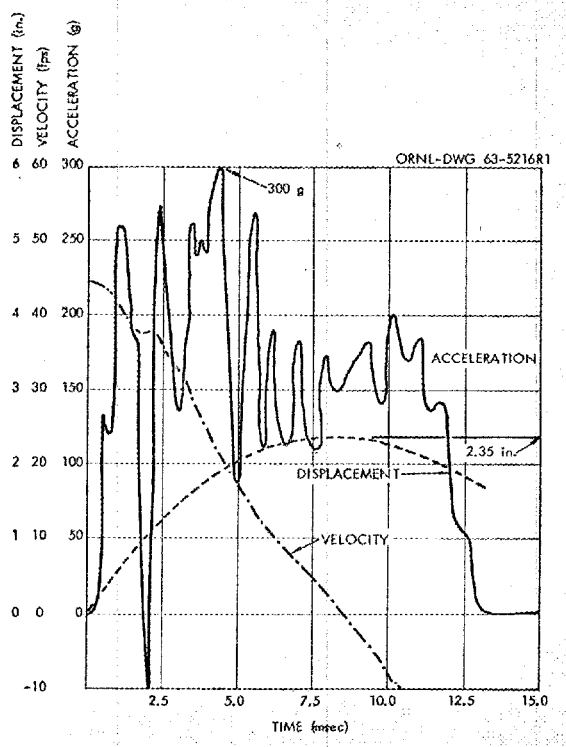

Fig. 4.24. Acceleration, Velocity and Displacement Record for a 30-ft End Drop of an Aluminum Honeycomb Buffer Model.

violated. The Hanford shipments of a strontium carbonate dry precipitate fall in these categories. In addition, the buffer provides a good thermal shield if the cask is involved in a fire (see Sect. 3.9.2).

4.6 Energy Absorption Properties of Lead and Steel

When two objects collide, some energy is dissipated in both bodies. If the collision is perfectly elastic (approached in the limit for low velocities and hard materials), the velocities of the two objects are defined after collision, based on the velocities before collision and the masses of the objects. If the collision is completely plastic, then the coefficient of restitution is zero and all the energy is absorbed in deformation of the two objects.

The proposed regulations (CFR Title 10, Part 72) indicate that a cask should be able to withstand the impact of a solid, unyielding object without exceeding the ultimate strength of any part of the cask or deforming the cask to the extent that fission products are released. This specification is hypothetical in that a solid, unyielding object cannot be obtained;

however, it can be approached. Thus, all the impact energy must be dissipated in plastic deformation of the cask, assuming that friction and shock waves produced by the impact dissipate a negligible amount of energy.

In the piston impact tests of the 1.3- and 6-ton casks discussed previously in Sect. 4.3.1, an indentation was formed in the steel shell roughly 2-1/2- to 3-piston diameters across; lead under the bent shell was pushed out of the way; the shell was cleanly sheared around the edge of the piston; and the lead, which is rather incompressible (Poissons ratio of .4 to .45), under the piston was pushed out of the way (see Fig. 4.25). Some fraction of the impact energy was required to effect each of these deformations.

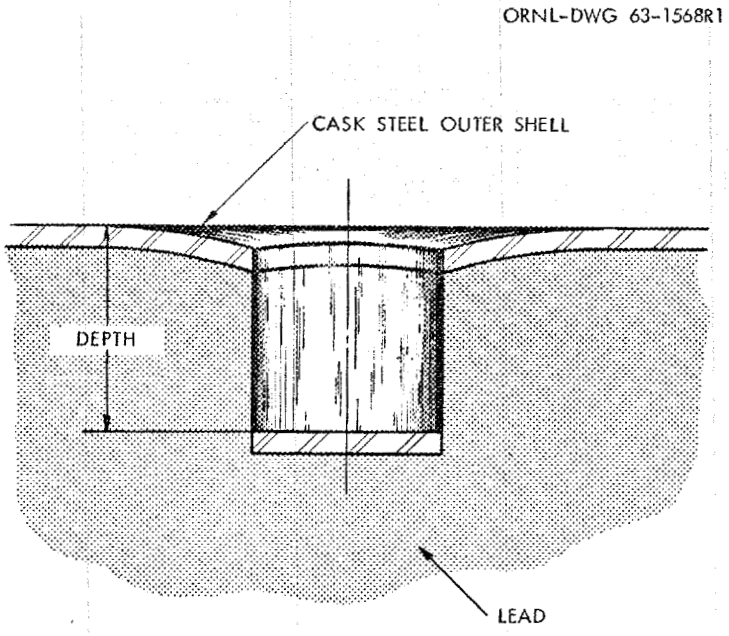

Fig. 4.25. A Schematic Cross Section of the Puncture Produced by the Impact of a Cask on a Piston.

4.6.1 Lead Penetration Tests

There has been an appreciable amount of work done on the determination of the amount of energy required to shear through and indent a steel plate, and penetrate into lead. The work that has been done to date in this area, along with equations that appear to describe the phenomona, is reported in this section. This data must be recognized as preliminary in nature, yet

useful in determining the effect of a piston impact on a steel-shelled, lead-shielded cask.

In order to better examine the properties of lead when impacting on a piston, without having to account for unknown amounts of energy dissipated in bending and shearing steel, four stainless-steel 4-liter beakers and one 2-liter beaker were filled with lead and dropped onto a 3/4-in.-diam piston such that the piston impacted on the lead at the mouth of the beaker. These drop specimens are shown in Fig. 4.26.

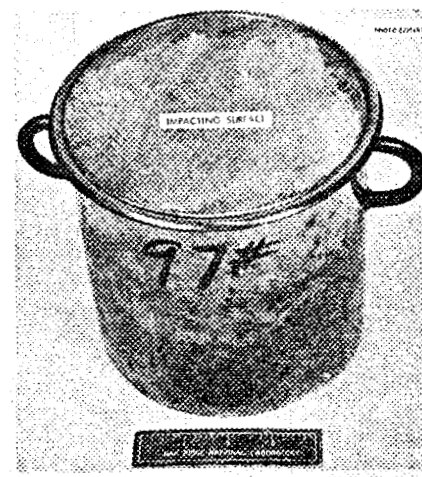

Fig. 4.26. Four-Liter Beaker Containing Lead Prior to a Piston Drop.

A full 4-liter beaker weighs about 100 lb and a 2-liter beaker 50 lb. The beaker-to-piston-diameter ratio in the large beakers was about 8.7 to 1, so the lead behaved approximately like an infinite body.[48] Side effects on the smaller 50-lb weights were neglected.

The normal method of recording such data is to plot the impact energy, E, against V, the volume of the indentation. This is done in Fig. 4.27.

The slope of the line passing through the data points has the dimensions of in.-lb/in.^{3} or lb/in.^{2}; this pressure is sometimes known as the dynamic-flow pressure.[49]

The dynamic-flow pressure, P, for elastic collisions is given by Tabor[50] and is of the form

$$P^5 = \frac{K''wh_1}{(D_1)^3} \tag{27}$$

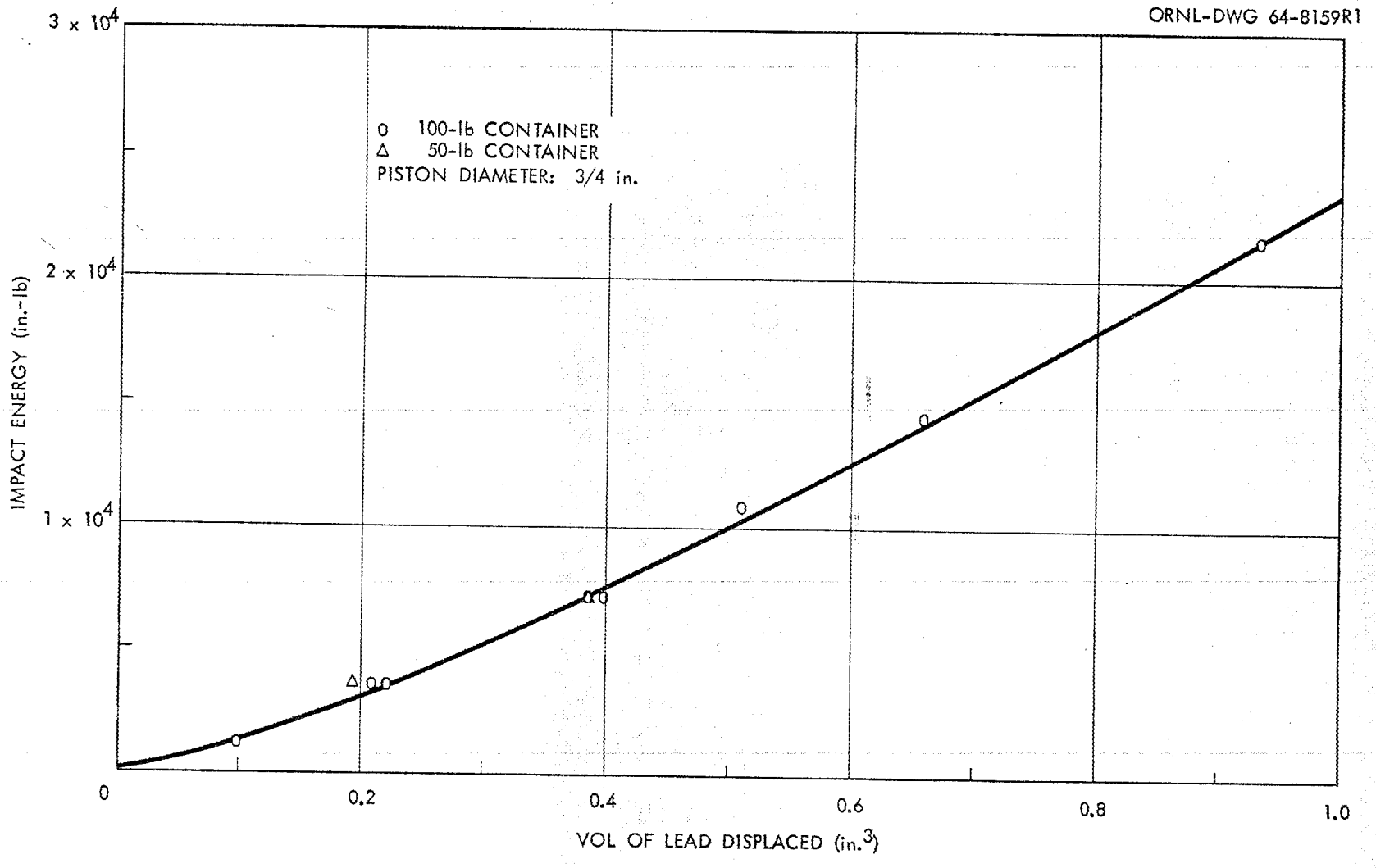

Fig. 4.27. Volume of Lead Displaced in Penetration Tests of Small Containers as a Function of Impact Energy.

where w is the container weight, h_1 the drop height, D_1 the diameter of the indenter, and K" a constant. If an equation of this form can be used to describe plastic collisions of a container dropped onto a flat-headed piston, then the data points in Fig. 4.27 may be described as follows:

Rewriting Eq. (27) and substituting the impact energy, E, for wh_1,

$$P = K'E^{1/5}(1/D)^{3/5} \quad . \tag{28}$$

But P, the dynamic flow pressure, may be replaced by $\frac{dE}{dV}$, the slope of the line obtained when E is plotted against V. Thus,

$$\frac{dE}{dV} = K'E^{1/5}(1/D)^{3/5} \tag{29}$$

Integrating and solving for E,

$$E^{4/5} = K(1/D)^{3/5}V + C \tag{30}$$

Since V = 0 when E = 0, then C = 0.
The constant K was determined from one data point in Fig. 4.27 and was determined to be 2.61×10^3 with the dimensions of $(\text{lb/in.}^2)^{4/5}$.
The equation

$$E^{4/5} = 2.61 \times 10^3(1/D)^{3/5}V \tag{31}$$

is plotted in Fig. 4.27 as the solid line and appears to describe all the data points quite well.

4.6.2 1.3-ton Cask Puncture Tests

Equation (30) was also used to describe the relationship between the impact energy and volume of lead displaced for a series of puncture tests in which a piston had to punch through a steel surface prior to contacting the lead. The volume was measured from the original cask surface. These tests were performed by dropping a 1.3-ton cask onto a 2-in.- and a 1.43-in.-diam steel piston. In addition, two puncture tests were conducted in which the 1.3-ton cask had a small portion of the outer steel shell removed so that the piston impacted directly upon the exposed lead. The data points of volume displaced versus impact energy are shown

in Fig. 4.28. The points in curves A and B were obtained by impacting the steel shell of the cask onto the two different pistons, and in curve C by impacting the exposed lead onto the 2-in.-diam piston. The difference between curves A and C is the energy required to shear through and indent the steel shell by the 2-in.-diam piston.

Attempts have been made to predict this amount of energy; once it is obtained, the value may be used to predict the constant C in Eq. (30).

The length of the cut produced by the 2-in.-diam piston is 2π or 6.28 in. In order to determine the approximate force in pounds required to make this long a cut, the thickness of the stock should be multiplied by the length of the cut and by the shearing strength of the material.

The energy required to puncture the material is then determined by multiplying this force in pounds by the distance through which it acts; that is, the thickness of the material.

Mathematically,

$$E_s = t\ell\sigma_s t = t^2\ell\sigma_s \tag{32}$$

where

t = thickness of material,

ℓ = the length of the cut, and

σ_s = the shearing strength of the material.

In normal metalworking, only a fraction of this energy (20 to 80%) is generally required for puncture since fracture of the metal occurs before penetration is complete. This, however, is true when the metal stock is backed by a die and not a soft material, such as lead. In this latter case, much of the steel surrounding the piston is affected, bending inward and creating a dished surface. It seems reasonable, however, that the total energy required will still be a function of the diameter of the piston and the thickness of the steel.

Thus, the entire amount of energy predicted in Eq. (32) has been used to estimate the energy required to shear and indent the steel shell. In most cases, Eq. (32) does, in fact, predict the energy required within 10% of the measured values. The one case in which it does not is discussed in Sect. 4.6.3.

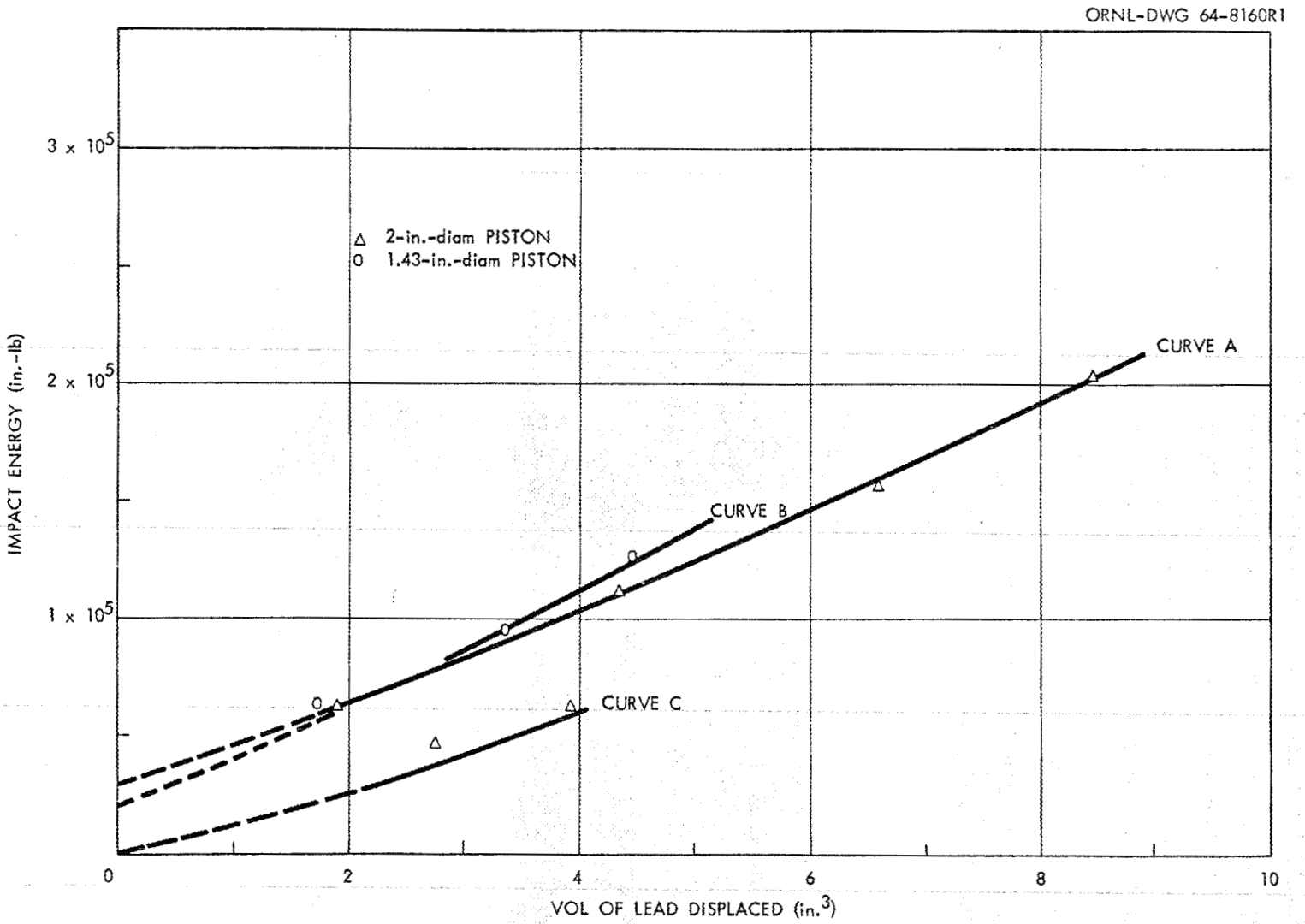

Fig. 4.28. Volume of Lead Displaced in Penetration Tests of 1.3-ton Casks as a Function of Impact Energy.

The approximate shearing strength of steels is given in Table 4.13.

Table 4.13. Approximate Resistance to Shearing in Dies* (Ref 51)

Material	Annealed State Resistance to shearing, psi	Hard, cold-worked Resistance to shearing, psi
Steel 0.10C	35,000	43,000
Steel 0.20C	44,000	55,000
Steel 0.30C	52,000	67,000
Steel 0.40C	62,000	78,000
Steel 0.60C	80,000	102,000
Steel 0.80C	97,000	127,000
Steel 1.00C	115,000	150,000
Stainless Steel	57,000	---

*Available test data do not agree closely.

The outer steel shell of the 1.3-ton cask was analyzed and found to have a carbon content of 0.13 percent. Interpolating from Table 4.13 for cold worked steel, $\sigma = 46{,}600$ psi. Since the shell thickness is 0.312 in. and the length of steel cut produced by a 2-in.-diam piston is 2π, the energy required to shear and to indent the steel shell is:

$$E_s = t^2 \ell \sigma_s = (.312)^2 (2\pi)(46{,}600) = 28{,}600 \text{ in.-lb}$$

From Eq. (3) when $V = 0$, $C = E^{4/5}$. Substituting 28,600 in.-lb for E, $C = 3.70 \times 10^3$. By substituting this value of C into Eq. (30) and picking one data point from curve A, the value of K was determined to be 2.47×10^3. That is,

$$E^{4/5} = 2.47 \times 10^3 \, (1/D)^{3/5} V + 3.70 \times 10^3 \qquad (33)$$

Equation (33) is plotted in Fig. 4.28 as the solid line, curve A, and describes all data points well.

In the case of the 1.43-in. piston, the diameter is smaller and thus less energy is required to shear and indent. From Eq. (32)

$$E_s = t^2 \ell \sigma_s = (.312)^2 (1.43\pi)(46{,}600) = 20{,}500 \text{ in.-lb}$$

and

$$C = E_s^{4/5} = 2.82 \times 10^3$$

The impact energy should be predicted by

$$E^{4/5} = 2.47 \times 10^3 (1/1.43)^{3/5} V + 2.82 \times 10^3 \qquad (34)$$

Equation (34), plotted in Fig. 4.28 as the solid line, curve B, agrees quite well with the data points for the 1.43-in.-diam piston impacts.

In the case of curve C, Eq. (33) was used with the constant C reduced from 3.70×10^3 to zero. This implies that no energy is required to shear through the outer steel shell and all of the impact energy is absorbed in displacing lead. (The data points plotted are those in which part of the steel shell was removed and the cask dropped onto the 2-in.-diam piston impacting on the exposed lead.) Again, the equation does a reasonable job of fitting the data.

4.6.3 6-ton Cask Penetration Tests

Two different casks weighing 11,350 lb (nominal 6-ton casks) were dropped on three different size pistons. The first cask, with an outer shell thickness of 0.375 in., was dropped onto a 2- and a 4-in.-diam piston. Equation (30) was used to correlate the energy-volume relationship, and Eq. (32) was used to predict the intercept of the curve. The constant K, as determined from one data point is somewhat less than K determined for Eqs. (31) and (33) as can be seen in Eq. (35).

$$E^{4/5} = 1.77 \times 10^3 (1/D)^{3/5} V + C \qquad (35)$$

The carbon content of the steel shell was 0.13% and from Table 4.12 for cold worked material, $\sigma_s = 46{,}600$ psi. For the 2-in.-diam piston $C = [(.375)^2 (2\pi)(46{,}600)]^{4/5} = 5.94 \times 10^3$. Substituting this in Eq. (35),

$$E^{4/5} = 1.77 \times 10^3 (1/D)^{3/5} V + 5.94 \times 10^3 \qquad (36)$$

Letting D = 2 in., Eq. (36) is plotted as the solid line, curve A, in Fig. 4.29.

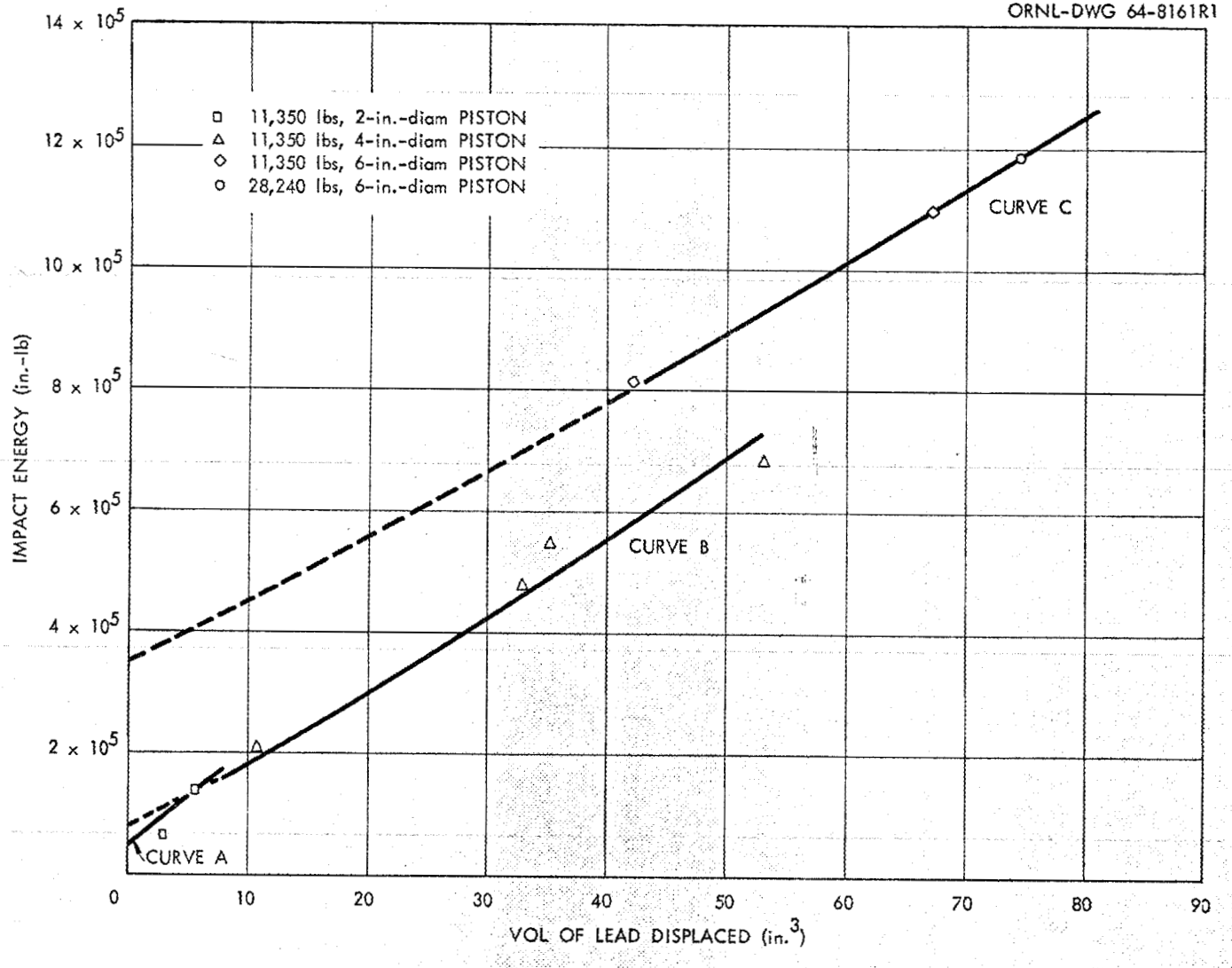

Fig. 4.29. Volume of Lead Displaced in a Piston Drop vs Impact Energy.

Since it requires twice the energy to shear through the shell with a 4-in.-diam piston as a 2-in.-diam piston, the constant C for the former is $[(.375)^2(4\pi)(46,600)]^{4/5} = 8.60 \times 10^3$.
Substituting this in Eq. (35),

$$E^{4/5} = 1.77 \times 10^3 (1/D)^{3/5} V + 8.60 \times 10^3 \qquad (37)$$

Letting D = 4 in., Eq. (37) is plotted as the solid line, curve B, in Fig. 4.29. Both Eqs. (36) and (37) appear to describe the data points quite well.

When Eqs. (35) and (32) were used to predict the line slope and intercept describing the data obtained when the second nominal 6-ton cask were dropped onto a 6-in.-diam piston (this cask had an outer shell thickness of 0.5 in., a carbon content of 0.2% and a σ_s = 55,000 psi), a problem arose. The slope was well predicted but the intercept calculated from Eq. (32) appeared to be about 35% below the value that would best describe the data points. That is, Eq. (32) predicted the energy required to shear and indent the steel shell at 260,000 in.-lb, whereas curve C indicates this energy (and intercept) should be about 350,000 in.-lb.

The reason for this difference is presently unresolved, but data obtained at Franklin Institute indicate that as the steel shell gets thicker, the indentation around the point of impact of a piston covers a larger area for any given piston diameter. As the affected area increases, more energy is required before penetration through the steel is actually achieved.

It is possible that for outer steel shells thicker than 0.5 in., Eq. (32) may continue to underestimate the energy required to shear through them. Additional experimental work will be required to determine the form of Eq. (32) when computing the energy absorption of thick shells.

4.6.4 Recommended Cask Outer Shell Thicknesses[52]

Franklin Institute has developed a curve from impact data of the outer carbon steel shell thickness required to keep a particular weight cask from penetration of the outer shell in a 3-1/2-ft free fall onto a 6-in.-diam piston (see Fig. 4.30). If the shell thickness is greater than that given by the curve for a given weight, shell penetration should not occur. The

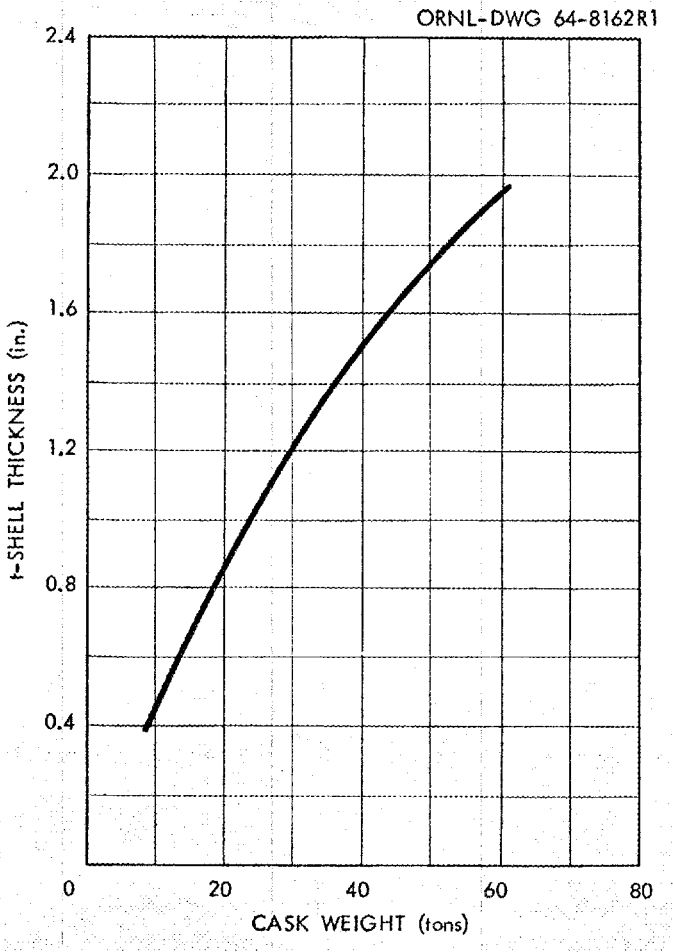

Fig. 4.30. Approximate Shell Thickness Required for no Penetration vs Cask Weight. Drop specification: 3-1/2-ft Drop onto a 6-in.-diam piston.

original data from which the curve was derived is of a preliminary nature.

It is possible that as additional data are obtained, this curve may be somewhat modified.

4.7 Some Useful Formulas in Cask Design

According to Sect. 4.2, a cask, when regarded as a simple beam and supported at its ends along the major axis, must be able to withstand 10 times the cask weight without exceeding the ultimate strength of any part of the cask.

To meet this specification, the outer shell of the cask is normally considered to be the only supporting member; this assumption provides a

conservative, but simple, method of analyzing the cask.

The stress in the outer steel shell of the cask supported at the ends of its major axis is given by

$$S = \frac{M_b C}{I} \tag{38}$$

where

S = the maximum bending stress, lb/in.^{2}

M_b = the bending moment, in.-lb

C = distance from the central axis to outermost fiber, in.

I = moment of inertia, in.^{4}

But M_b is

$$M_b = \frac{WL}{8} \tag{39}$$

where

W = the cask weight, lb

L = the length of span between the supports, in.

then for uniform load of 10 times the cask weight, Eq. (39) may be written

$$M_b = \frac{10\ WL}{8} \tag{39a}$$

The moment of inertia, I, for circular and rectangular cross sections are given by Eqs. (40) and (41).

The moment of inertia about a horizontal axis through the centroid for the circular cross section given in Fig. 4.31 (a) is

$$I = \frac{\pi}{4}\,(r_2^4 - r_1^4) \tag{40}$$

and for the rectangular cross section, given in Fig. 4.31 (b) is

$$I = 1/12\ [b_2(d_2)^3 - b_1(d_1)^3] \tag{41}$$

Example 4.3. Determine the maximum stress in the outer shell of the cask used to transport Yankee fuel elements. The dimensions of the cask are given in example 3.3. Assume that the cask weight is 75,000 lb.

Solution. From example 3.3, the cask is a cylindrical design with a 45-in.-OD and a 1-in. stainless steel outer shell thickness; i.e. r_1 = 43/2 in. and r_2 = 45/2 in., and from Eq. (40),

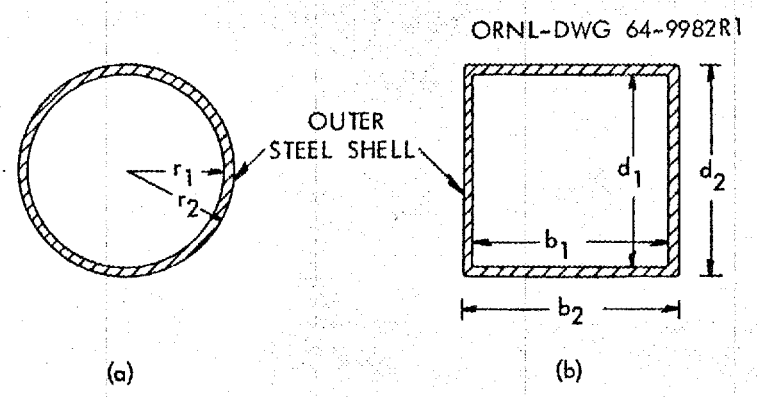

Fig. 4.31. Typical Circular and Rectangular Cross Sections.

$$I = \frac{\pi}{4}\left[\left(\frac{45}{2}\right)^4 - \left(\frac{43}{2}\right)^4\right]$$

$$= 33{,}400 \text{ in.}^4$$

If the weight of the cask is 75,000 lb and its length is 150 in., then from Eq. (39a)

$$M_b = \frac{(10)(75{,}000)(150)}{8} = 1.41 \times 10^7 \text{ in.-lb}$$

From Eq. (38)

$$S = \frac{M_b C}{I} = \frac{(1.41 \times 10^7)(45/2)}{3.34 \times 10^4}$$

$$= 9{,}500 \text{ psi}$$

Since the ultimate strength of stainless steel is approximately 75,000 psi, the cask meets this criteria.

As indicated in Sect. 4.2, the code also requires that the lid and lid-closing mechanism (normally bolts) must be able to withstand at least 60 times the weight of the lid plus the contents of the cask without exceeding the ultimate strength of the bolts. The purpose of this specification is to prevent the cask lid from breaking loose in an impact in which the contents are thrown against the lid and the weight of both the lid and contents act against the lid closure bolts.

Since the specification requires that

$$60(W_\ell + W_c) = B\,\sigma_u A_B \tag{42}$$

where

W_ℓ = weight of lid, lb

W_c = weight of contents, lb

B = number of bolts

σ_u = ultimate strength of bolts, psi

A = cross-sectional area of bolt, in.^{2}

Equation (42) may be solved for the required number of bolts if the ultimate strength of the bolt material is specified. This was done for stainless steel bolts whose ultimate strength is 75,000 psi, and the results are shown in Fig. 4.32.

Thus, if a lid plus contents of a cask weighed 7500 lb, eight 1-in. bolts would be required to meet this specification. For a cask lid plus contents weight of 12,000 lb, eight 1-1/4-in. bolts or sixteen 7/8-in. bolts would be required.

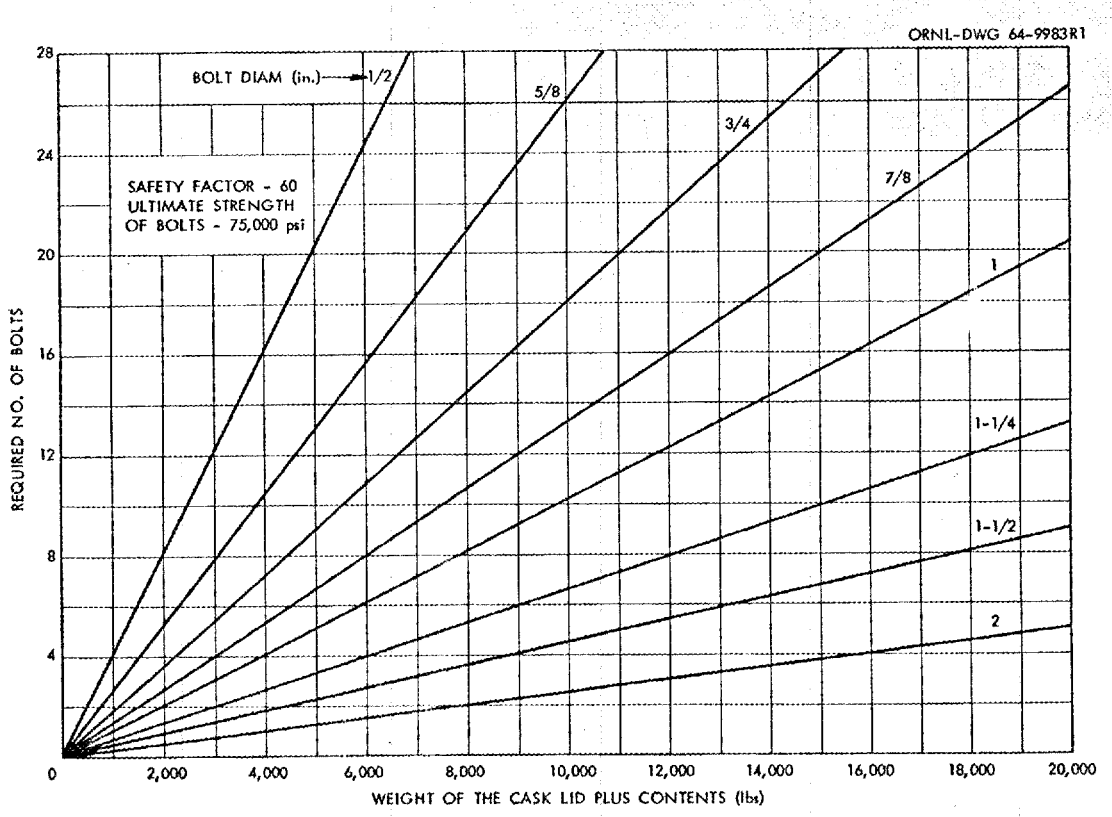

Fig. 4.32. Number of Bolts Required as a Function of the Weight of the Cask Lid Plus Contents.

4.8 Design Considerations

At this point, it is important to re-emphasize the difficulty in translating some cask performance specifications into design specifications.

Useful calculations concerning shipping cask design can be made on the basis of a static system as have been done in Sect. 4.7. However, to a large degree, assurance of impact resistance must presently be based on actual cask tests rather than some analytic model.

It is necessary, therefore, to examine and understand the manner in which the casks behave under various impact conditions and exercise some judgment in cask design based on these results.

It is obvious that, in order not to fail, much of the kinetic energy that the cask has at the time of impact must be absorbed in places other than the cask shell (assuming that fracture or rupture of the cask shell constitutes failure). This energy must be absorbed in the lead shielding, cask fins, a buffer, the vehicle transporting the cask if it is adequately tied down, or in the object that the cask strikes. This last energy sink has been administratively ruled out in the proposed regulations.

The energy absorption capabilities of lead have already been discussed in Sect. 4.6. However, reasonable amounts of energy may also be absorbed in the deformation of steel fins.

One design which may be used to insure that the fins bend under an impact loading and do not stiffly transit the full shock to the cask surface is to prebend the fins as shown in Fig. 4.33. In this design, the fins will bend no matter in which direction the impact occurs.

In order to take advantage of the vehicle as an energy absorber, the cask must be securely attached to rigid support members of the vehicle frame which are capable of absorbing appreciable amounts of energy in deformation before the cask is released.

Cask buffers have been used to protect the cask during shipment. Surrounding buffers were discussed in Sect. 4.5. In addition to this type, Du Pont has employed a shock absorbing draft gear when its cask was attached to the railcar as a floating load. The draft gear, which is similar to a railcar coupler, is capable of absorbing some energy during impact as the cask moves against the gear's action.

ORNL-DWG 63-5227R1

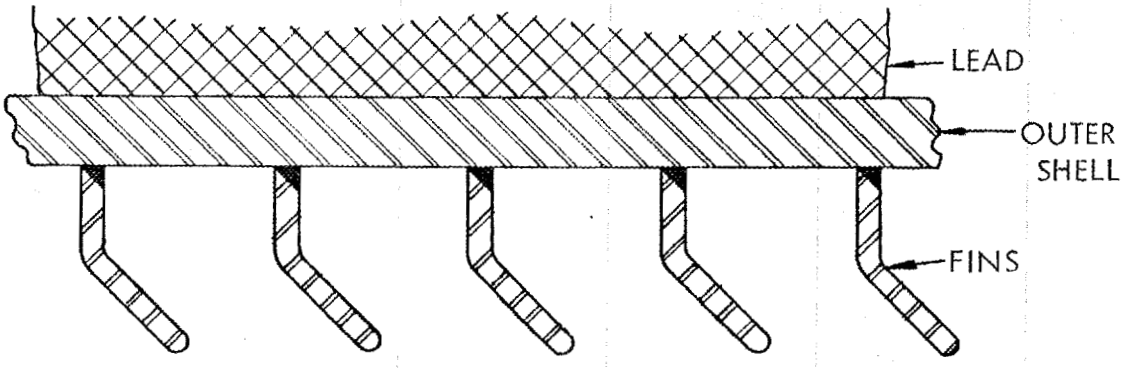

Fig. 4.33. Proposed Fin Design.

Good cask design practices dictate that the cask shell should be designed with a minimum number of areas in which high-stress concentrations would occur in the event of an accident. Obvious areas are points of metal discontinuity, unprotected trunnions, cask corners, and edges. Welds should be full penetration.

One of the most damaging types of impact for a lead-shielded cask, other than the penetration type, is the corner or edge impact since high localized stresses can produce cracking in the shell or weld areas.

The drawing in Fig. 4.34 shows a schematic lead-shielded cask design which has a number of desirable features suggested as a result of the testing program. All welds are full penetration. The cask corners have been rounded off to remove potential high stress areas since shielding in these areas is not necessary. The cover plate, which has been recessed to prevent direct impact on the bolts, is bolted into a heavy steel ring that should withstand the pinching effect (the casks tend to assume an oval shape) in a horizontal, side drop. The heavy inner shell prevents cavity deformation that could damage radioactive material at the time of

ORNL-DWG 64-7251R1

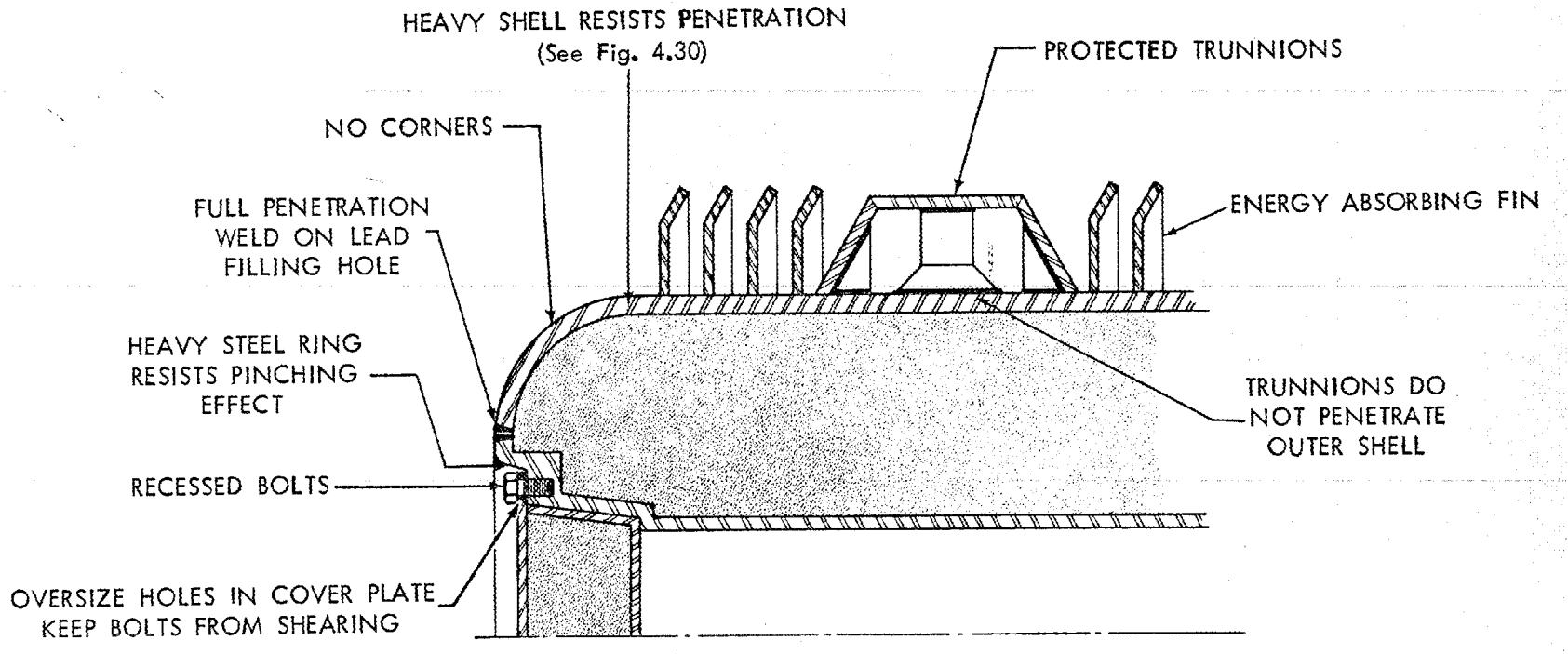

Fig. 4.34. Schematic of a Cylindrical Cask Design Incorporating Desirable Safety Features Based on Impact Tests for Horizontally Transported Casks.

impact. Energy absorbing fins have been welded to the outer shell and the trunnions have been protected.

4.9 Tiedowns

One aspect of cask design, which is often underrated, is the method of tiedown of the cask to the skid or to the vehicle. (Skids are used on casks to make the casks safer to handle and to spread the weight of the cask over a wide area.) The object of the tiedowns is not only to keep the containers in position during normal travel, but also to reduce the effect of a severe accident should one occur.

Casks weighing over 500 lb must be fitted with skids or otherwise designed so that excessive floor loadings will be prevented. Normally, cask skids are designed so that the floor loading is less than 500 lb/ft^2. For overseas shipments, the floor loading limit posed by most cargo ships is generally somewhat greater, ranging from 850 to 1000 lb/ft^2.

There are two schools of thought on the method of tiedowns, both of which have merit. The first is that the cask should be rigidly fastened to the vehicle, essentially becoming a part of it; and in case of accident, the vehicle body could crush, absorbing appreciable amounts of energy of the cask-vehicle system, reducing the amount of energy that the cask itself would have to absorb. The second is that the load should be "floating" but restricted in movement which would allow, to some extent, controlled deceleration of the cask in the event of an accident.

Most of the tiedowns to date have been of the rigid type and have been satisfactory. However, the Du Pont 70-ton cask has employed the floating-load concept, in which the tiedown bolts allow limited motion of the cask relative to the car if the frictional forces between the cask and the flat car are overcome.

Draft gears, which are put on railcar couplers to take up the shock of coupling, have been suggested as energy absorbers for floating loads and are capable of absorbing up to about 40,000 ft-lb of energy each.

Hanford's policy of tiedowns for their buffered cask on railcars has been somewhat different. Since the buffer that is attached to the cask is designed to reduce the number of g's that the cask body will be

subject to, the tiedowns are designed to break with a severe shock (about 12 g), allowing cask and buffer to roll free; this would reduce the chance of it being crushed by the colliding railcars. The buffered cask tiedowns are shown in Fig. 4.35.

It is probably unnecessary to require tiedowns to withstand continuous or static loadings much greater than 20 g's since such loadings would start to destroy the vehicle, even though short-duration shock loadings can go much higher without appreciable vehicle damage. In any case, the tiedowns must be adequate and good rigging practices must be followed. Figure 4.36 shows the results of poor rigging practices in tying down a 7-ton cask to a trailer bed. The cask was centered, and chains and boomers (a chain tightener) were used to fasten the load in place. Not enough blocking was used around the bottom of the skid. In transit, vibration caused the boomers to open, and the load shifted with the result that the trailer almost tipped over.

Two acceptable, common methods of tiedowns are the four-way tie and the basket hitch. The former method is used for heavier loads and the latter method for lighter ones. Figure 4.37 shows a schematic drawing of the two methods. Figure 4.38 shows a 7-ton cask tied down by the four-way tie method.

Best rigging practices for a rigid tiedown entail tying the cask down with a cable looped around a strong support member in the vehicle, and then fastened to itself by means of Crosby clamps. In this way, the chance of the cables accidentally coming loose during transit is practically eliminated. If turnbuckles are used to tighten the tiedown cables, they must be spiked to prevent their vibrating open. Bolts can be used to fasten the cask to the transporting vehicle and, where applicable, are preferred over blocking the cask in place with lumber.

The general tiedown procedures suggested by the Idaho Operations Office, Idaho Falls, Idaho, are reported below.[53]

These procedures can be used as a guide; however, due to the variety of shipping containers all applicable shipments and handling thereof must be acceptable to the AEC safety engineer who may direct additional action as the situation demands.

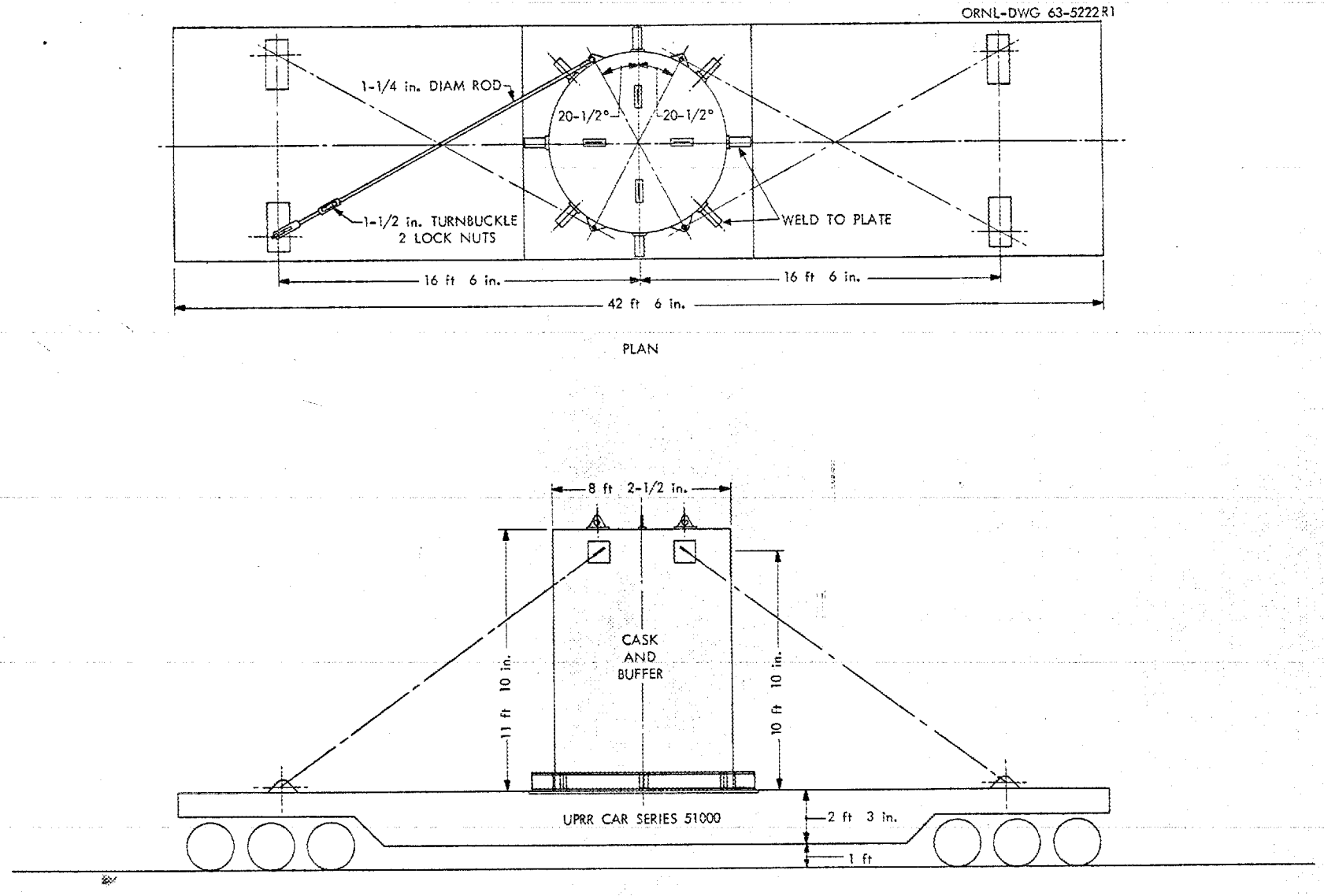

Fig. 4.35. Tiedown of Hanford's Buffered Cask.

ORNL-PHOTO 52969R1

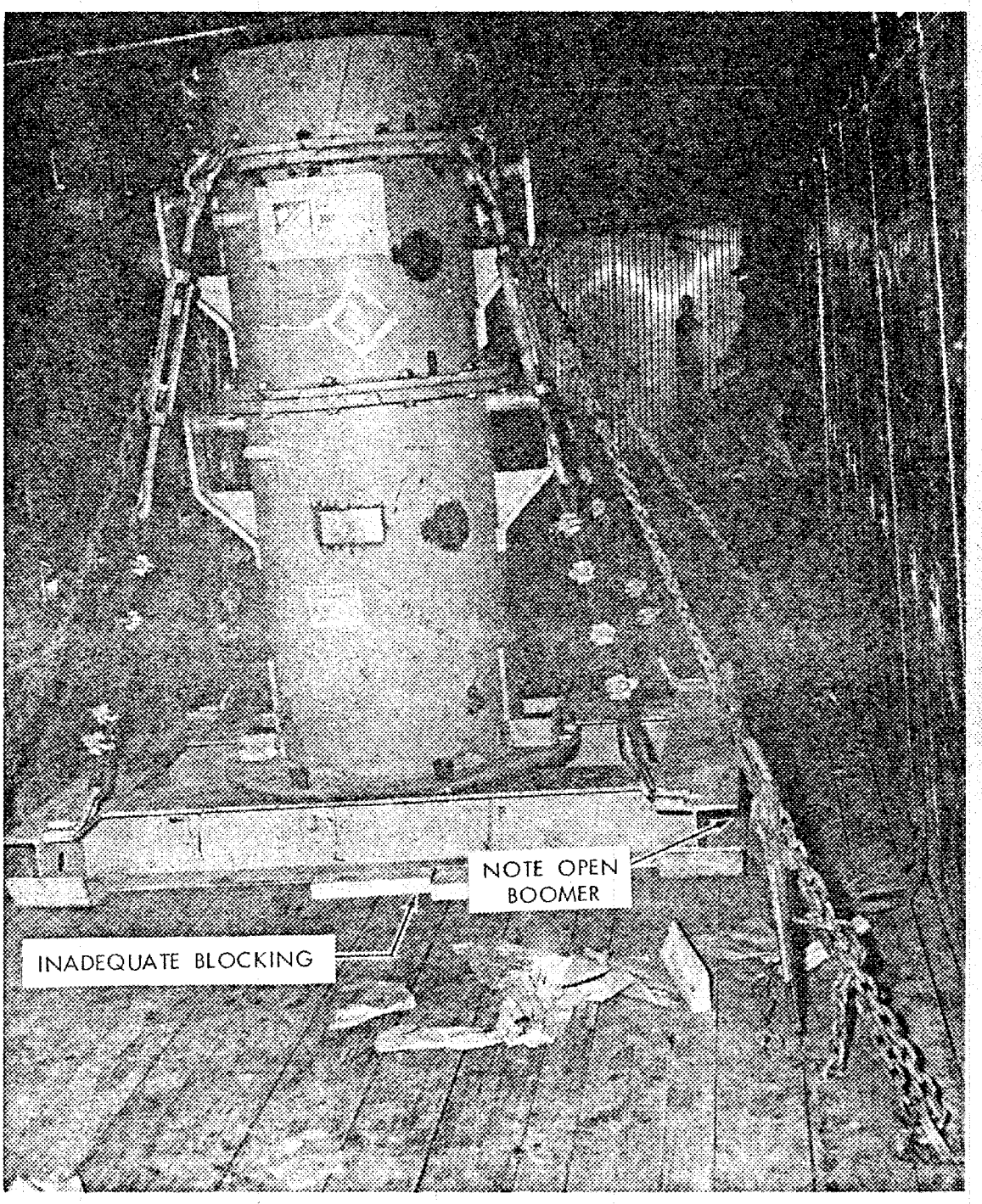

Fig. 4.36. Results of Poor Rigging Practice on a 7-ton Cask.

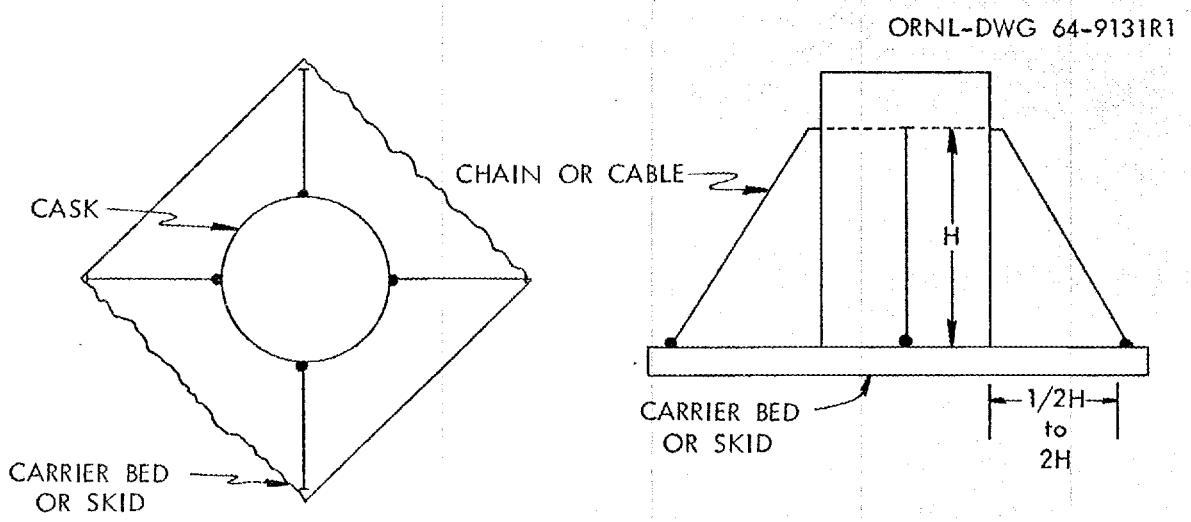

A. A Typical Four-Way Tie-Down for Heavy Containers.

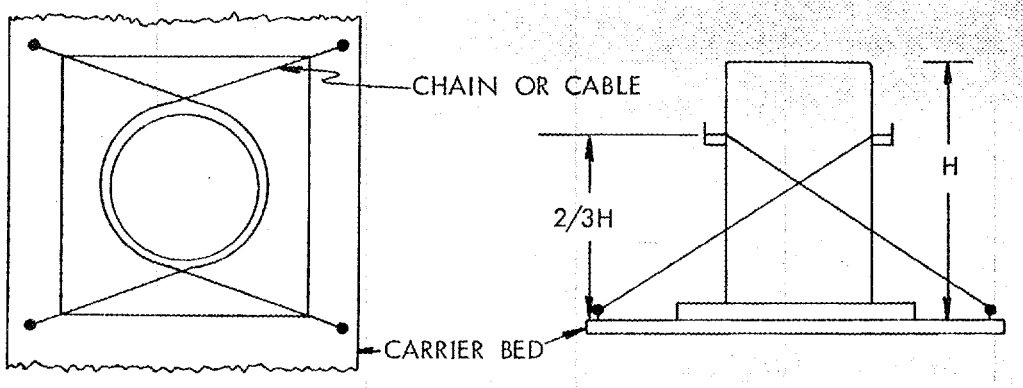

B. A Basket Hitch Tie-Down for Light Containers.

Fig. 4.37. A Schematic Drawing of Two Typical Tie-Down Methods.

ORNL PHOTO 52994R1

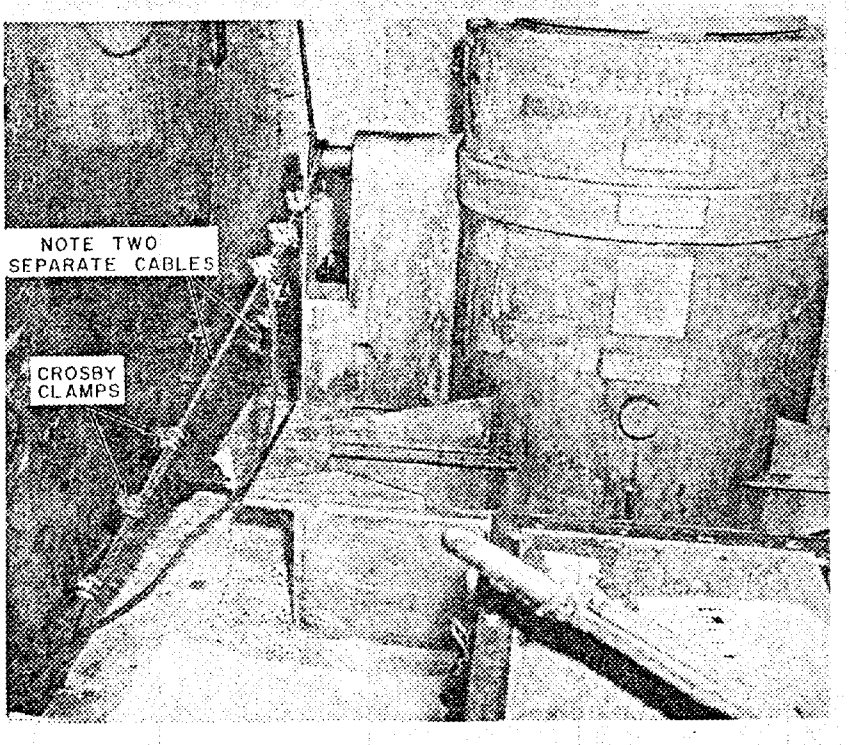

Fig. 4.38. A Four-way Tiedown on a 7-ton Cask.

a. Good rigging practices must be observed at all times.

b. The vehicle must be in good operating condition, of adequate capacity to carry the load, and provided with tie rings or other acceptable means of securing the load to the frame.

c. The load must be positioned on the vehicle with consideration for: minimum stress on the carrier, good tie-down positioning, and acceptable wheel load and drivability.

d. All radioactive materials being moved must normally be secured; however, some specific movements may be accepted when suitably confined in an enclosed bed.

e. Chains must be used to tie down short-haul shipments (< 100 miles) when in compliance with all the following conditions:

   (1) Chain hooks and boomers must be in good condition and of adequate size for weights involved.

   (2) Pads or blocks should be used to eliminate sharp corners or edges.

   (3) Boomer handles shall be wired to prevent opening.

(4) Hooks must be of sufficient depth to hold a full link.

(5) Containers weighing more than three tons should be secured from four directions with independent chain tie-downs.

(6) Containers weighing less than three tons may be secured with two chains independently boomered and opposing each other with a basket hitch.

(7) Tie points on containers shall be such that the containers are held securely and chains cannot work or vibrate loose.

(8) Knots in chains must not be permitted.

f. Cables should normally be used to secure long-haul shipments (> 100 miles) in compliance with the following conditions:

(1) Cable should be in good condition. Five-eighths-inch-diameter improved plow steel wire rope should be provided for tie-down of containers weighing up to 15,000 lb.

(2) Two cable clips of the Crosby type (see Fig. 4.38) should be minimum for securing cables on containers weighing up to 3,500 lb.

(3) Three cable clips of the Crosby type should be minimum for securing cables on containers weighing over 3,500 lb.

(4) The base end of all cable clips shall be on the live (or connecting) end of the cable and spaced approximately 6 rope diameters apart.

(5) Cables shall be drawn tight and shall be protected from sharp edges or corners as necessary.

(6) Opposing cable basket hitches may be used on containers weighing up to 15,000 lb. Above 15,000 lb four independent cable ties should be the minimum.

Additional discussion of tiedowns is given in the booklet, "Shipping Radioactive Material," by R. V. Batie and D. E. Patterson, Safety and Fire Protection Bulletin No. 6, USAEC, revised October, 1960.

5. SHIELDING

5.1 Problem

The problem of proper shield design is important. On the one hand, the shielding must be adequate to reduce the external radiation from the largest expected source to acceptable tolerance levels; on the other, the cask should be as light as possible since unnecessary bulk adds both to the initial cost and, most particularly, to the recurring shipping charges. In order to minimize fuel cycle costs, the shipping cask must be optimized to obtain the largest fuel-to-cask-weight ratio consistent with limitations on heat transfer, criticality, structural integrity, and cask weight.

5.2 Regulation

The ICC's Tariff No. 15 (see appendix 1) specifies that the external radiation level should not exceed 200 mrem/hr at the accessible surface of the cask, nor 10 mrem/hr at a distance of one meter from the source. The proposed CFR Title 10, Part 72, suggests the dose not exceed 200 mrem/hr at the accessible surface of the cask, nor 10 mrem/hr at one meter from the accessible cask surface. This difference in wording can cause difference in the shielding and weight of a cask. It is hoped that these differences will be resolved in the near future in favor of the "accessible cask surface."

In addition, according to the proposed Code of Federal Regulations, if a single cask has exclusive use of a vehicle (whether rail or truck), the radiation level should not exceed 10 mrem/hr at a distance of 3 meters from the cask surface. If any material in the cask which aids in shielding is lost (such as cooling water lost in an accident), the radiation level should not exceed 1 rem/hr at one meter from the accessible cask surface.

5.3 Comments on Shielding Design

Since there are many texts and reference documents concerning the subject of shielding, some of which are noted in references 54-58, the theory and calculational methods will not be discussed here.

Shielding calculations are either based on the results of the "moments method" or are "Monte Carlo" calculations. The moments-method calculations give the gamma-ray dose rate from a point source in an infinite, homogeneous medium; various media may be considered. The results are often used for finite media by integrating over all sources. This normally introduces only a small error. If the shield is laminated, this method is generally inadequate, and Monte-Carlo methods must be employed. The Shielding Design Code[59] (SDC) is an example of a code that analytically integrates the point kernel for point, line and surface sources. Volume sources are reduced to surface or line sources in accordance with information experimentally determined or theoretically calculated from Monte Carlo treatments of volume sources.

The SDC code was designed to accept a source containing 12 energy groups, to predict the shielding necessary to reduce the dose rate to a specified level, or to predict the dose rate through a known or existing shield thickness. The source may be a point, line, disk, plane, slab, cylinder, or an annular cylinder and may have an isotropic or cosine distribution. Materials, which are available for shielding in this code, include water, aluminum, iron, lead, uranium, four types of concrete (normal, barytes, magnetite, and ferrophosphorus), and glass with a density of 2.67, 3.27, or 6.22 gm/cc. The code is written for the IBM-7090, and a typical running time is one minute for up to 12 separate problems. It is particularly suited for parametric shielding studies as well as design work.

The "Monte Carlo" method is a statistical treatment of the radiation transport problem which usually requires the use of a digital computer. In principle, it can handle any geometry; but in practice, generally only simple geometries are treated. The method is not well suited to parametric studies because of cost.

Information on shielding codes which are presently available may be obtained by writing or calling:

Radiation Shielding Information Center
Oak Ridge National Laboratory
P. O. Box X
Oak Ridge, Tennessee

5.4 Comments on Cask Shielding Material

5.4.1 Types of Casks

The most common material of construction used in the United States for a gamma shield is lead, due to its low cost (about $0.12/lb), high density, and its ability to be easily fabricated, even in odd shapes.

Lead, alone, is used extensively for shielding small radioactive isotope sources. When larger sources are transported, the lead must be encased in steel for fabrication, protection, and handling purposes. Disadvantages to using lead as the primary shielding material are several fold. For example, lead contracts appreciably upon solidification from the molten state (over 3% by volume)[60] and thus care must be taken during the pouring of large steel-encased shields so that unwanted voids are not inadvertently introduced. In addition, lead often does not wet or bond to stainless steel satisfactorily, which also contributes to the formation of unwanted voids. If the radiation source material produces appreciable heat, uncontrolled air spaces or gaps must be avoided to keep source temperatures at a minimum.

Fire presents a hazard to lead-filled casks. Lead has a high coefficient of thermal expansion, quite a bit greater than steel which is normally used to encase it (Fig. 5.1). It is evident that high pressures may develop in the cask, which could result in broken welds and subsequent loss of shielding, if it is subject to a fire. Certainly if leaks do not occur, then there will be permanent damage to the steel shell if the fire is hot enough.

The British have performed some heat tests on small lead-filled, steel-shelled casks[33] and found that even the use of controlled voids left in the cask shield to provide thermal expansion space for the lead was not entirely satisfactory. Melting of the lead would not always take place around the void area, thus did not prevent pressure buildup and the loss of lead in other areas. In addition, the position of the void after cooling, even if no lead was lost, was not predictable and could result in areas of inadequate shielding.

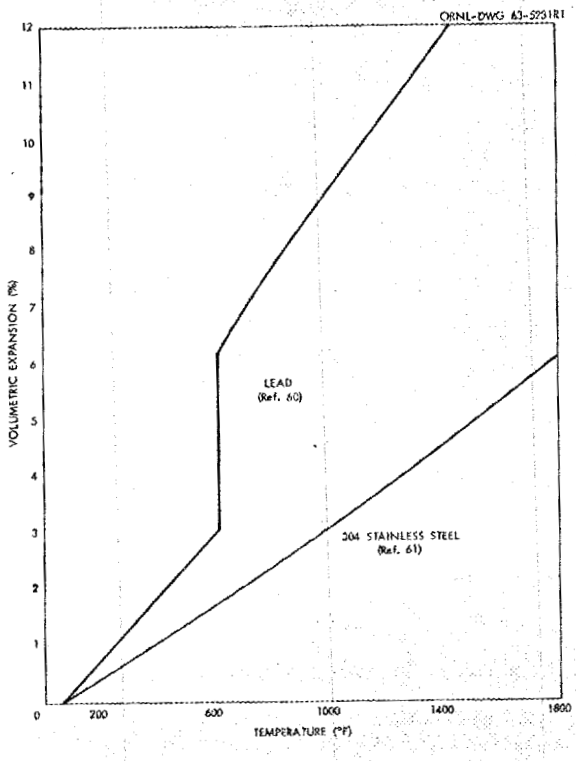

Fig. 5.1. Volumetric Expansion of Lead and Steel as a Function of Temperature.

A very difficult decontamination problem can arise if any welds in the steel shell break permitting contaminated coolants to leak between the shell and the lead shielding. The situation is dangerous since the cask cannot be completely decontaminated and the presence of trapped liquids inside the steel shell presents an explosion hazard in case the cask is involved in even a small fire.

Attempts have been made to counter some of the objections to lead as a shielding substance. In small containers, a lead-bismuth alloy can be used with a controlled coefficient of thermal expansion (see Sect. 3.8). Thus, the shielding expansion will present no problem if exposed to fire. The alloy, however, is expensive and has a low melting point.

For small casks which contain small heat sources, it is possible to insulate the outside of the container for fire protection (see Sect. 3.9).

The approximate weight of a lead-shielded cylindrical cask may be quickly estimated from Fig. 5.2, which presents the weight per foot of an annular shield and the total weight (<u>not</u> per foot) of two end plugs.

ORNL-DWG 64-6669R1

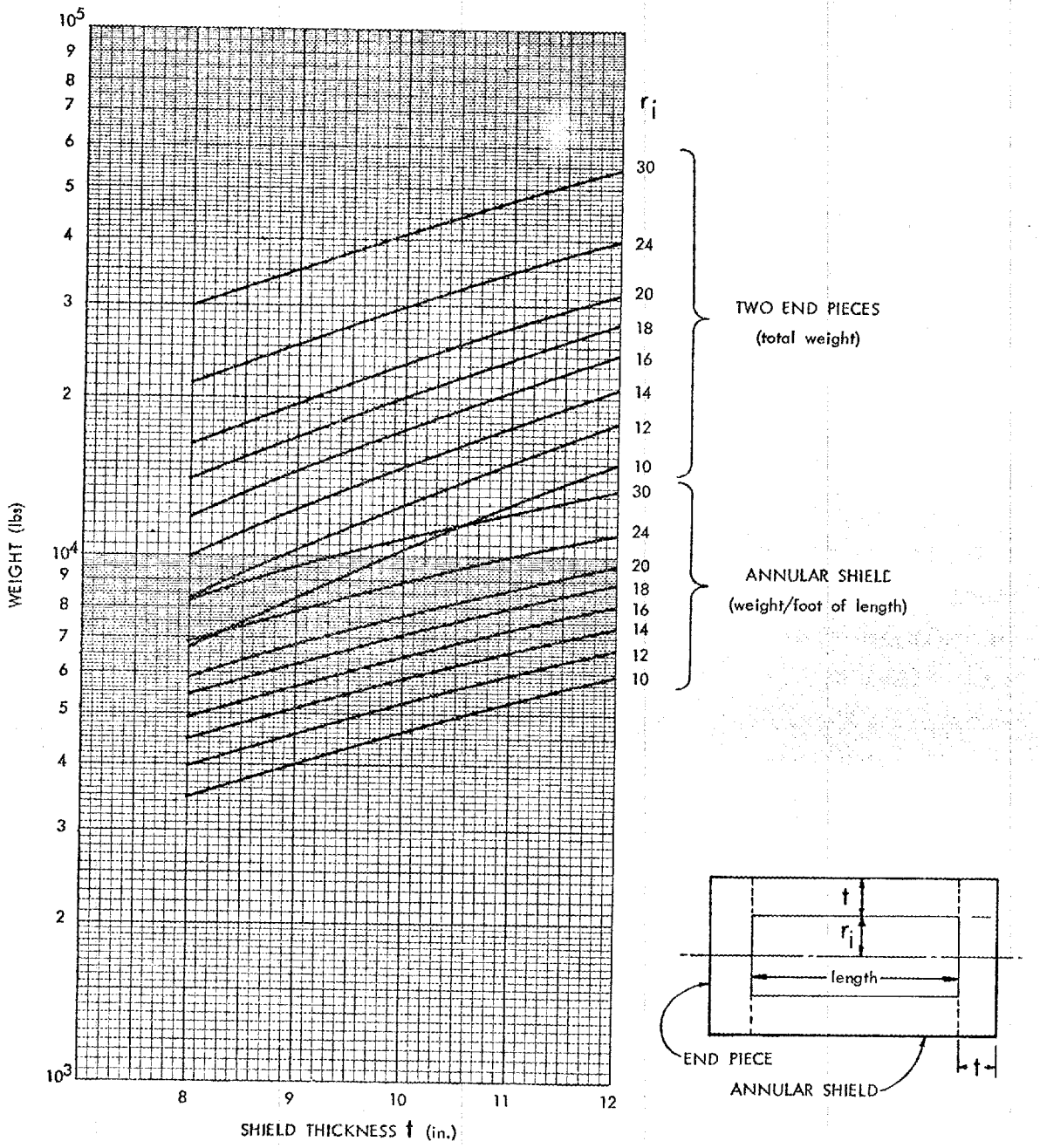

Fig. 5.2. Weight of a Cylindrical Lead-Shielded Cask; Inside radius, r_i, as a parameter.

Problem 5.1. Determine the weight of a cylindrical cask whose inside diameter is 32 in., shielding is 10-in. thick, and the cavity is 8-1/2 ft long.

Solution. From Fig. 5.2, the weight per foot of a 10-in.-thick annular cylinder of lead, whose inside radius is 16 in., is 5950 lb/ft. The weight of the 8-1/2-ft-long cylinder is

$$(8.5 \text{ ft})(5950 \text{ lb/ft}) = 50{,}500 \text{ lb}$$

The weight of two end plugs of the cask whose thickness is 10 in. and whose inside radius is 16 in. is 17,400 lb. The total weight of lead is 17,400 + 50,500 = 67,900 lb.

The weight of steel shell containing the lead is obviously a function of the steel thickness and container size, but is approximately 15% of the weight of the lead. The approximate total cask weight without any skid is, therefore, (1.15)(67,900) = 78,000 lb.

The British have made a number of large casks from cast iron or cast steel containing no lead or other high-density material. This eliminates the problem of differential thermal expansion found in the lead cask with their steel shells. The shielding does not melt under the action of a normal petroleum fire, and the impact qualities are apparently improved.

The total cost of a steel cask is comparable to a lead cask with the same cavity size; since the steel cask weighs more, its unit cost is less, around \$0.40 to \$0.50 per lb. It has been reported that in England expected costs of steel casks ordered in large (45 cask) quantities might have unit costs as low as \$0.18/lb.[62,63]

The main disadvantage with steel casks is that, for an identical cavity size, a steel cask is larger and weighs considerably more than a lead-shielded cask. This, in turn, means that transportation charges will normally be proportionally higher for the steel cask. The weight ratio obtained by using denser material is shown in Fig. 5.3 as a function of cavity volume (the weight ratio is also a function of the source strength).

Depleted uranium has been used for shielding in small casks. Uranium has an advantage over lead because it is a much more dense metal (18.8 compared to 11.34 gm/cc) and, for the same cavity size, will be a smaller unit and weigh less. This advantage tends to disappear as the cavity size becomes large (Fig. 5.3).

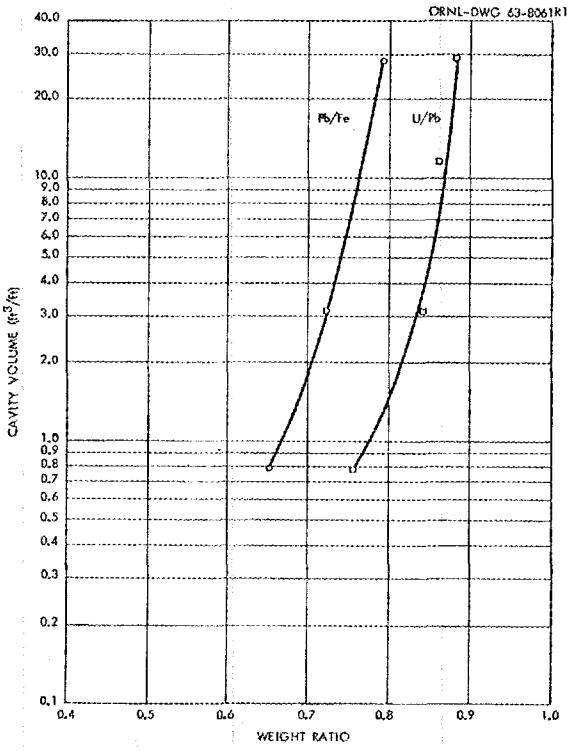

Fig. 5.3. Approximate Weight Ratio of Shielding Material vs Cavity Volume per foot of length for cylindrical casks.

Uranium is structurally about as strong as steel; but when heated, as in a fire, goes through phase changes which are accompanied by grain growth and expansion.

Due to its pyrophoric nature, uranium shields should be encased in steel, even though it is difficult to get large solid pieces to burn.

Uranium may be cast and machined, or rolled in sheets, formed, and welded. An uranium casting is generally limited by the size of the equipment, the maximum size presently being around 6000 lb. However, sheets that have been rolled and formed may be nested and welded into a modular type of construction of almost any size.

Unassayed depleted uranium may be obtained from the government as UF_6 at a base coat of about $1.15/lb of contained uranium. The uranium hexafluoride must be reduced, using conventional methods, and then cast or rolled. The total cost of a uranium cask from a vendor would be in the order of $5.00/lb, which is quite expensive when compared to the cost of a lead-filled carrier at roughly $1.00/lb, but the price may be justified to obtain a maximum cavity volume for minimum shield weight.

Another material that has excellent shielding properties is tungsten, whose specific gravity is 19.3. Additional work is needed to determine whether tungsten, or one of its alloys is a completely satisfactory shielding material for shipping casks from a mechanical point of view; its costs are high, but for large casks is about $5/lb or less.

6. CONTAMINATION

6.1 Problem

A radioactive-materials shipping container may become contaminated with radioactive material during an underwater loading operation or by leakage of the contained source material. Strict limits have been set for maximum external contamination and for internal coolant activity content. When these limits are exceeded prior to shipment, the cask must be decontaminated before shipment can be permitted.

6.2 Regulations

Under the proposed AEC regulations, the cask must be checked for external contamination prior to release for shipment.

The check is made by wiping (or smearing) an area of approximately 100 square centimeters with a clean absorbent paper (filter paper), applying moderate finger pressure, and measuring contamination on the paper through standard counting techniques for beta-gamma and alpha activity. The transferable contamination must not exceed the limits given in Table 6.1.

Table 6.1. External Contamination Limits

Radiation	Type Reading	Limit
α	Smear	≤ 500 d/min/100 cm^2
β, γ	Smear	≤ 4000 d/min/100 cm^2

The proposed regulations also require that the cask coolant, either liquid or gaseous, be sampled prior to shipment and that the coolant activity be below the limits given in Table 6.2.

Table 6.2. Limits of Coolant Activity

Type of Coolant	Radiation	Limit
Liquid	α	10^{-7} curies/ml
	β, γ	10^{-5} curies/ml
Gas	α	10^{-10} curies/ml
	β, γ	10^{-7} curies/ml

Contamination of casks may arise from corrosion products which have become radioactive in the reactor and have deposited on the surfaces of the fuel elements.

It is, therefore, of interest to determine whether the contamination is due to corrosion products or fission products; if due to fission products, a ruptured fuel element may be suspected. The suspect element should be removed, examined, and if ruptured, should be canned in a separate container prior to shipment to prevent further contamination of the shipping container.

6.3 Fission Product Release from Fuels

The purpose of this section is to briefly note the methods of fission-product release from fuel elements and the effect of various parameters on this release.

Fission products can be released from fuel elements by melting or oxidation of the fuel and diffusion or recoil of the radioactive isotopes through the fuel. The release rate is affected by the temperature, form of the material, method of manufacture, material purity, burnup of the fuel, and geometry of the element.[64,65]

Temperature of the fuel, which is the only variable that the cask designer has any control over, is the most important. As the temperature of the fuel increases, the percent release of the fission products also increases. If the fuel is clad and the cladding is intact, then the fission products will be contained; on the other hand, if the cladding is ruptured, the release will contaminate the primary coolant of the cask.

It has been shown in experiments, however, that only a small fraction of the fission products that are released from the hot environment of the fuel will contaminate the air for any length of time. Most of the isotopes that are released, with the exception of the rare gases, deposit on cooler surfaces. Thus, cooler surfaces, such as the inner surface of a dry cask wall, will tend to function as a fission product trap for many isotopes if any should be accidentally released.

7. RADIOLYTIC DECOMPOSITION AND PRESSURE BUILDUP IN CASK COOLANTS

Cask coolants, which are used to improve the heat transfer from the radioactive fuel elements to the heat sink (the atmosphere), are subject to radiolytic decomposition by the radioactive source. The cask coolant is normally water, but in some cases other substances, such as alcohol, are added during winter operation to depress the freezing point.

The decomposition of water by gamma rays and subsequent reactions of the products are thought to occur in the following manner:[66]

$$3H_2O \rightarrow H_2 + H_2O_2 + OH + H \qquad (43)$$

$$H_2 + OH \rightarrow H_2O + H \qquad (44)$$

$$H_2O_2 + H \rightarrow H_2O + OH \qquad (45)$$

$$H + OH \rightarrow H_2O \qquad (46)$$

Equation (43) indicates how the free radicals OH and H are produced, along with H_2 and H_2O_2. Equations (44), (45), and (46) indicate a back reaction in which the H_2 and H_2O_2 are destroyed and water is reproduced.

These back reactions may be interrupted by the presence of some readily oxidizable material, such as the bromide ion. This ion would remove the OH and H radicals from solution and allow some of the H_2 to escape from solution to any gas space above the solution.

Any foreign material that interrupts the back reactions causes the equilibrium overpressure to increase; it is, therefore, important that the water used as the primary coolant be as pure as possible and free from such foreign material.

The rate of a radiolytic reaction is designated by "G" and is expressed in terms of the number of molecules formed per 100 ev of energy absorbed in the solution. This rate, for any particular solution, is a function of the type of radiation (due to the different ionization densities of the different types of radiation). For gamma rays, the value of G_{H_2} is equal to 0.45 molecules per 100 ev in both neutral and acid solutions (ref 67). If no material is present which would interrupt the back reactions [Eqs. (44), (45), and (46)], the equilibrium pressure of hydrogen and oxygen over the solution should be quite low, i.e. in the range of a few psi.[68]

Equilibrium pressure from radiolytic decomposition is reached when the back reaction is equivalent or equal to the forward reaction; that is, when the products are destroyed as fast as they form. There are many factors which affect the back reaction, and equilibrium pressures are quite difficult to predict with any degree of accuracy; however, the following statements can be made.

Pure water is the best liquid coolant for large radioactive sources, since almost all the hydrogen formed will recombine with oxygen in the water quickly to reform water, according to Eqs. (44), (45), and (46), thus creating very little excess pressure. However, it is possible that impure canal water can fill the cask during underwater loading (some casks are loaded in this manner) and may remain in the cask during the period of transportation.

Canal water can contain halogens and materials, like $CuSO_4$, which have been added to retard algae growth. These contaminating materials can disrupt the back reactions and allow equilibrium pressures to increase to higher levels, possibly to a few atmospheres.

This estimate was verified when water samples from two different canals were sealed in a closed container and irradiated in a cobalt-60 source.[69] Overpressure from the water of the first canal leveled off at about 0.83 atm and from the second canal at about 1.9 atm. Equilibrium was reached at an absorbed dose of about 4×10^8 rads.

The difference in equilibrium pressures of the two samples may be attributed to the fact that the second canal used unfiltered process water which contains around 80 ppm hardness, whereas the water for the first canal was processed through an anion-cation resin bed and is filtered.

It appears from the data available, that deionized water is a satisfactory primary coolant and would be expected to produce overpressures of less than 1 atm of radiolytic decomposition products in a closed sealed container. In fact, it is quite possible that temperature changes in the primary coolant could cause greater pressure changes than those caused by radiolytic decomposition of deionized water.

8. ACCIDENTS

8.1 Accident Analyses

There are two types of shipping containers that are used to transport radioactive materials; these are type A and type B. Type A containers are intended to prevent dispersal of the radioactive contents under conditions normally incident to transport and during minor accidents. Type B containers are intended to prevent the release of the contents under conditions normally incident to transport and during a maximum credible accident relative to the mode of transport.[70]

This specification, issued by the International Atomic Energy Agency (IAEA), is, in essence, accepted by most countries; however, the method of proving that a specific cask meets this requirement has not yet been agreed upon.

It would be easier to define a "maximum credible accident" if the probabilities for any given accident were known for any given mode of transportation. The investigation of these probabilities have formed a basis for studies performed by Knapp,[71] Leimkuhler,[72] Stewart,[73] and others.[74,75]

Knapp's paper presented an analysis of the frequency and severity of an accident occurring with the three main modes of transportation – rail, air, and truck. The frequency analysis was based on available statistics in the mid-1955's, and the severity analysis was based on interpretation of photographs of accidents so that estimates of the chances of a radioactive release could be made. His results indicated that the chances of a severe accident, which could result in the release of radioactive material, were roughly the same for all modes of transportation.

A more extensive analysis of motor vehicle (truck) accidents whose cost of damages exceeded $100 was carried out by Leimkuhler[72] in which he found that the average annual accident frequency of all trucks based on a four-year period was 3.63 accidents per MVM (million vehicle miles). This frequency was dependent upon the time of year the shipment was made. Table 8.1 illustrates the variation of accident frequency averaged over each quarter and Table 8.2 indicates the variation in the number of accidents

reported by time and day for the last quarter of 1959. Data was not available to translate the information given in Table 8.2 into accident rates, but there is evidence that indicates the vehicle-miles traveled each quarter-day is roughly constant;[76] thus, the accident rate would vary as the number of accidents given in Table 8.2.

Table 8.1. Average Accident Frequency per MVM Each Quarter (1956-1959)

1st Quarter	2nd Quarter	3rd Quarter	4th Quarter
4.28	3.28	3.34	3.65

Table 8.2. Number of Accidents Reported by Time and Day in the Last Quarter of 1959

Reported Accidents	6 a.m. to 12 noon	12 noon to 6 p.m.	6 p.m. to 12 midnight	12 midnight to 6 a.m.
Weekdays (ave)	403	430	272	245
Saturday	268	215	162	291
Sunday	97	116	135	104

It was also determined in this study that, in general, as the speed of the vehicle increased, the chance for an accident also increased; that fire occurred in about 1% of collision accidents and 2% in overturn accidents. This report is probably the most complete analysis of motor vehicle accidents available at this time.

An extensive analysis of rail accident statistics has been made by Stewart[73] for the years 1958 through 1960. Accidents reported are those in which the cost of damages exceeded $2000. His results indicate that the average freight-train damage caused by derailments increases sharply for train speeds in excess of 30 mph, and the accident frequency is about 2.85 per million freight-train miles.

8.2 Hazards Analyses of Shipping Casks

Every newly designed cask that is expected to transport large quantities of radioactive materials is subject to a hazards analysis; such an analysis provides an insight to the problems and difficulties that may be encountered during shipment.

It has been the purpose of this manual to provide, and/or discuss, all of the available data that could aid in compiling a hazards analysis for a new cask. Such an analysis has been, in the past, time consuming, expensive, and a source of frustration to the many people required to produce such an analysis. These frustrations have stemmed partly from the lack of data and analytical techniques available to adequately analyze casks under accident conditions and partly from a lack of a firm framework of specifications within which a cask is to be judged.

It is hoped that with the intense interest shown by the AEC, Contractors, foreign governments, and the IAEA, that standardized reporting procedures and techniques will remove such hazards analyses from the realm of an art to that of a science.

In spite of, or possibly because of, the lack of standardized reporting procedures and techniques, it is of interest to examine the hazards analyses that have already been made for various shipping casks. Several such analyses are reported in references 77 through 81.

ACKNOWLEDGMENTS

Many people have contributed, both directly and indirectly, to this report. It would be impossible to note all the contributions, although quite often their work may be found in the list of references. Of particular help were J. P. Nichols, D. K. Trubey, S. K. Penny, B. F. Maskewitz, A. D. Callihan, C. J. Hochanadel, and S. J. Ball of ORNL; F. J. Stanek, Hayes International Corporation; and H. G. Clarke, The Franklin Institute.

APPENDIX 1

REGULATIONS APPLYING TO THE TRANSPORT OF RADIOACTIVE MATERIALS

Before a cask design for a specific job is undertaken, it is mandatory that the design engineer become thoroughly familiar with the regulations to which the cask must conform. This could entail a variety of regulations by local, state, federal, and international groups, depending on expected uses of the cask.

The most important proposed federal regulations which affect the particular aspect of cask design discussed have been presented at the start of each section. The source of many of the regulations which affect interstate as well as international transportation of radioactive materials is given below.

The Interstate Commerce Commission has been made responsible by Public Law 86-710 of the 86th Congress for regulations of shipments of radioactive materials by common carriers on land (except the United States mails) and water in the United States.

These regulations may be found in the following publications:

(1) Tariff No. 15, ICC Regulations for Transport of Explosives and Other Dangerous Articles by Land and Water in Rail Freight Service and by Motor Vehicle and Water, T. C. George, Agent, published by the Bureau of Explosives (B of E) of the American Association of Railroads (A.A.R.), 63 Vesey St., New York 7, N. Y., August 23, 1963.

(2) Tariff No. 10, Motor Carriers Explosives and Dangerous Articles Tariff, F. G. Freund, Agent, published by the B of E of the A.A.R., 1424 16th St. N.W., Washington 6, D. C.

(3) Code of Federal Regulations, Title 49, Par. 71 to 78, covering the packaging, labeling, and transportation of dangerous articles. (Revised Jan. 1, 1963) This regulation is almost identical to Tariff No. 15.

The transportation of radioactive materials in aircraft in the United States is regulated by the Civil Aeronautics Board and is covered in

(4) Code of Federal Regulations, Title 14, Part 49, "Transportation of Explosives and Other Dangerous Articles," Revised Jan. 1, 1963.

(5) Civil Aeronautics Board Official Air Transport Restricted Articles Tariff No. 6-C Governing the Transportation of Restricted Articles by Air, B. H. Smith, Agent, Air Traffic Conference of America, 1000 Connecticut Ave., N. W., Washington 6, D. C., April 1, 1962.

(6) Federal Aeronautics Administration Regulations Part 103, Transportation of Dangerous Articles and Magnitized Materials, Superintendent of Documents, U. S. Government Printing Office, Washington 25, D. C.

International air traffic of radioactive materials is covered by the following document.

(7) International Air Transport Assn. (IATA) Regulations Relating to the Carriage of Restricted Articles by Air, 9th ed., April 1, 1964. Terminal Centre Building, Montreal 3, Que, Canada.

Transportation of radioactive material by water is subject to regulations prescribed by the Commandant of the United States Coast Guard.

Applicable regulations are:

(8) Code of Federal Regulations, Title 46, Part 146, "Transportation or Storage of Explosives or Other Dangerous Articles or Substances and Combustible Liquids on Board Vessels," (July 1, 1958).

(9) Water Carrier Tariff No. 6, H. A. Campbell, Agent, published by the B of E of the A. A. R., 63 Vesey St., New York 7, N. Y.

More specific regulations concerning the shipment of special nuclear material may be found in:

(10) Code of Federal Regulations, Title 10, Part 70, "Licensing of Special Nuclear Materials" (proposed), Federal Register, March 5, 1963.

(11) Code of Federal Regulations, Title 10, Part 71, "Regulations to Protect Against the Accidental Conditions of Criticality in the Shipment of Special Nuclear Materials," (proposed) Federal Register, March 5, 1963.

(12) Code of Federal Regulations, Title 10, Part 72, "Regulations to Protect Against Radiation in the Shipment of Irradiated Fuel Elements," (proposed) Federal Register, Sept. 23, 1961.

In addition, the N5.5.2 Committee of the American Standards Association (sponsored by the American Institute of Chemical Engineers, 345 East 47 St., New York 17, N. Y.) has published several drafts of "An American Standard of Good Practice for Design and Operation of Shipping Containers for Irradiated Solid Fuel from Nuclear Reactors."

The U. S. Atomic Energy Commission has published a summary of the Interstate Commerce Commission, United States Coast Guard, Federal Aviation Agency, and the United States Post Office regulations in the

(13) Handbook of Federal Regulations Applying to Transportation of Radioactive Materials, USAEC Division of Construction and Supply, Superintendent of Documents, Washington 25, D. C., May, 1958.

Regulations sponsored by the IAEA, which were written by a panel of men from nine member countries and which, it is hoped, will form a basis or be compatible with transport regulations of member countries, are noted below.

(14) Regulations for the Safe Transport of Radioactive Materials, Safety Series No. 6, International Atomic Energy Agency, Vienna, 1961.

To this end, an Interagency Committee on the Transportation of Radioactive Materials, made up of representatives from the USAEC, ICC, Coast Guard, U. S. Post Office, Federal Aviation Agency, and the Bureau of Explosives, have met to formulate a set of rules acceptable to all United States government agencies and compatible with the safety regulations adopted by the International Atomic Energy Agency.

APPENDIX 2

Availability of Machine Codes

There are a number of information sources concerning nuclear codes. Nuclear Science and Engineering has included a section for code descriptions in its publication. Nuclear Science Abstracts, which is available in most libraries, is useful in locating references to both domestic and foreign codes. International Business Machines Data Processing Division publishes the Nuclear Computing Technical Bulletin which lists available codes and their descriptions. These codes are available upon request from:

Data Processing Library Services
International Business Machine Corporation
112 E. Post Road
White Plains, New York

The Argonne Code Center at the Argonne National Laboratory, Argonne, Illinois, under the auspices of the American Nuclear Society, is another source of available nuclear codes. Abstracts are distributed periodically to persons on their mailing list.

Additional code information is available in the Nuclear Code Abstracts.

Appendix 3

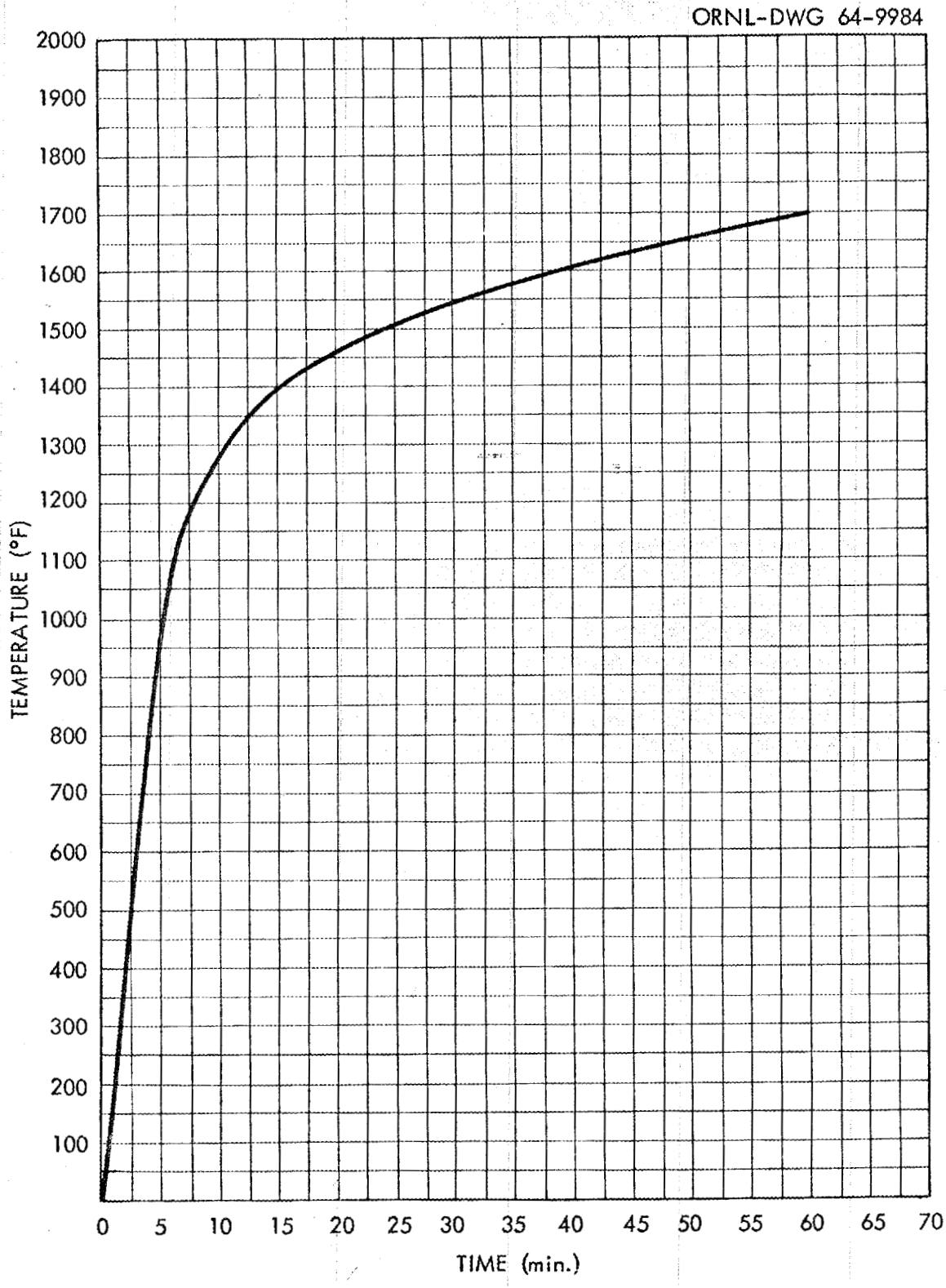

The Standard Time-Temperature Curve for a One-Hour Fire.

REFERENCES

1. Nuclear Safety Guide, TID-7016, Rev 1, p 8 (1961).

2. H. C. Paxton et al., Critical Dimensions of Systems Containing U-235, Pu-239 and U-233, TID-7028, June, 1964.

3. J. K. Fox and L. W. Gilley, Critical Experiments with Arrays of ORR and BSR Fuel Elements, ORNL-2609, p 34 (Oct. 16, 1958).

4. L. O. Gunnels, Battelle Memorial Institute, personal communication.

5. J. D. Anthony, Neutron Blackness Tester for Use Under Water, DP-373 (December 1961).

6. H. C. Paxton, Critical Data for Nuclear Safety Guidance, LAMS-2415 (May 16, 1960).

7. C. L. Schuske and G. H. Bidinger, Nuclear Safety Measurements on Systems Containing Boron and Enriched Uranium, RFP-246 (Oct. 24, 1961).

8. C. L. Brown, Calculated Critical Parameters for Slightly Enriched Uranium Rods in Light Water, HW-69273 (April, 1961).

9. J. K. Fox and L. W. Gilley, Critical Experiments with Arrays of ORR and BSR Fuel Elements, ORNL CF-58-9-40 (Oct. 2, 1958).

10. R. M. Ball, A. L. MacKinney and S. H. Mortensen, Marty Critical Experiments Summary of 4% Enriched UO_2 Cores of NMSR, BAW-1216 (May, 1961).

11. E. E. Gross, B. W. Colston, and M. L. Winton, Nuclear Analyses of the NS Savannah Reactor with Zircaloy or Stainless Steel as Fuel Element Containers, ORNL-3261 (April, 1962).

12. B. G. Carlson, The S_n Method and the SNG and SNK Codes, LASL T-1-159 (Jan. 26, 1958).

13. E. E. Gross and J. H. Marable, "Static and Dynamic Multiplication Factors and their Relation to the Inhour Equation," Nu. Sci. and Eng. 7 (4), 281 (1960).

14. E. B. Johnson and R. K. Reedy, Jr., Neutron Multiplication by Experimental Gas Cooled Reactor Fuel Assemblies, ORNL-TM-433 (Nov. 27, 1962).

15. Data in part from "Safety Summary Report for Shipping MTR-Type Irradiated Fuel Elements from NASA Plum Brook Reactor Facility, Sandusky, Ohio, to USAEC Savannah River Plant, Dunbarton, S. C.," National Lead Company, Aug. 3, 1964.

16. Personal communication with E. D. Arnold. Information based on data from J. F. Perkins and R. W. King, "Energy Release from the Decay of Fission Products," Nu. Sci. and Eng. 3, 726 (1958) and J. O. Blomeke and M. F. Todd, Uranium-235 Fission Product Production as a Function of Thermal Neutron Flux, Irradiation Time and Decay Time, ORNL-2127 (Oct. 1, 1958).

17. F. Kreith, Principles of Heat Transfer, p 217, International Textbook Co., Scranton, Pa., 1958.

18. A. I. Brown and S. M. Marko, Introduction to Heat Transfer, 3d ed., p 71, McGraw-Hill, New York, 1958.

19. F. A. Brooks and W. Miller, "Availability of Solar Energy," p 36, Introduction to the Utilization of Solar Energy, McGraw-Hill, New York, 1963.

20. W. H. McAdams, Heat Transmission, 3d ed., p 173, McGraw-Hill, New York, 1954.

21. Personal communication with S. J. Ball.

22. M. Jakob, Heat Transfer, p 235, vol 1, John Wiley and Sons, Inc., New York, 1949.

23. W. H. McAdams, Op.Cit., p 68-69.

24. J. S. Watson, Heat Transfer from Spent Reactor Fuels During Shipping: A Proposed Method for Predicting Temperature Distribution in Fuel Bundles and Comparison with Experimental Data, ORNL-3439 (May 27, 1963).

25. W. H. McAdams, Op.Cit., p 72-76.

26. O. H. Klepper, Radient Interchange Factors for Heat Transfer in Parallel Rod Arrays, ORNL-TM-583, (Dec. 26, 1963).

27. A. R. Irvine, letter to H. E. Goeller, dated May 22, 1961.

28. A. R. Irvine, personal communication.

29. E. C. Lusk, Patent No. 3,005,105, issued Oct. 17, 1961.

30. E. C. Lusk and J. E. Gates, "New Developments in the Design of Shipping Casks for Irradiated Fuel Elements," Nuclear News 6(6) June 1963.

31. B. E. Bader, Heat Transfer in Liquid Hydrocarbon Fuel Fires, SC-R-64-1366, December, 1964.

32. Letter to L. B. Shappert from J. W. Langhaar, Subject: Open-air Fires with JP-4 Fuel - Results of Study and Tests by Armour Research Institute and Sandia Corporation Summary of Information Obtained in Visit to Sandia Nov. 5-6, 1963 and Pertinent to the Cask Testing Program, dated Jan. 3, 1964.

33. F. E. Dixon, "The Design of Shielded Containers to IAEA Standards," Summary Report of AEC Symposium on Packaging and Regulatory Standards for Shipping Radioactive Material, Germantown, Maryland, Dec. 3-5, 1962, TID-7651, p 331.

34. R. A. Robinson et al., Isotopes Development Center Progress Report, Safety Testing Program, Nov.-Dec. 1962, ORNL-TM-486 (April 8, 1963).

35. R. A. Robinson et al., Isotopes Development Center Progress Report, Safety Testing Program, January-February 1963, ORNL-TM-566 (June 4, 1963).

36. L. H. Horn, Fire Tests of Shipping Containers and Cobalt-60 Teletherapy Head, COO-274 (March 31, 1963).

37. L. H. Horn, Fire Test of Wooden-Jacket Shield for Radioisotope Shipping Container, COO-277 (March 23, 1964).

38. F. Kreith, Op.Cit., p 153.

39. W. I. Thisell and J. W. Langhaar, Static and Impact Tests on 15-ton Cask for Shipping Irradiated Fuel, DP-843 (Aug. 1963).

40. H. G. Clarke and W. E. Onderko, "Model Impact Tests Pertaining to Shipping Containers," Summary Report on AEC Symposium on Packaging and Regulatory Standards for Shipping Radioactive Materials, Germantown, Md., Dec. 3-5, 1962, TID-7651, p 238.

41. Unpublished data from H. G. Clarke of Franklin Institute.

42. E. A. Ripperger, Model Studies of Buffered Shipping Containers for Fission Products, Structural Mechanics Research Laboratory, University of Texas, HW-77963 (May 1963).

43. C. W. Smith et al., "Application of External Impact Energy Sorption to Large Radioisotope Shipping Casks," Summary Report of the AEC Symposium on Packaging and Regulatory Standards for Shipping Radioactive Material, Germantown, Md., Dec. 3-5, 1962, TID-7651, p 265.

44. C. Schroeder, "Aluminum Shock Absorber Fails, Crushes at Specified Loads," p 141, Materials in Design Engineering, May 1961.

45. J. M. Lewallen and E. A. Ripperger, "Energy Dissipating Characteristics of Trussgrid Aluminum Honeycomb," The University of Texas, SMRL-RM-5.

46. E. A. Ripperger and M. D. Reifel, "Size Effects of Trussgrid Aluminum Honeycomb," The University of Texas, SMRL-RM-6.

47. J. R. McGehee, "A Preliminary Experimental Investigation of an Energy Absorbing Process Employing a Frangible Metal Tubing," NASA TN D-1477 (Oct. 1962).

48. E. P. Unksov, An Engineering Theory of Plasticity, p 229, Butterworths, London (1961).

49. Werner Goldsmith, Impact, p 93, Edward Arnold, London (1960).

50. D. Tabor, The Hardness of Metals, p 115-139, Clarendon Press, Oxford, (1951).

51. T. Baumeister (ed.), Mechanical Engineers Handbook, 6th ed., p 13-15, McGraw-Hill, New York, 1958.

52. H. G. Clarke, personal communication.

53. Letter from C. R. Shaber to J. F. Sommers and R. E. Hayden, Sha-127-61A-M, Phillips Petroleum Company, Idaho Falls, Idaho (June 14, 1961).

54. E. P. Blizard (ed.), Reactor Handbook, Vol III, Part B, Shielding, 2nd ed., Interscience, New York, 1962.

55. H. Goldstein, Fundamental Aspects of Reactor Shielding, Addison-Wesley, Reading, Mass., 1959.

56. B. T. Price, C. C. Horton, and K. T. Spinney, Radiation Shielding, Pergamon Press, 1957.

57. T. Rockwell III, Reactor Shielding Design Manual, McGraw-Hill, New York, 1956.

58. H. Goldstein and J. E. Wilkins, Jr., Calculation of the Penetration of Gamma Rays, NYO-3075 (1954).

59. E. D. Arnold and B. F. Maskewitz, Shielding Design Calculation Code for Fuel Handling Facilities, ORNL-3041 (in preparation).

60. Lead in Modern Industry, Lead Industries Assn., New York, 1952.

61. T. Lyman (ed.), Metals Handbook, American Society of Metals, 8th ed., Vol 1, p 422 (1961).

62. H. E. Goeller and W. H. Lewis, Trip Report: UKAEA Facilities at Risley and Windscale; Eurochemic Facilities at Mol, Belgium, and French AEC Facilities at Marcoulle, France, ORNL CF-60-1-104, p 17 (Jan. 25, 1960).

63. R. Morris, Atomics, p 29, February, 1963.

64. G. W. Parker et al., "Release of Fission Products on Out-of-Pile Melting of Reactor Fuels," Nuclear Safety Program, Semiannual Progress Report for Period Ending June 30, 1962, ORNL-3319, p 11 (Aug. 1962).

65. J. A. Lane et al., A Study of the Problems Associated with the Release of Fission Products from Ceramic Fuels in Gas Cooled Reactors, ORNL-2851, p 16 (Oct. 29, 1959).

66. A. O. Allen, "Radiation Chemistry of Aqueous Solutions," J. of Ph. and Colloid Chem. 52, 479 (1948).

67. A. O. Allen, The Radiation Chemistry of Water and Aqueous Solutions, Van Nostrand and Company, Princeton, N. J., p 33 (1961).

68. C. J. Hochanadel, personal communication.

69. H. Kubota, personal communication.

70. Regulations for the Safe Transport of Radioactive Materials, Safety Series No. 6, IAEA, Vienna, 1961.

71. H. A. Knapp, "Cost and Safety Considerations in Transport of Radioactive Materials," pp 54-67 in Proceedings of the 1958 AEC and Contractor Safety and Fire Protection Conference, June 24-25, 1958, TID-7569.

72. F. Leimkuhler, Trucking of Radioactive Materials, The Johns Hopkins Press, Baltimore, Md., 1963.

73. K. B. Stewart, Rail Accident Statistics Pertinent to the Shipment of Radioactive Materials, HW-76299, Jan. 21, 1963.

74. J. T. Thompson and F. F. Leimkuhler, An Operations Research Study of the Transportation of Highly Radioactive Materials (a progress report), NYO-7832 (April, 1959).

75. F. F. Leimkuhler, M. J. Karson, and J. T. Thompson, Statistical Analysis of the Frequency and Severity of Accidents to Potential Highway Carriers of Highly Radioactive Materials, NYO-9771 (July, 1961).

76. Lewis L. Strauss, The Federal Role in Highway Safety, House Doc. 93, 86th Cong., Washington, D. C., 1959.

77. E. C. Watson et al., The Consequences of Accidental Releases During Shipments of Radioactive Cesium and Strontium, HW-69561 (Rev.)(Del.) June, 1961.

78. C. W. Smith, Strontium-90 Shipping Cask Criteria and Hazards Evaluation, HW-68081 (Jan. 13, 1961).

79. L. B. Shappert and A. M. Rom, Evaluation of 1WW Carrier Design for Conformance with Code of Federal Regulations, Title 10, Part 72, ORNL-TM-154 (Feb. 26, 1962).

80. Stanray Corp., SS Savannah Cask Safeguards Report, ST-51, Appendix C, (June 19, 1961).

81. R. A. Wiesman et al., Shipment of Irradiated Yankee Fuel Elements, WCAP-1859 (Jan., 1962).

DISTRIBUTION

1. A. E. Aikens, AEC, Washington
2. T. A. Arehart
3. R. F. Barker, AEC, Washington
4-8. Chris Beck, AEC, Washington
9. W. G. Belter, AEC, Washington
10. C. E. Bettis
11. R. E. Blanco
12. J. C. Bresee
13. R. E. Brooksbank
14. K. B. Brown
15. F. R. Bruce
16. A. D. Callihan
17-31. D. C. Costello, AEC, Washington
32. F. L. Culler, Jr.
33. R. L. Donahue
34-38. G. K. Ellis, AEC, Washington
39. D. E. Ferguson
40. J. H. Gillette
41. H. M. Glen
42. J. C. Glynn, AEC, Washington
43. H. E. Goeller
44. K. W. Haff
45. J. B. Henson
46. A. R. Irvine
47. W. A. Johnson, ORO
48. A. B. Joseph, AEC, Washington
49. E. M. King
50. J. A. Lane
51. J. A. Lieberman, AEC, Washington
52. C. D. Luke, AEC, Washington
53. A. J. Mallett, ORGDP
54. J. L. Matherne
55. J. D. McLendon, Y-12
56. W. T. Mee, Y-12
57. J. L. Myers, Paducah
58. C. E. Newlon, ORGDP
59. J. P. Nichols
60-64. D. E. Patterson, AEC, Washington
65. A. F. Perge, AEC, Washington
66. T. W. Pickel
67. W. A. Pryor, ORO
68. W. F. Schaffer
69-89. L. B. Shappert
90. A. E. Spaller
91. J. W. Ullmann
92. J. S. Watson
93. M. E. Whatley
94. B. W. Wieland
95. R. G. Wymer
96-97. Central Research Library
98-99. Document Reference Section
100-102. Laboratory Records
103. Laboratory Records-RC
104. ORNL Patent Office
105. R & D, ORO
106-121. DTIE